Studies on the silicon dynamics and those impacts on diatom blooms in a shallow eutrophic lake

October 2013

Hiroyuki Arai

Studies on the silicon dynamics and those impacts on diatom blooms in a shallow eutrophic lake

A Dissertation Submitted to
the Graduate School of Life and Environmental Sciences,
the University of Tsukuba
in Partial Fulfillment of the Requirements
for the Degree of Doctor of Philosophy in
Integrative Environmental Science
(Doctoral Program in Integrative Environmental Sciences)

Hiroyuki Arai

Contents

Abstract

Silicon (Si) is one of the essential nutrients for diatoms. In Lake Kasumigaura, a shallow eutrophic lake, increasing trends of dissolved Si (DSi) and total Si (TSi) concentration were detected during the last three decades (mean DSi concentration measured by a colorimetric method in the 1980s and 2000s was 1.3 mg l^{-1} and 4.0 mg l^{-1}, respectively). The observation of such long-term trends is rare; therefore, detailed analysis could be useful to understanding Si dynamics in inland waters. The objectives of this study are fourfold: (i) to detect the long-term trend of Si concentrations and discuss the factors of the trend, (ii) to assess the contribution of DSi release from suspended solids (SS) to the increasing trend of DSi observed in the lake by laboratory experiments, (iii) to calculate the Si budgets in the lake based on the long-term database and compare with the chronological sediment information, and (iv) to assess the factors for long-term changes in diatom abundance by database analysis and model simulation, especially focusing on the relationships between diatoms and DSi.

Based on statistical analysis, we found that the increases in DSi and lithogenic Si accounted for most of the TSi increase (44% and 45%, respectively) and that biogenic Si (BSi), consisting of diatom frustules, also increased with them. Increases in DSi concentration were not detected near the mouth of the inflowing rivers, suggesting that the increase was caused by in-lake processes. Because the increase in SS caused by sediment resuspension had been observed in the lake for the same period, we considered

that DSi release from SS containing diatom frustules contributed to the increase.

The results of the laboratory experiments in which surface sediments were stirred in lake waters showed that the change in DSi concentration depended mainly on SS concentration, water temperature, and the elapsed time of diatom frustules dissolution. An estimation of the released amount of DSi from SS using the sediment resuspension model was (1.0–2.7) × 10^9 g y^{-1} in the 2000s, which was about 30–90% of the increase in the DSi outflow of 3.0 × 10^9 g y^{-1} from the 1980s to the 2000s. We also determined the DSi release rates from bottom sediments to be 4.3 × 10^9 g y^{-1}, which was about 2–4 times higher than the estimated DSi amount released from SS. These findings suggest that the sediment resuspension might be the cause of the latest DSi increase.

Budgetary calculations based on the database showed that 60–70% of DSi inputs from the inflowing rivers could ultimately be accumulated as diatom frustules in bottom sediments in the lake during the 27 years. The sediment BSi analyzed in the dated cores revealed that the BSi amount accumulated in the lake from 1980–2007 was (2.0–2.6) × 10^{11} g, close to the amount based on the database of (1.3–2.4) × 10^{11} g. Although the gross sedimentation rates of BSi likely increased, the net sedimentation rates of BSi significantly decreased from (6–10) × 10^9 g y^{-1} in the 1980s to (2–6) × 10^9 g y^{-1} in the 2000s, suggesting fast BSi recycling in recent years caused by an increase in sediment resuspension and regeneration of DSi.

Diatom abundance increased during the last three decades. Based on the monthly dataset, N:P:Si ratios suggested that Si was the element mostly limiting diatom growth after DSi depletion. The seasonal relationships between DSi and diatoms showed a hysteresis loop, representing as follows: (i) diatom growth by uptake of DSi in a better state (e.g., at optimal temperature), (ii) rapid sinking of diatoms after DSi depletion, and

(iii) no diatoms with DSi supply from river inputs and release. The relationships were mostly characterized as a two-round loop during the 1980s (spring and autumn diatom blooms), while a one-round big loop during the 2000s (extensive winter–spring blooms). Modeling and simulation of major processes involved in DSi (inflows, outflow, uptake by diatoms, and release from bottom and SS determined by the laboratory experiments) and diatoms (outflow, sinking, and growth limited by light condition, water temperature, and DSi concentration) could reproduce a two-round and one-round loop during the 1980s and 2000s, respectively. The peaks of diatom blooms declined with the release from resuspended sediments removed, indicating the impacts of the recent release on diatom blooms in the lake. Simulation also suggested that the sediment resuspension might cause the change of the loop from two-round to one-round mainly through degradation of light condition. These findings implicate the significance of the interactions between sediments and water to phytoplankton blooms.

The products of this dissertation might be useful for lake management as basic information relevant to Si and diatoms.

Keywords: Silicon, Diatoms, Suspended solids, Sediments, Release, Budgetary analysis, Model simulation, Lake Kasumigaura

List of Tables

List of Figures

Chapter 1

Introduction

1.1 Purpose of this study

Silicon (Si) is the second most common element of the earth's crust. It occurs as silicate minerals in association with igneous, metamorphic, and sedimentary rocks. They undergo physical, chemical, and biological weathering. The products of weathering include both particulate components (e.g., clays) and dissolved silicate. The latter consists of $Si(OH)_4$ (dominant with a pH of less than 9.8), $Si(OH)_3O^-$ (dominant with a pH of more than 9.8), and those polymers as a result of dehydration synthesis (Alexander et al. 1954).

It is well known that part of dissolved Si (DSi) produced in weathering is used in aquatic ecosystems by diatoms, sponges, chrysophytes, radiolarians, and silicoflagellates (Conley et al. 1993). Diatoms form a major part of the aquatic food chain and play a critical role in marine biogeochemical cycles, especially in the sequestration of carbon dioxide from the atmosphere via the biological pump (Schelske 1999; Ittekkot et al. 2006). Diatoms need plentiful Si which is present in their cell walls, i.e., frustules, as amorphous silica (i.e. SiO_2). Freshwater diatoms have more silica per

unit of biovolume than marine species (Conley et al. 1989). Therefore, Si dynamics could affect the phytoplankton dominance, food web, and biogeochemical cycling in both marine and freshwater ecosystems (Kristiansen and Hoell 2002). In addition, terrestrial plants such as paddy rice take up a significant portion of DSi (Sommer et al. 2006). Recent evidence supports that the flux of DSi transferred from the land to the oceans is primarily leakage out of the internal terrestrial biogeochemical cycle (Derry et al. 2005; Conley et al. 2006).

While the loadings of nitrogen (N) and phosphorus (P) are enhanced by the human activities, a decreasing trend of the loadings of DSi, which tends to be taken by diatoms in the eutrophicated stagnant waters such as dammed reservoirs, has been observed globally (Humborg et al. 1997; Conley et al. 2000; Duan et al. 2007; Li et al. 2007). For example, Humborg et al. (1997) showed the decreases in the DSi load in the Danube River–Black Sea system and indicated the impacts of the construction of “Iron Gates”. In addition, Teodoru et al. (2006) suggested that the large number of impoundments on the Danube and its tributaries changed DSi transport to the coastal Black Sea. In Japan, few observational data suggested a decrease in the loadings of DSi. The Foundation of River & Watershed Environment Management (2007) reported that the mean DSi concentration of the limited 18 Japanese rivers in the 2000s was lower than that in the 1940s and 1950s, opposite to the trends of N and P. However, the report pointed out the scarcity of long-term Si monitoring data fractionated to be dissolved, biogenic, and lithogenic Si makes it difficult to elucidate the cause.

Following the DSi trapping in the eutrophicated stagnant waters, the consequent change in the N: P: Si stoichiometric ratio of the river water flowing into the coastal sea may be advantageous to nonsiliceous algae (potentially harmful such as some of

dinoflagellates) but disadvantageous to diatoms (siliceous and mostly benign). This is called as the “silica deficiency hypothesis” (Officer and Ryther 1980; Humborg et al. 1997; Ittekkot et al. 2000). For instance, Humborg et al. (1997) showed that the decrease in the DSi load of the influent rivers and the consequent changes in Si:N ratio of the Black Sea nutrient load seem to be responsible for dramatic shifts in phytoplankton species composition from diatoms to coccolithophores and flagellates in the sea. In Japan, where DSi supply by natural weathering is comparatively huge due to geological condition (mainly igneous rock) and high rainfall, Harashima et al. (2006) implied the sensitivity of the ecosystem to Si processes in the aquatic continuum composited of Lake Biwa, the Yodo River, and the Seto Inland Sea. Moreover, Harashima (2007) developed “silica deficiency hypothesis” further to the “extended silica deficiency hypothesis” as follows. While the diatoms effectively draw down the substances from the upper layer with their sinking after the spring bloom (biological pump), other algae do not. This will cause the retention of the surplus nutrient and biogenic substances in the upper layer and lead further to eutrophication of upper layer substantially. The role of Si or N: P: Si stoichiometric ratio was suggested not only in marine environment but also in freshwater ecosystems such as natural lakes (Koszelnik and Tomaszek 2008). However, evidence for significant effects of Si dynamics on aquatic ecosystems in stagnant waters is sparse in the world (Humborg et al. 1997; Harashima 2007).

This research is a case study to obtain new fundamental knowledge of a long-term Si dynamics and those impacts on diatom blooms in a shallow eutrophic lake using several biogeochemical techniques. The target area is Lake Kasumigaura, where various forms of Si have been monitored for the last three decades. With regard to the social

significance of use of lake water, detailed analysis in such a shallow eutrophic lake is important. The objectives are fourfold: (i) to detect the long-term trend of Si concentrations and discuss the factors influencing the trend, (ii) to estimate the DSi release rate from SS and bottom sediments by laboratory experiments and assess the contribution of DSi release to the trend, (iii) to calculate the Si budgets in the lake based on the long-term database and compare with the chronological sediment information, and (iv) to assess the factors for the long-term changes in diatom abundances by model simulation. The products of this dissertation might be useful for lake management as basic information relevant to Si and diatoms.

1.2 Structure of this study

This dissertation is organized from 8 chapters. Chapter 1 explains the backgrounds and objectives of this study. Chapter 2 describes the study area, Lake Kasumigaura and its catchment. Chapter 3 addresses the long-term trend of various Si concentrations and the factors influencing the trend using the water quality and meteorological data. Chapter 4 estimates the DSi release rate from SS and bottom sediments by laboratory experiments and assesses the contribution of DSi release to the observed trend. Chapter 5 calculates the Si budget in the lake based on the long-term database and discusses the budget with the chronological sediment information. Chapter 6 addresses the long-term changes in the abundance and seasonality of diatom blooms and assesses the factors using simplified box model, especially focusing on the impacts of DSi increase on diatom blooms.

Chapter 2

Study area

Lake Kasumigaura is the second largest shallow lake in Japan, located in the Ibaraki Prefecture, approximately 50 km northeast of Tokyo. Lake Kasumigaura refers group of contiguous lakes, which includes Nishiura and two smaller lakes (Kitaura and Sotonasakaura). In this study, "Lake Kasumigaura" indicates only Nishiura (**Figure 2.1**). It has a surface area of 171.5 km^2, a mean depth of 4 m, and a maximum depth of 7.3 m. Mean water retention time is about 200 days. The lake is so shallow that vertical stratification is easily destroyed by a moderately strong wind. The lake has two large bays, Takahama-iri and Tsuchiura-iri. The Koise and Sakura rivers are the main rivers influent into Takahama-iri and Tsuchiura-iri, respectively. Water tends to flow through the lake from the northwest, where Takahama-iri and Tsuchiura-iri are located, to the southeast, to the effluent Hitachitone River. Its catchment area of 1426 km^2 (excluding the lake area) consists of paddy fields, plowed fields for other row crops, orchards (in total of 51%), forest (30%), and urban, industrial, and residential uses (12%). Major surface geology in the catchment is loam. The climate of the area is similar to other regions on the Pacific side of Japan with the annual average air temperature of about 14°C and an annual precipitation of 1250 mm. The lake was turned from a brackish into

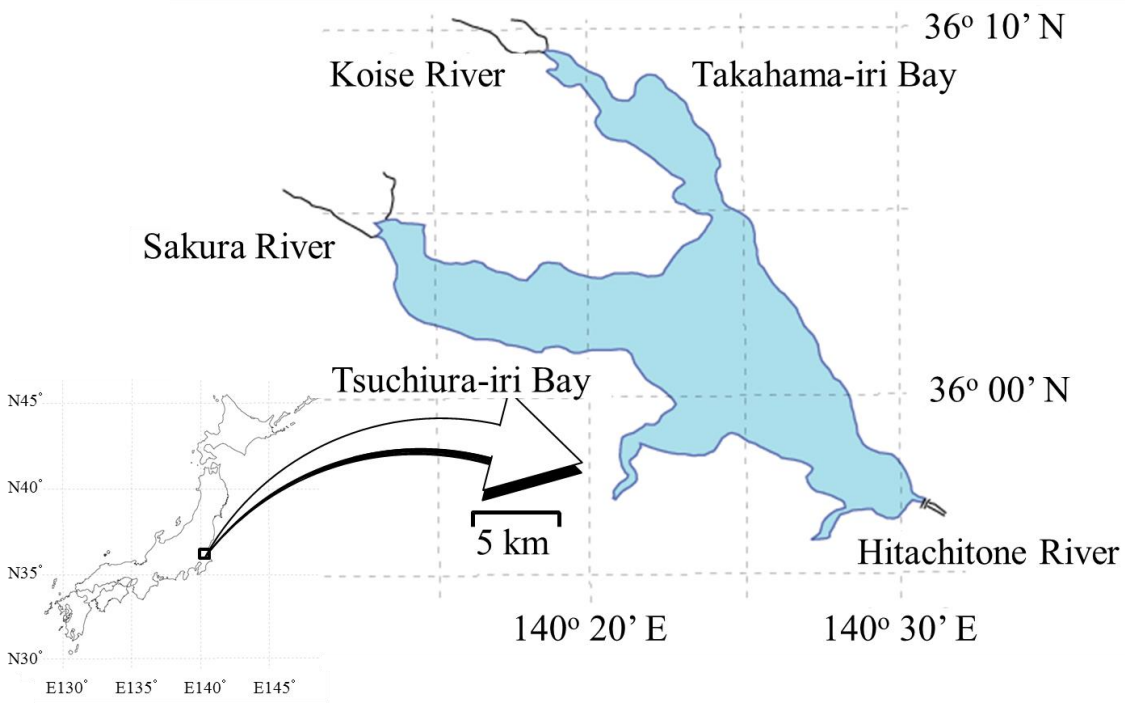

Figure 2.1 Lake Kasumigaura

a freshwater lake 5 years after a floodgate to the Pacific Ocean was implemented in 1963.

The lake is well known for eutrophication. Mean (min.–max.) chlorophyll *a*, total nitrogen (TN), and total phosphorus (TP) concentrations observed monthly at the center of the lake for 1980–2010 were 53 (3–140), 1040 (520–1990), and 94 (21–238) μg l^{-1}, respectively. Nitrogen and phosphorus load from the basin to the lake increased during the high economic growth period.

Considerable increases in turbidity and inorganic content in suspended solids (SS), due mainly to the resuspension of bottom sediments, were also observed in the lake from the late 1990s to mid 2000s, possibly causing the decline in primary production and the increase in phosphorus concentrations (Fukushima et al. 2005; Seki et al. 2006).

Chapter 3

Long-term changes of silicon concentrations in a shallow eutrophic lake

3.1 Introduction

Si is essential for diatoms, play an important role in the global primary production (Schelske 1999). In recent years, DSi load from land to coastal area may be declining globally, which are probably caused by human activities such as dam construction and N and P emission promoting diatom sinking and sedimentation in dammed reservoirs (Humborg et al. 1997; Li et al. 2007). Similar trend was observed in Japan; however, few monitoring of Si makes it difficult to elucidate the long-term Si dynamics in stagnant waters (The Foundation of River & Watershed Environment Management 2007). In fact, few studies investigated long-term trends of Si concentrations in inland waters around the world. Among the few studies, Vesely et al. (2005) showed the increasing trends of DSi concentration in five glacial lakes in the Bohemian Forest over

the last two decades. They concluded that the higher mobility of Si from the soil to surface waters resulted from a decrease in dissolved Al and faster dissolution of biogenic Si (BSi). Several studies indicated that, as a consequence of diatom sedimentation, Si was released back to the water column (Rippey 1983; Schelske et al. 1988; Szczepocka and Szulc 2006).

Annual changes in DSi concentrations and diatom abundances were assessed in many studies. Bailey-Watts (1976b) assessed the Si budget in the shallow, eutrophic Loch Leven based on the monitoring of DSi and BSi in the water column and on laboratory experiments determining diatom cell sinking rates and Si release rates from diatom frustules and sediments. The authors suggested that the incorporation of diatom frustules into the sediments and the release of DSi from the sediments were more important than the inflows and outflow in the lake. Cornwell and Banahan (1992) calculated the Si budget in shallow, ultraoligotrophic Lake Toolik based on the monitoring of DSi concentrations in streams and the water column and on estimated Si burial and release rates; these estimations were obtained through analyzing pore water and BSi concentrations in ^{210}Pb-dated sediment, respectively. Although the internal cycling of DSi was about half of the flux through inflows, the study indicated that internal cycling can supply a significant part of the biologically utilized amount in the lake. Also, the budgets in other shallow lakes reported in previous studies suggested that Si cycling within lakes played an important role in determining the available Si for diatoms (e.g., Gibson et al. 2000; Miretzky and Cirelli 2004). On the other hand, Hoffman et al. (2002) found that the main source and export of DSi in the North basin of Lake Lugano, permanently stratified below a 100-m depth, were river input and final burial of diatom frustules in the bottom sediment, respectively, indicating that the North

basin of Lake Lugano acted as an important permanent sink for Si. Although a number of studies have assessed the annual Si budgets in shallow lakes, detailed studies analyzing the long-term Si dynamics are scarce.

In Lake Kasumigaura, various forms of Si have been monitored for the last three decades and several trends were detected. Understanding the dynamics of Si in a shallow eutrophic lake is extremely valuable. Therefoer, the objectives of the present chapter are twofold: (1) to detect the long-term trend of Si concentrations in Lake Kasumigaura, and (2) to discuss the factors influencing this trend.

3.2 Materials and methods

3.2.1 Silicon concentrations and other water qualities in Lake Kasumigaura

The database of water quality used for this study was based on the investigation by two institutes during April 1980 – March 2007. The National Institute for Environmental Studies (NIES) collected surface waters once a month at 10 sites (A1–A4, B1–B3, and C1–C3; **Figure 3.1**). C1 is located at the center of the lake. Water filtered through 0.45-μm glass-fiber was analyzed by inductively-coupled plasma (ICP) to determine the concentrations of DSi (expressed as DSi_{ICP} in this chapter) and other elements (B, Ca, K, Mg, Na, and Sr). Diatom, SS, and chlorophyll *a* concentrations taken by a column-sampler (upper 2 m) and data on basic water quality (e.g., water temperature, pH, DO, transparency observed in the field) were also used for statistical analysis. Diatoms were counted on an inverted microscope and quantified as biovolume by

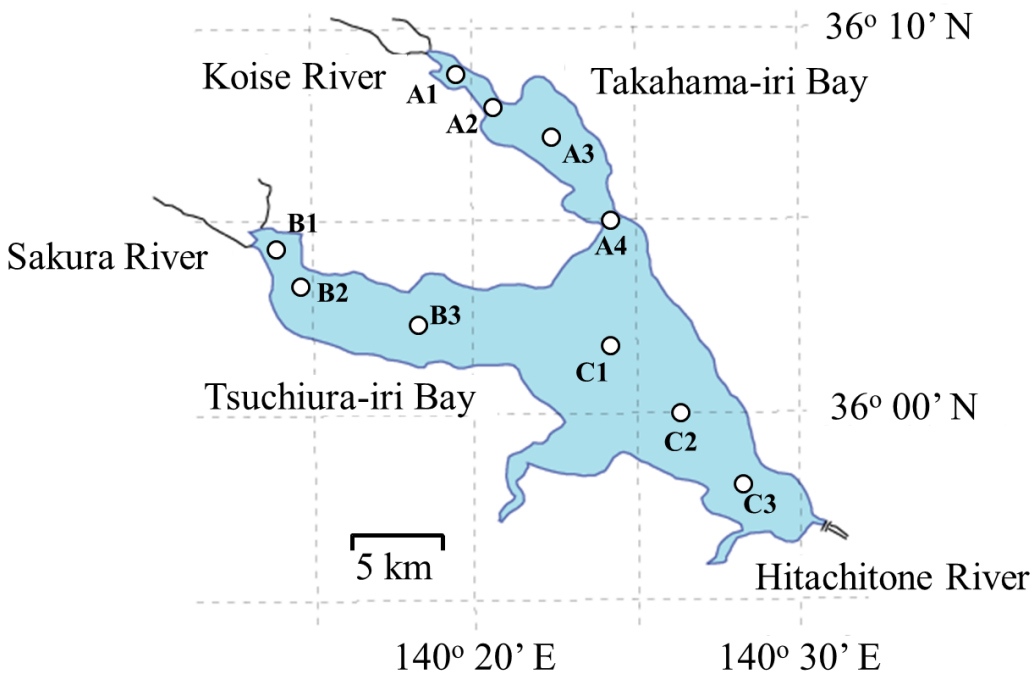

Figure 3.1 Sampling points in Lake Kasumigaura

multiplying counted cell number by mean cell volume.

The Kasumigaura River Office (KRO) collected surface waters once a month at 3 sites. They are relatively close to A2, B2, and C1; therefore, we call them by the same names as the NIES stations for the sake of simplicity. The concentrations of DSi were measured by silicomolybdate yellow colorimetric method JIS K 0101 after filtering the sampled water through a 0.45-μm membrane filter. In this chapter, "DSi_{col}" indicates the Si determined by the colorimetric method. Total Si (TSi) concentrations were determined by the same method as DSi_{col} after alkaline digestion of solids in water as specified by method JIS K 0101.

Monthly precipitation data at Tsukuba meteorological weather station were obtained from the web site (http://www.jma.go.jp/jma/) and used for analysis.

Particulate Si (PSi) concentrations were estimated through the subtraction of DSi_{col} from TSi at C1. PSi consists of biogenic and lithogenic one. In Lake Kasumigaura, BSi concentrations could be estimated from diatom concentrations and mean Si density of diatom frustules (1.1×10^{-10} mg μm^{-3}), determined by averaging the values found in Bailey-Watts (1976a) and Sicko-Goad et al. (1984). Lithogenic Si (LSi) concentrations were estimated through the subtraction of BSi from PSi.

3.2.2 Silicon concentrations of the rivers inflowing Lake Kasumigaura

Si concentrations of the main rivers inflowing Lake Kasumigaura were used in this study. In 1994, DSi_{ICP} concentrations of 10 rivers (Sakura, Koise, Sonobe, Ono, Hanamuro, Seimei, Sannou, Amano, Shin, and Takahashi Rivers) were seasonally

measured by NIES (N = 4). In 2007, DSi_{col} concentrations of 5 rivers (Sakura, Ono, Seimei, Tomoe, and Hokota Rivers) were measured almost monthly by KRO (N = 11). Only 3 rivers (Sakura, Ono, and Seimei Rivers) were investigated by both institutions. In addition, we measured both DSi_{ICP} and DSi_{col} concentrations of 12 rivers (Sakura, Koise, Sonobe, Ono, Hanamuro, Seimei, Kajinashi, Ichinose, Hishigi, Shin, Tomoe, and Hokota Rivers) by ICP and colorimetric method, respectively, in December 2009 (**Figure 3.2**). There was no rainfall for 3 days before almost all samplings.

3.3 Results

3.3.1 Long-term trends of silicon concentrations in Lake Kasumigaura

Mean (min.–max.) of DSi_{col}, DSi_{ICP}, and TSi concentrations were 2.4 (0.0–9.3), 3.1 (0.0–10.3), and 4.7 (0.1–22.2) mg l^{-1}, respectively, at C1 during April 1980 – March 2007. Although we cannot make a fair comparison because of the difference in the sampling date, about 80% of DSi_{ICP} concentrations were larger than DSi_{col} concentrations at C1, which might be caused by the difference in the method for analysis. The annual average DSi_{col} and TSi concentrations significantly increased (p < 0.001), along with DSi_{ICP} concentrations (p < 0.01), at C1 during this period (**Table 3.1**; **Figure 3.3**). The annual maximum of each Si concentration and the minimum of TSi also significantly increased (p < 0.001), except in 2006, when declines were observed. From the 1980s to 2000s, the averages of DSi_{col}, DSi_{ICP}, and TSi concentrations at C1 changed from 1.3, 2.2, and 2.2 to 4.0, 4.8, and 8.4 mg l^{-1}, respectively, which represents

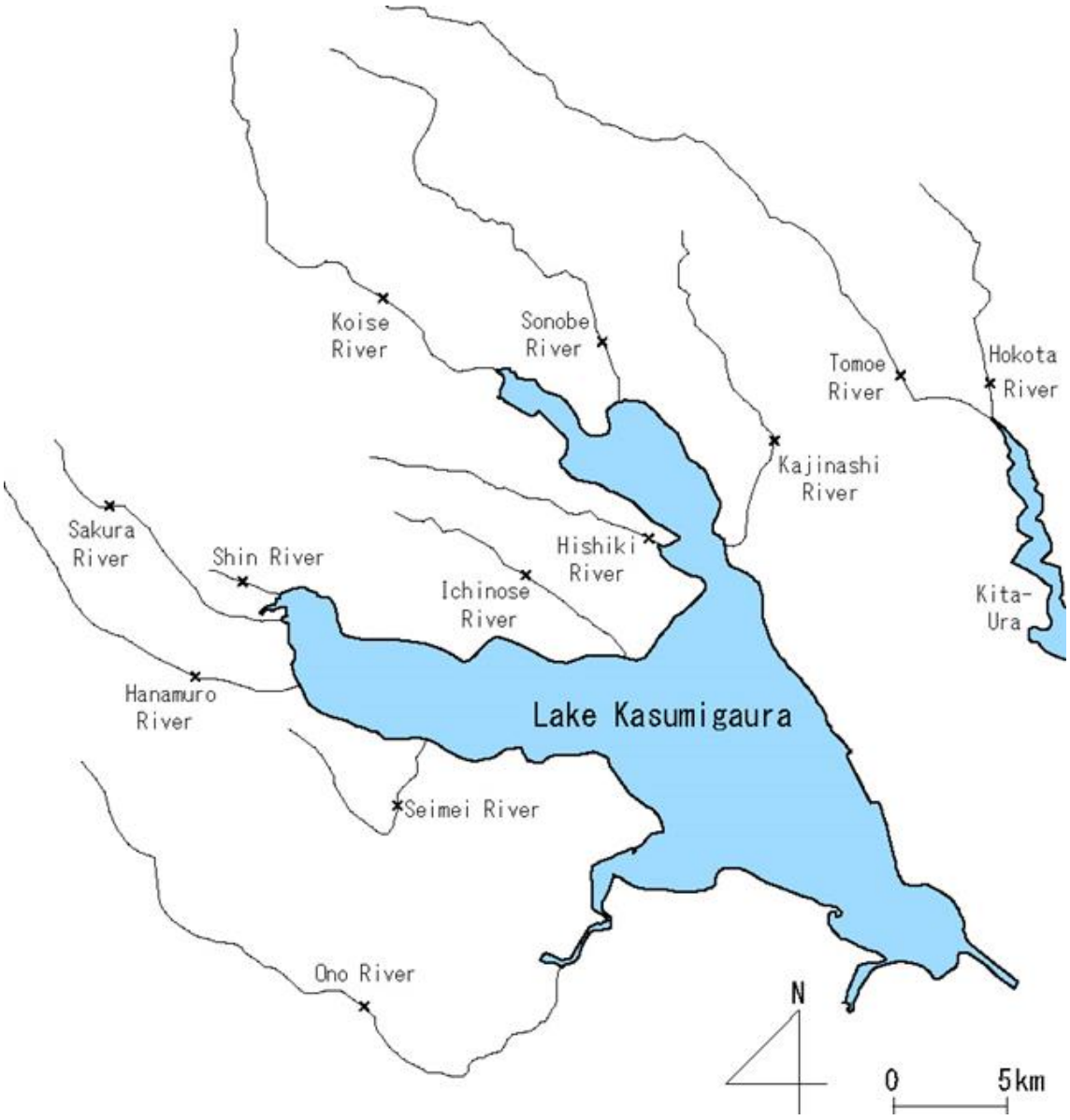

Figure 3.2 Sampling points of river water in Lake Kasumigaura Basin

Table 3.1 Mean Si concentrations in the 1980s/1990s/2000s and yearly trends detected by t-test

Site	Mean concentrations in the 1980s/1990s/2000s (mg l^{-1})		
	DSi_{col}	DSi_{ICP}	TSi
A1		8.1/ 7.1/ 7.1 $^{-}$	
A2	3.0/ 4.0/ 5.1 $^{+++}$	5.4/ 4.9/ 5.8	4.8/ 7.2/ 9.4 $^{+++}$
A3		3.4/ 3.6 /5.0 $^{++}$	
A4		2.6/ 3.0/ 4.9 $^{++}$	
B1		7.2/ 6.0/ 7.3	
B2	2.1/ 3.1/ 4.6 $^{+++}$	4.5/ 4.5/ 6.2 $^{+}$	3.7/ 6.9/ 10.4 $^{+++}$
B3		2.7/ 3.1/ 4.9 $^{+}$	
C1	1.3/ 2.4/ 4.0 $^{+++}$	2.2/ 2.8/ 4.8 $^{++}$	2.2/ 4.8/ 8.4 $^{+++}$
C2		2.2/ 2.9/ 4.9 $^{++}$	
C3		2.2/ 3.0/ 5.0 $^{++}$	

+, increase; -, decrease

+ or -, $p < 0.05$; ++ or --, $p < 0.01$; +++ or ---, $p < 0.001$

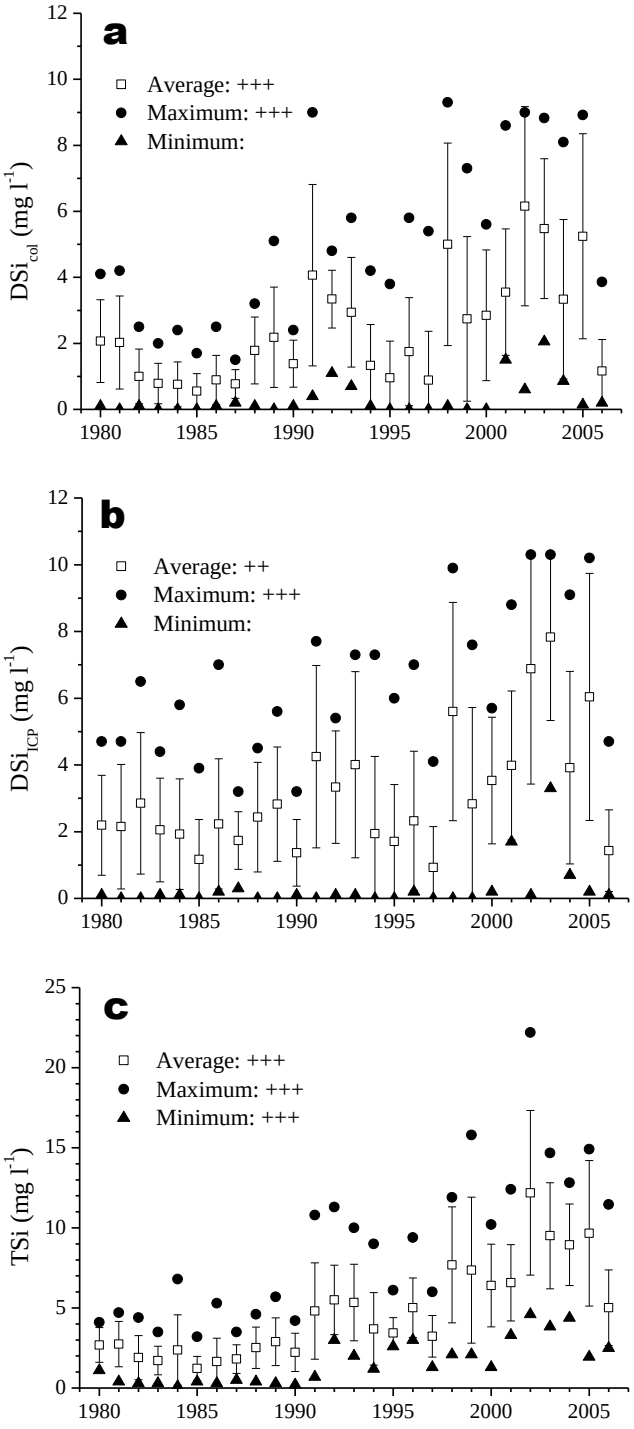

Figure 3.3 Changes in DSi_{col} (**a**), DSi_{ICP} (**b**), and TSi (**c**) concentrations at C1 during 1980–2006. Bars indicate standard deviations. Legends (+, ++, +++, –, – –, and – – –) are the same as in Table 3.1

210, 120, and 290% increases, respectively. On the other hand, ratios of change for the other dissolved elements (B, Ca, K, Mg, Na, and Sr) were within ± 15% (data not shown).

Similar Si changes were also observed at A2 and B2 (**Table 3.1**). With the exception of DSi_{ICP} at A2, increasing trends of DSi_{col}, DSi_{ICP}, and TSi concentrations were detected; however, these increases (37–180%) were lower than those at C1. Increasing trends of DSi_{ICP} concentrations were seen around the center of the lake, such as at A4 and B3 (**Table 3.1**). In contrast, DSi_{ICP} concentrations decreased at A1, near the Koise River ($p < 0.05$), and a clear trend was not detected at B1, near the Sakura River. The temporal and spatial variations of DSi_{ICP} concentrations in **Figure 3.4** represent the DSi loads from inflowing rivers and progressive decreases in DSi as the flows approach the center of the lake. The concentrations at C1 were transiently higher than those at the stations near the inflowing rivers (A1 and B1) in every summer during the period of 2002–2005.

Changes in the annual averages of DSi_{col}, BSi and LSi concentrations at C1 are shown in **Figure 3.5**. Increasing trends of DSi_{col}, BSi and LSi concentrations were detected ($p < 0.001$). The increases in DSi_{col}, BSi and LSi accounted for 44, 11 and 45%, respectively, of the TSi increase of 6.2 mg l^{-1} from the 1980s to 2000s.

3.3.2 Relationships between silicon concentrations and other water quality items

DSi_{col} concentration was positively correlated with DSi_{ICP} concentration (**Table 3.2**). DSi_{col}, DSi_{ICP}, and BSi concentrations were also related to LSi concentration. In

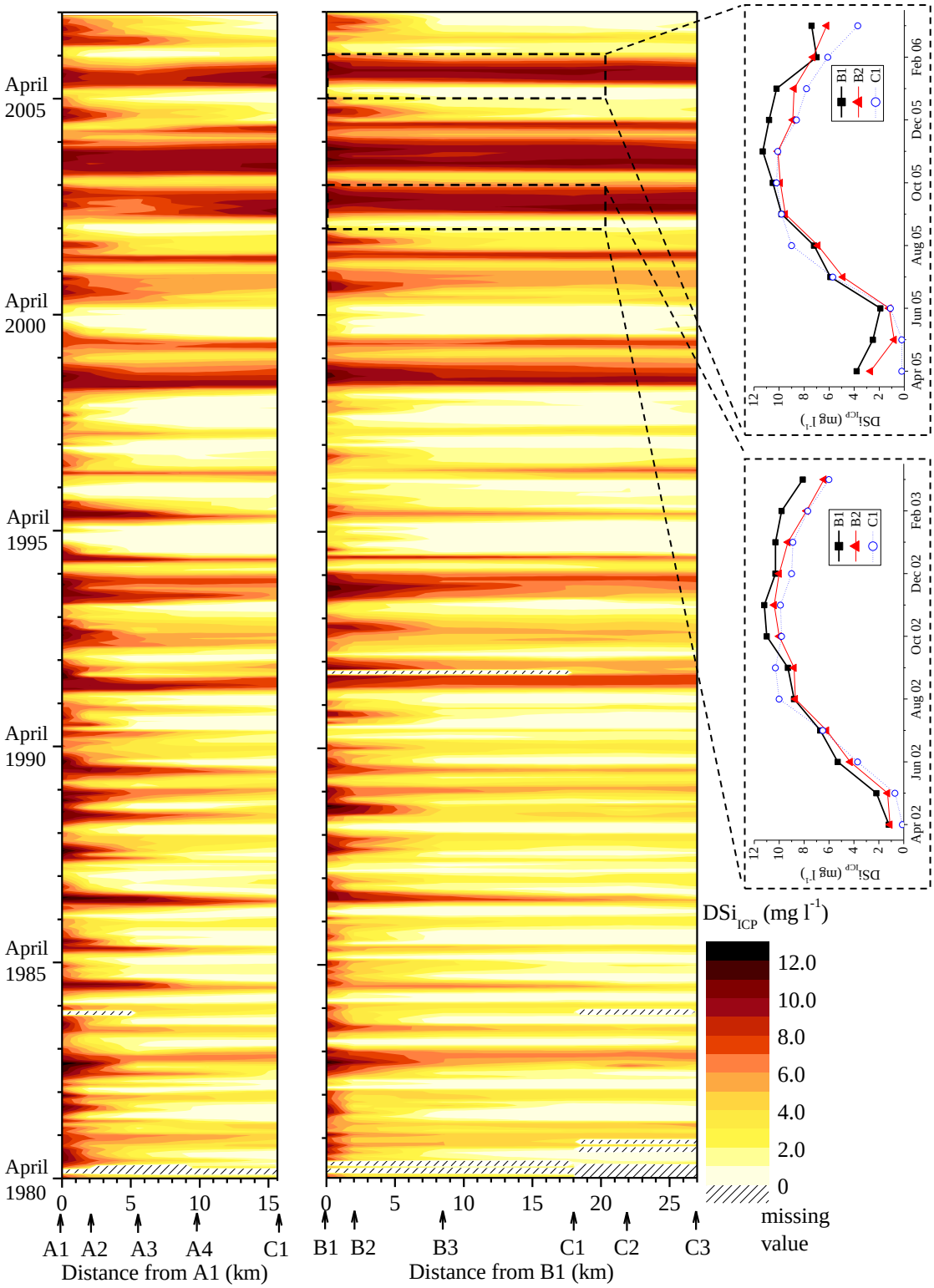

Figure 3.4 Temporal and spatial variation of DSi_{ICP} concentrations in Lake Kasumigaura during April 1980 – March 2007

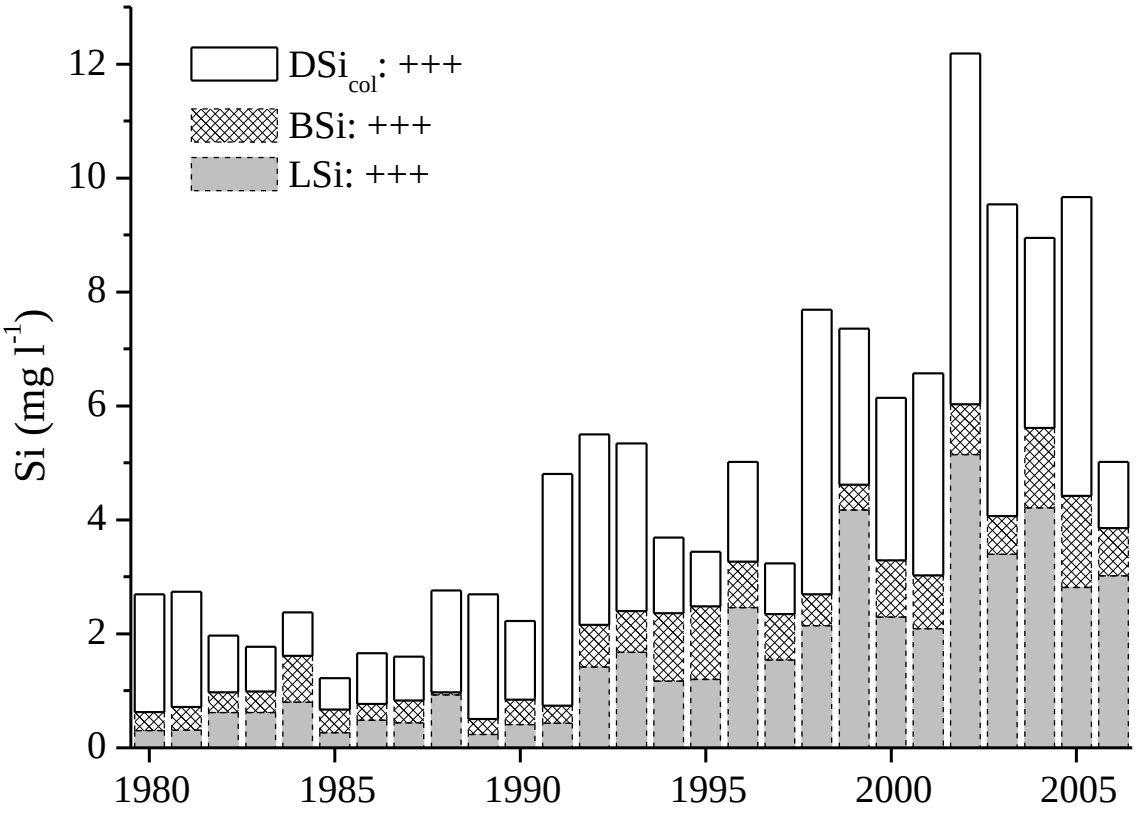

Figure 3.5 Changes in annual averages of DSi_{col} concentration (observed) and BSi and LSi concentrations (estimated) at C1 during 1980–2006. Legends (+, ++, +++, –, – –, and – – –) are the same as in Table 3.1

Table 3.2 Correlation coefficient matrix of annual mean water quality items at the center of Lake Kasumiguara and annual precipitation at Tsukuba meteorological weather station during 1980–2006. N = 27 for all relationships except pH versus others (N = 24). Legends (+, ++, +++, –, – –, and – – –) are the same as in Table 3.1

	DSi_{col}	DSi_{ICP}	BSi	LSi	SS	ISS	Chl-a	WT	pH	DO	Transp	PT
DSi_{col}		0.95	0.30	0.64	0.61	0.64	-0.27	-0.03	-0.55	-0.35	-0.61	0.27
DSi_{ICP}	+++		0.27	0.60	0.61	0.63	-0.26	-0.09	-0.46	-0.35	-0.56	0.23
BSi				0.53	0.64	0.61	-0.05	0.04	0.16	-0.07	-0.59	-0.22
LSi	+++	+++	++		0.88	0.88	-0.24	0.08	-0.21	-0.37	-0.75	0.01
SS	+++	+++	+++	+++		0.97	-0.15	0.10	-0.22	-0.29	-0.87	0.13
ISS	+++	+++	+++	+++	+++		-0.38	0.15	-0.26	-0.37	-0.78	0.08
Chl-a								-0.17	0.33	0.32	-0.13	0.20
WT									0.16	-0.40	-0.08	0.20
pH	--	-								0.22	0.11	-0.21
DO								-			0.08	-0.21
Transp	---	--	--	---	---	---						-0.22
PT												

ISS, inorganic suspended solids estimated by Seki et al. (2006); *Chl-a*, chlorophyll *a*; *WT*, *pH* and *DO*, water temperature, pH and dissolved oxygen at 0.5 m depth; *Transp*, transparency; *PT*, precipitation

addition, each Si concentration was significantly related to SS, inorganic content of SS, and transparency. These correlations indicate that the Si increases were related to sediment resuspension. In fact, the increase in LSi appears to be directly caused by it. In contrast, DSi, BSi, and LSi were insignificantly correlated with chlorophyll *a*, water temperature, DO, and precipitation.

3.4 Discussion

3.4.1 Potential causes of the silicon increase around the center of Lake Kasumigaura

3.4.1.1 Watershed

Contrary to the detected trends around the center of the lake, DSi_{ICP} concentrations near the inflowing rivers did not increase, suggesting that the loads from the inflowing rivers had not increased. DSi loads through rivers were compared between different two years (**Table 3.3**). In 1994, the average (min.–max.) of annual mean DSi_{ICP} concentration of the 10 NIES-monitored inflowing rivers was 12.7 (9.9–15.6) mg l^{-1}, with that of the 3 "overlapping" rivers (i.e., the Sakura, Ono, and Seimei Rivers) being 12.2 (10.6–13.3) mg l^{-1}. In 2007, the average (min.–max.) of annual mean DSi_{col} concentrations of the 5 KRO-monitored rivers was 9.4 (7.8–10.9) mg l^{-1}, with the 3 "overlapping" rivers being 8.8 (7.8–9.8) mg l^{-1}. In addition, the investigation showed that the ratio of DSi_{col} to DSi_{ICP} concentration was 0.98 (r^2 = 1.00). These results suggest that DSi concentrations of inflowing rivers did not increase but rather decreased. The discharge of inflowing

Table 3.3 Mean DSi concentrations at 15 rivers inflowing Lake Kasumigaura in 1994, 2007, and 2008–2009. Standard deviations were noted in parentheses. There was no rainfall for 3 days before almost all samplings

Rivers	DSi_{ICP} (mg l^{-1})	DSi_{col} (mg l^{-1})	DSi_{ICP} (mg l^{-1})	DSi_{col} (mg l^{-1})
	in 1994 (N = 4)	in 2007 (N = 11)	in 2008 and 2009 (N = 2～3)	
Amano	11.4 (3.5)	-	-	-
Hanamuro	13.7 (3.2)	-	14.9 (1.2)	15.2 (0.9)
Hishiki	-	-	11.6 (1.1)	11.9 (0.6)
Hokota	-	10.9 (1.5)	14.6 (0.9)	14.9 (0.4)
Ichinose	-	-	11.3 (0.6)	11.6 (0.2)
Kajinashi	-	-	12.8 (1.5)	12.9 (1.1)
Koise	9.9 (3.2)	-	11.6 (0.9)	12.0 (0.5)
Ono	12.6 (2.6)	8.8 (1.2)	12.0 (0.7)	12.2 (0.4)
Sakura	10.6 (2.6)	7.8 (1.3)	12.0 (0.7)	12.2 (0.4)
Sannou	15.2 (2.6)	-	-	-
Seimei	13.3 (4.5)	9.8 (3.0)	13.4 (1.3)	13.7 (0.8)
Shin	15.6 (4.9)	-	17.4 (1.5)	17.9 (0.7)
Sonobe	12.2 (4.0)	-	12.7 (1.0)	13.2 (0.6)
Takahashi	12.4 (3.1)	-	-	-
Tomoe	-	9.6 (1.6)	13.2 (1.3)	13.4 (0.8)
3 riveres average[a]	12.2 (3.2)	8.8 (2.1)	12.5 (1.2)	12.7 (1.0)
All riveres average	12.7 (3.5)	9.4 (2.0)	13.1 (1.9)	13.4 (1.7)

[a] Sakura, Ono, and Seimei River

rivers also did not increase; therefore, DSi loads through the rivers could not have caused the increase in DSi concentrations in the lake.

3.4.1.2 In-lake processes

Changes in the rate of DSi uptake by diatoms might cause the observed changes in Si concentrations. However, no decrease in volume concentrations of diatoms at C1 was detected. Bailey-Watts (1976a) and Sicko-Goad et al. (1984) suggested that the BSi contents in freshwater diatom cells are almost in the same order among species. These considerations suggest that the diatom production could not have caused the increasing trend.

BSi dissolution is one of the important process in several lakes (e.g., Bailey-Watts 1976b). For living diatoms, frustules are protected from dissolution by an organic coating (Lewin 1962; Kristiansen and Hoell, 2002), which are degraded by bacterial activity (Bidle and Azam 1999). Some diatoms also secrete macromolecules which have been suggested to protect against dissolution (Hoagland et al. 1993). In many studies, primary source of DSi release was frustules of dead diatoms accumulated in bottom sediments. DSi release rates from lake sediments were enhanced by increases in water temperature and pH (Rippey 1983; Loucaides et al. 2008). In Lake Kasumigaura, however, the annual average water temperature and pH have not significantly increased during the last three decades. On the other hand, the turbidity increase due to sediment resuspension observed in the lake from the late 1990s caused the increase in LSi concentration, and might provide the opportunity for increases in DSi concentration through regeneration of Si. DSi of sediment pore water might also be released with

resuspension. However, surface sediments less than 2 cm depth were affected by sediment resuspension (Seki et al. 2006), and DSi concentrations of those pore water were considered to be not so different from those in the water column; therefore, the DSi release from pore water might be neglected. Fukushima et al. (2005) roughly discussed the causes for the increased resuspension like the changes in meteorological condition, physical properties of sediments, benthic ecosystem, aquatic plants, and geomorphologic conditions. The plausible causes were suggested such as the changes in the organic content and water content of the sediments perhaps resulted from the recovery of the lake from hyper-eutrophicated condition and/or the transition from blackish water to freshwater; however, the authors indicated that the further investigation was needed.

3.5 Conclusions

Significant increases in Si concentrations were observed at the center of the lake over the last three decades. Dissolved and lithogenic Si accounted for 44% and 45% of the increase in total Si concentration of 6.2 mg l^{-1} from the 1980s to 2000s, respectively, and that biogenic Si, consisting of diatom frustules, also increased with them. DSi concentrations did not increase near the mouth of the inflowing rivers, suggesting that the DSi increase was caused by in-lake processes. We assumed the contribution of release from SS derived from sediments, which had increased in the lake from the late 1990s to mid 2000s, to be the cause of this DSi increase.

The final publication is available at www.springerlink.com.

Chapter 4

Silicon release from suspended solids and bottom sediments in a shallow eutrophic lake

4.1 Introduction

As a result of statistical analysis, DSi release from resuspended seiment was suspected as a major factor of DSi increase observed at the center of the lake. In fact, several studies indicated that, as a consequence of diatom sedimentation, Si was released back to the water column (Rippey 1983; Schelske et al. 1988; Szczepocka and Szulc 2006). The importance of Si cycling within a lake was indicated in several studies (Bailey-Watts 1976b; Cornwell and Banahan 1992; Gibson et al. 2000; Miretzky and Cirelli 2004); however, previous studies focused on DSi release from bottom sediments, but not on release from SS derived from sediments. Sediment resuspension tends to occur in shallow lakes by relatively strong wind. Those lakes are often used by human activities and consequently eutrophicated; therefore, it is important to assess the DSi

release from SS in such lakes.

The objectives of the present chapter are twofold: (1) to estimate the DSi release rates from SS and bottom sediments by laboratory experiments, and (2) to assess the contribution of DSi release to the increasing trend of DSi observed in the lake.

4.2 Materials and methods

4.2.1 Sampling

We sampled the surface sediments with an Ekman-Birge type bottom sampler at the center of the lake (C1) in August 2008 and June and October 2009 (**Figure 4.1**). Sediments at A3 and B3 were also sampled in August 2008. Lake waters were collected at A3, B3, C1, and C3 in August 2008, at B0 (located at Tsuchiura-Port) in November 2008, and at C1 in June and October 2009. Lake waters were filtered through 0.45-μm membrane filters. Filtrates and sediments were stored at 1°C under dark conditions before the incubation experiments. BSi contents of sediments were determined by colorimetric method after wet alkaline digestion according to DeMaster (1981).

4.2.2 Experiment design

4.2.2.1 Silicon release experiments from suspended solids

DSi release rates from SS were assessed in the laboratory (**Table 4.1A**). The sediments were mixed with lake water or distilled water at various SS concentrations (about 50–

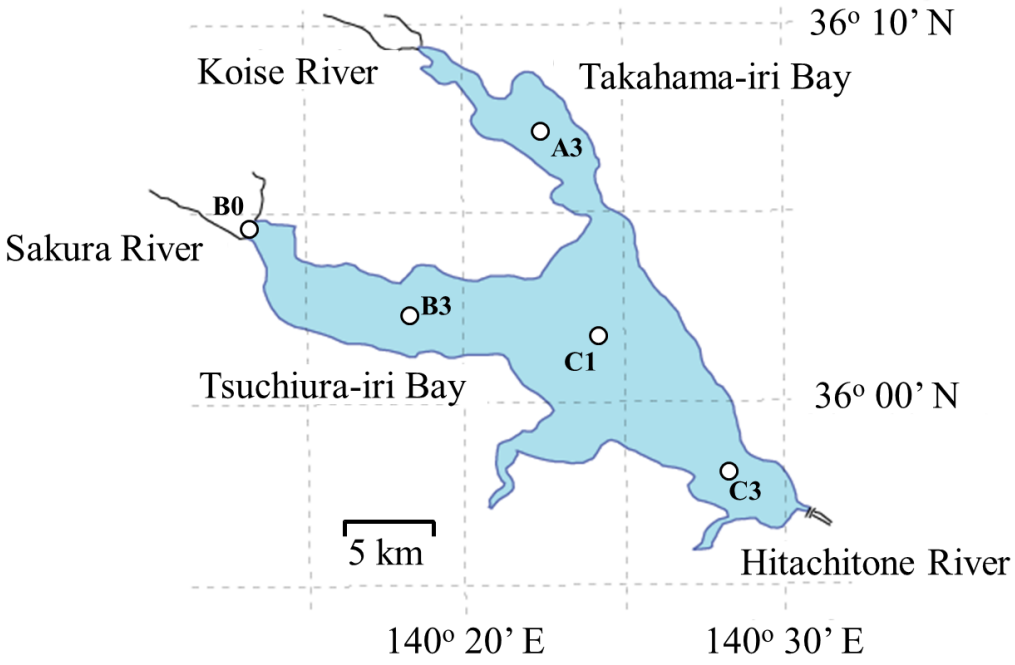

Figure 4.1 Sampling points in Lake Kasumigaura

Table 4.1 Summary of experimental design and results of DSi release experiments from SS (**A**) and bottom sediments (**B**)

(A) From suspended solids

Label	Sediment	SS conc.	Water			Sampling day	DSi_{col} (mg l^{-1})				Si release rate (mg g^{-1} day^{-1})		
	Site	(mg l^{-1})	Type[d]	Site	Temp.		Day 0	Day 1	Day 7 (or 8)	Day 28 (or 32)	Days 0–1	Days 1–7 (or 8)	Days 7 (or 8)–28 (or 32)
S1-1	A3[a]	500	DW		25°C	Day 0, 0.5, 1, 3, 8, 16, 32	0.11	0.43	0.81	1.59	0.64	0.11	0.06
S1-2	B3[a]	500	DW		25°C		0.06	0.38	0.84	1.55	0.63	0.13	0.06
S1-3	C1[a]	500	DW		25°C		0.09	0.35	0.80	1.47	0.53	0.13	0.06
S2-1	C1[b]	59	DW		25°C	Day 0, 1, 2, 3, 5, 7, 14, 21, 28	0.01	0.05	0.11	0.15	0.61	0.16	0.03
S2-2	C1[b]	100	DW		25°C		0.02	0.08	0.16	0.25	0.61	0.13	0.04
S2-3	C1[b]	210	DW		25°C		0.03	0.16	0.32	0.50	0.61	0.13	0.04
S2-4	C1[b]	360	DW		25°C		0.05	0.25	0.52	0.84	0.56	0.12	0.04
S3-1	C1[b]	56	LW	C1[b]	25°C	Day 0, 1, 2, 3, 5, 7, 14, 21, 28	0.12	0.18	0.30	0.63	1.07	0.34	0.28
S3-2	C1[b]	120	LW	C1[b]	25°C		0.14	0.26	0.48	1.09	1.01	0.32	0.24
S3-3	C1[b]	190	LW	C1[b]	25°C		0.14	0.40	0.66	1.58	1.37	0.23	0.23
S3-4	C1[b]	340	LW	C1[b]	25°C		0.19	0.51	1.05	2.47	0.95	0.27	0.20
S4-1	C1[c]	260	DW		1°C	Day 0, 1, 2, 3, 5, 7, 14, 21, 28	0.03	0.07	0.12	0.21	0.15	0.03	0.02
S4-2	C1[c]	240	DW		15°C		0.03	0.11	0.21	0.35	0.34	0.07	0.03
S4-3	C1[c]	240	DW		25°C		0.03	0.17	0.34	0.64	0.58	0.12	0.06
S5-1	C1[a]	530	LW	B0[g]	25°C	Day 0, 0.5, 1, 2, 4, 8, 16, 32	11.40	11.21	11.53	12.87	-0.36	0.09	0.11
S5-2	C1[a]	1600	LW[e]		25°C	Day 0, 1	4.71	5.08	-	-	0.23	-	-
S5-3	C1[a]	820	LW[f]		25°C		6.01	6.09	-	-	0.10	-	-
S5-4	C1[c]	230	LW	C1[c]	25°C	Day 0, 1, 2, 3, 7, 14, 21, 28	4.26	4.24	4.49	5.25	-0.09	0.18	0.16

(B) From bottom sediments

Label	Sediment		Water			Sampling day	DSi_{col} (mg l^{-1})				Si release rate (g m^{-2} day^{-1})		
	Site	Thickness	Volume	Site	Temp.		Day 0	Day 7	Day 14	Day 28	Days 0–7	Days 7–14	Days 14–28
B1-1	C1[b]	3.3 cm	750 ml	DW[d]	25°C	Day 0, 7, 14, 21, 28, 35, 42	0.5	6.9	11.6	15.9	0.089	0.064	0.030
B1-2	C1[b]	6.6 cm	500 ml	DW[d]	25°C		0.8	10.1	14.1	17.8	0.090	0.038	0.017
B1-3	C1[b]	9.9 cm	250 ml	DW[d]	25°C		1.6	16.6	17.7	19.5	0.070	0.005	0.004
B2-1	C1[b]	3.3 cm	750 ml	C1[b]	25°C	Day 0, 7, 14, 21, 28, 35, 42	0.5	6.9	9.9	14.2	0.099	0.047	0.033
B2-2	C1[b]	6.6 cm	500 ml	C1[b]	25°C		0.8	9.5	13.3	16.9	0.081	0.035	0.017
B2-3	C1[b]	9.9 cm	250 ml	C1[b]	25°C		1.6	17.4	18.1	19.2	0.074	0.003	0.003
							Day 0	Day 8	Day 104	Day 110	Days 0–8	Days 8–15	Days 104–110
B3-1	C1[c]	2 cm	700 ml	C1[c]	1°C	Day 0, 2, 4, 6, 8, 10, 15, 20, 25, 30, 44, 60 (, 90, 92, 99, 104, 106, 110, 200)	5.2	6.4	11.1	11.2	0.014	0.013	0.001
B3-2	C1[c]	4 cm	700 ml	C1[c]	1°C		4.3	6.6	0.6[h]	1.7[h]	0.026	0.016	0.018[h]
B3-3	C1[c]	2 cm	700 ml	C1[c]	15°C		4.8	9.3	-	-	0.051	0.024	-
B3-4	C1[c]	4 cm	700 ml	C1[c]	15°C		4.5	9.1	-	-	0.052	0.023	-
B3-5	C1[c]	2 cm	700 ml	C1[c]	25°C		4.6	12.4	0.6[h]	7.2[h]	0.086	0.038	0.099[h]
B3-6	C1[c]	4 cm	700 ml	C1[c]	25°C		4.9	12.2	0.6[h]	9.0[h]	0.083	0.041	0.127[h]
B3-7	C1[c]	6 cm	700 ml	C1[c]	25°C		5.0	12.4	25.2	25.4	0.082	0.036	0.002

[a] August 7th, 2008, [b] June 10th, 2009, [c] October 7th, 2009, [d] DW and LW indicate distilled water and lake water, respectively, [e] Mixture of lake waters sampled at A3, B3, C1, and C3 on August 7th, 2008, [f] Mixture of lake waters sampled at A3 on August 7th and at B0 on November 13th, 2008, [g] November 13th, 2008, [h] After replacing the overlying water by distilled water

500 mg l^{-1}) in a polycarbonate bottle (500 ml or 1 l) and stirred continuously by magnetic stirrer under dark conditions at room temperature (25°C). Two additional water temperature conditions, 1 and 15°C, were used, for which the samples were not stirred continuously but mixed once a day by hand. Aliquots of 3–10 ml were taken from the bottles at the beginning of the experiment, every day or every second day in the first week, and then every other week. pH, EC, and DO were measured to be 8.0–8.3, 290–330 μS cm^{-1}, and 5–8 mg l^{-1}, respectively, for the experiments using lake waters.

4.2.2.2 Silicon release experiments from bottom sediments

DSi release rates from bottom sediments were also assessed in the laboratory (**Table 4.1B**). Distilled or lake water was added to the sediments gradually in polyethylene bottles under dark conditions. In the series of experiments on B1 and B2, three sediment-water volume ratios were used at 25°C. In the series of experiments on B3, various sediment thicknesses and three water temperature conditions (1, 15, and 25°C) were used. Aliquots of 3–10 ml were taken from the bottles at the beginning of the experiment, every 2–7 days in the first month, and several times later. Before sampling, the water was stirred softly. In the experiments B3-2, -5, and -6, almost all of the water was siphoned, and the same volumes of new distilled water were replaced at Days 90 and 104. pH, EC, and DO were measured to be 6.7–7.8, 290–410 μS cm^{-1}, and 1–8 mg l^{-1}, respectively, for the experiments using lake water.

4.2.3 Analysis

All aliquots were filtered through 0.45-μm membrane filters and kept at 1°C, under dark conditions. DSi concentrations were determined by silicomolybdate yellow or blue colorimetric method. In the DSi release experiments from SS, the rate of change in DSi concentration was divided by SS concentration to estimate DSi release rate from SS as **Table 4.1A**, calculated in mg g^{-1} day^{-1}. Meanwhile, in the DSi release experiments from bottom sediments, the rate of change in DSi concentration was divided by the cross-sectional area to estimate DSi release rate from bottom sediments as **Table 4.1B**, calculated in g m^{-2} day^{-1}.

For checking the budget in the system, aliquots of 30 ml were taken at the start and end of experiments S4-3 and S5-4, respectively. Aliquots of 20 ml were filtered through 0.45-μm membrane filters for analyzing BSi by the method according to DeMaster (1981). Aliquots of 10 ml were used for analyzing TSi by silicomolybdate yellow colorimetric method after alkaline digestion according to JIS K 0101.

4.3 Results

4.3.1 Silicon release rates from suspended solids

The BSi contents of sediments sampled at A3, B3, and C1 in August 2008 and at C1 in June and October 2009 were 23, 29, 38, 40, and 43 mg g^{-1}, respectively. DSi release rates from the sediments sampled at A3 and B3 were within ± 20% of the rate at C1 (**Table 4.1**, S1). C1 is representative of the center area of the lake; therefore, we applied

the rates obtained at C1 to the whole lake. DSi_{col} concentrations were approximately proportional to SS concentrations at the same condition in the experiment S2 and S3 (r^2 = 0.90–1.00, **Figure 4.2**). This result means that DSi release rates from SS were independent of SS concentrations in this experiment. DSi release rates in lake water were higher than those in distilled water (**Figure 4.2**). Loucaides et al. (2008) suggested that such an enhancement of the DSi release rate was due to the catalytic effect of seawater cations, which may cause the difference in the rates in this study. In addition, DSi release rates strongly depended on water temperature (**Table 4.1**, S4).

Changes in DSi_{col} concentrations from Day 0 for various combinations of sediment and lake water are shown in **Figure 4.3**. Concentration changes could be largely divided into two parts, until and after Day 1. Until Day 1, DSi release rates were quite different among used lake waters. DSi_{col} concentrations increased in S3 using C1 lake water in June 2009 (1.10 ± 0.16 mg g^{-1} day^{-1}), remained almost constant in S5-4 using C1 lake water in October 2009 (–0.09 mg g^{-1} day^{-1}), and decreased in S5-1 using B0 lake water (–0.36 mg g^{-1} day^{-1}). On the other hand, after Day 1, DSi release rates were not so different among the waters, but gradually decreased with time. DSi release rates of S3 during Days 0–1, 1–7, and 7–28 were 1.10 ± 0.16, 0.29 ± 0.04, and 0.24 ± 0.03 mg g^{-1} day^{-1}, respectively. Loucaides et al. (2008) determined the DSi release rates from fresh diatom frustules and two diatomaceous lake sediments in freshwater at 25°C under stirred, flow-through conditions, which were 0.6, 0.9, and 1.6 mg g^{-1} day^{-1}, respectively. They used BSi-rich materials; therefore, the results in this study were lower than those values but of the same order.

TSi concentrations of S4-3 and S5-4 were not so different between the start and end of the experiment (± 10%, within the measurement error); therefore, the closed system

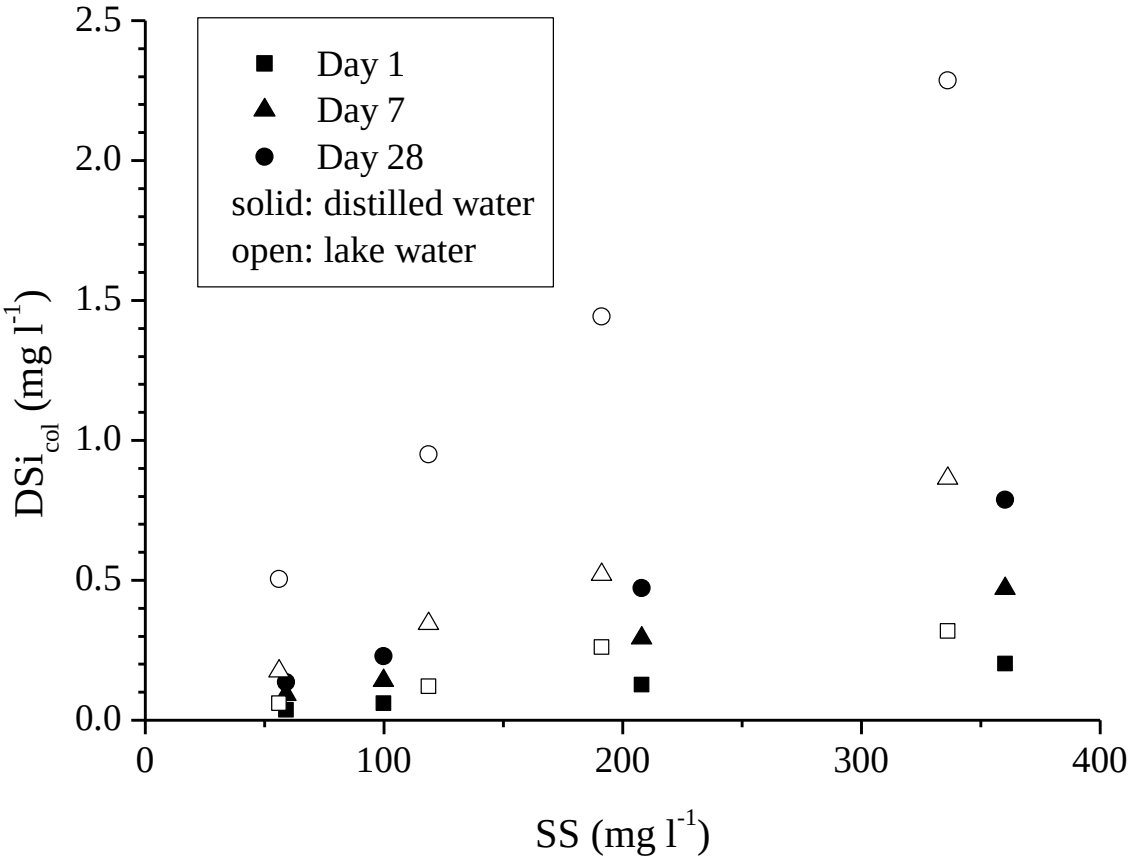

Figure 4.2 Relationship between SS concentrations and DSi_{col} concentrations using the sediments sampled at C1 in June 2009. Distilled water and lake water sampled at C1 in June 2009 were used. DSi_{col} concentrations at Day 0 were subtracted from those at each day. Details are shown in Table 4.1 (S2 and S3)

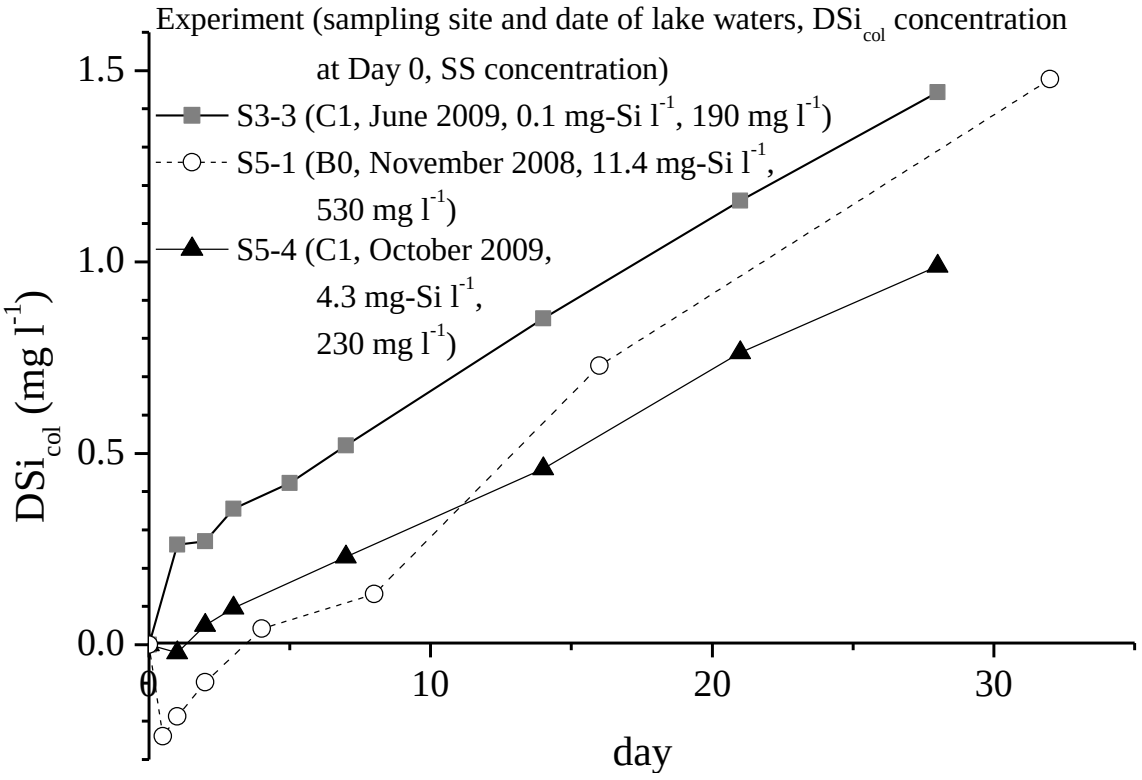

Figure 4.3 Changes in DSi_{col} concentrations released from SS. DSi_{col} concentrations at Day 0 were subtracted from those at each day. Details are shown in Table 4.1 (S3-3, S5-1, and S5-4)

was confirmed. The sum of DSi_{col} and BSi concentrations was nearly the same between them (± 8%; for example, DSi_{col} and BSi concentrations in the experiment S5-4 were 4.3 and 10.2 mg l^{-1} at Day 0 and 5.3 and 8.5 mg l^{-1} at Day 28, respectively), suggesting that the main source of DSi was BSi, mostly consisting of diatom frustules. In addition, DSi release rates from LSi are typically five orders of magnitude slower than those from BSi (Hurd 1983), and as such, we expected a negligible influence of LSi on DSi release. The estimated degradation ratios of BSi of S3 at Days 1, 7, and 28 were 2.7 ± 0.4, 7.1 ± 0.5, and 20.0 ± 2.0%, respectively. The ratios of S5-1 at Day 32 and S5-4 at Day 28 were 7.3% and 6.5%, respectively, and they were lower than those of S3. The variability may be affected by diatom frustules. Bailey-Watts (1976b) determined the degradation ratio of BSi using dead diatom frustules at 20°C under dark conditions, which were 17% after 38 days and 19% after 50 days, and my values at Day 28 were not far from those.

4.3.2 Silicon release rates from bottom sediments

DSi release rates from bottom sediments were not significantly different between distilled water and lake water (initial concentration was 0.1 mg-Si l^{-1}), indicating that the catalytic effect of cation was saturated by release from sediments in this experiment (**Table 4.1**, B1 and B2). The release rates were also independent of sediment thickness in the range of this experiment (**Table 4.1**, B3). On the other hand, they largely depended on water volume (B1 and B2) and temperature (B3). The rates during Days 0–8 at 1, 15, and 25°C were 0.020 ± 0.006, 0.051 ± 0.001, and 0.084 ± 0.002 g m^{-2} day^{-1}, respectively. Also, they gradually decreased with time (**Figure 4.4a**). In series B3, DSi release rates at 25°C during Days 0–8, 8–15, and 15–25 were 0.084 ± 0.002, 0.039 ±

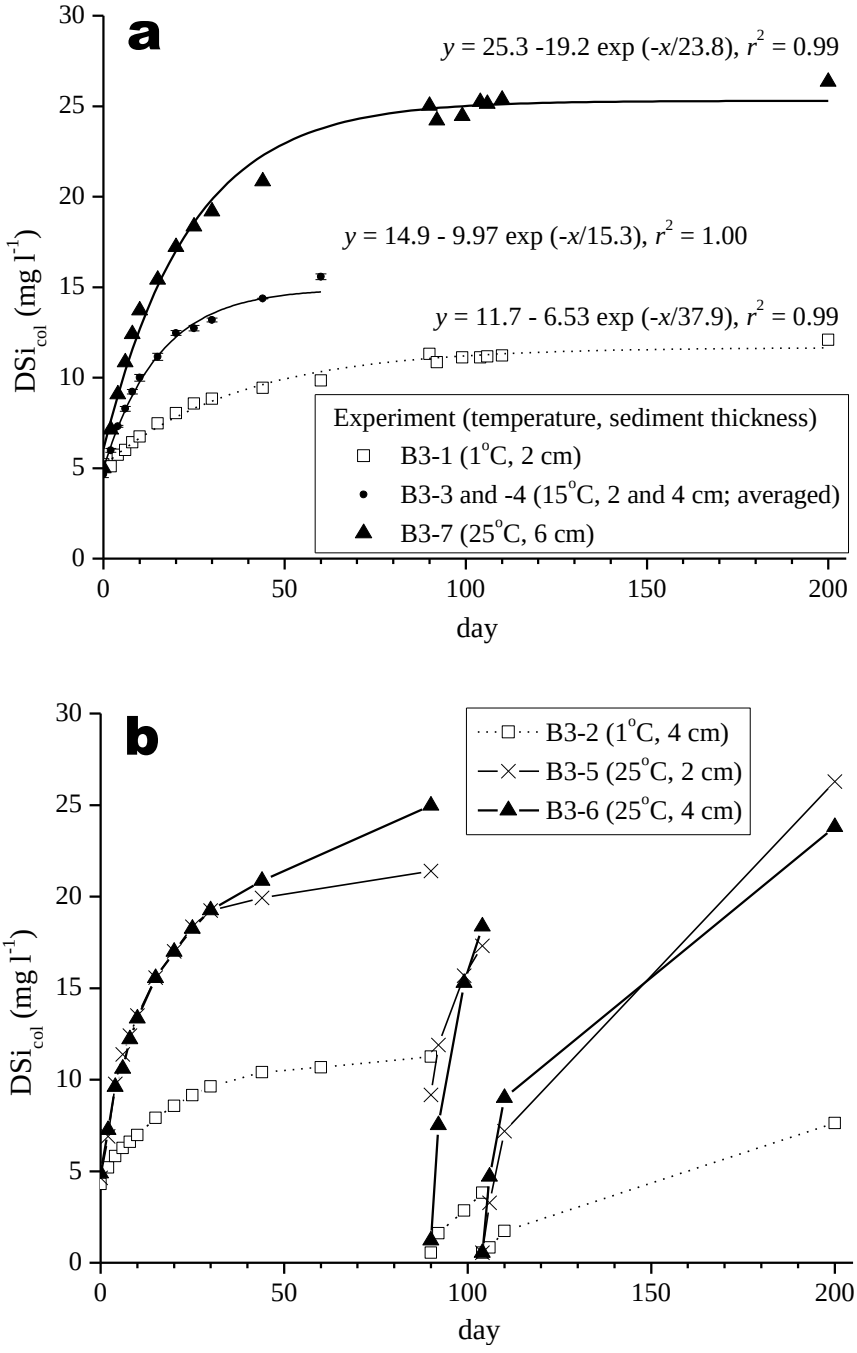

Figure 4.4 DSi_{col} concentrations in the series of the experiment B3 with no water replacement (**a**) and with replacing the overlying water by distilled water at Days 90 and 104 (**b**)

0.002, and 0.023 ± 0.001 g m^{-2} day^{-1}, respectively. DSi_{col} concentrations gradually reached constant values, depending on water temperature. After replacing the old water with distilled water in the experiments of B3-2, -5, and -6, DSi release rates were much enhanced (**Figure 4.4b**). This result suggests that the decrease in the rates with time was not caused by a change in sediment qualities, such as aging of diatom frustules, but caused by the change in overlying water qualities, such as DSi concentration. The variance of the rates among the three water volumes in the experiments of B1 and B2 also supports this consideration because the rates were independent of sediment thickness. Bailey-Watts (1976b) and Rippey (1983) measure DSi release rates in laboratory cores sampled at shallow eutrophic lakes (0.02–0.10 and 0.05–0.39 g m^{-2} day^{-1}, respectively), and my results in the first week were within those values.

4.4 Discussion

4.4.1 Factors influencing the silicon release rates from suspended solids

The experimental conditions were aerobic, as was the field condition; therefore, no anaerobic biodegradation of diatom frustules should have occurred. DSi uptake by diatoms (that might be alive in the sediments) can be neglected under dark conditions. Therefore, inorganic processes are the focus of the following discussion. Experimental results revealed that DSi release rates from SS depended mainly on water temperature and used lake waters whose DSi_{col} concentrations had a large variability (0.1–11.4 mg l^{-1}). The latter was observed only at the beginning of the experiment, but the rates were

nearly constant among lake waters after Day 1. Notably, the rate during Day 0–1 was negative in B0 lake water, whose DSi_{col} concentration was the highest. These results suggested that the DSi_{col} concentrations were not only affected by dissolution of diatom frustules, but also by the transport of adsorbed Si on SS. The dissolution of LSi can be neglected (Hurd 1983). From these considerations, the change in DSi_{col} concentration in the DSi release experiment from SS can be expressed as follows:

$$\frac{dC_{DSi}}{dt} = -\frac{d\alpha}{dt} SS - \frac{dC_{BSi}}{dt} \qquad (4.1)$$

where C_{DSi} is the DSi_{col} concentration (mg l^{-1}), t is the time (day), α is the Si adsorbed on the surface of SS (mg g^{-1}), SS is the suspended solids concentration derived from sediments (g l^{-1}), and C_{BSi} is the BSi concentration (mg l^{-1}). α can be described as following equation:

$$\alpha = \alpha' X \qquad (4.2)$$

where α' is the Si adsorbed on the carrier (mg mg^{-1}) and X is the carrier content of SS (mg g^{-1}). X was assumed to be constant in this experiment. Therefore, when the Si dissolved in water comes to equilibrium with the Si adsorbed on SS, α depends only on the surrounding DSi_{col} concentration and can be expressed as following formula:

$$\alpha = \gamma C_{DSi} \qquad (4.3)$$

where γ is a constant (l g^{-1}). Using Eq. 4.3, the change in the DSi concentration C_{DSi} can be determined by the following equation:

$$\frac{dC_{DSi}}{dt} = -\frac{1}{1+\gamma SS}\frac{dC_{BSi}}{dt} \qquad (4.4).$$

In the field, the adsorption equilibrium can be assumed. The constant γ and the change in BSi concentrations (dC_{BSi}/dt) are unknown and can be determined as described below.

Experimental results suggested that the Si dissolved in water and adsorbed on the surface of SS might not have been at equilibrium on Day 0, but had reached equilibrium by Day 1 at the latest. Therefore, we can assume that α was independent of C_{DSi} on Day 0 and dependent on it on Day 1 ($\alpha_1 = \gamma C_{DSi,1}$). Applying this assumption to Eq. 4.1, the following equation was obtained:

$$\frac{C_{DSi,1} - C_{DSi,0}}{SS} = -(\alpha_1 - \alpha_0) - \frac{C_{BSi,1} - C_{BSi,0}}{SS} = \alpha_0 - \frac{C_{BSi,1} - C_{BSi,0}}{SS} - \gamma C_{DSi,1} \qquad (4.5)$$

where the subscripts indicate the days since the experiment started. The values of α_0 are specific to the used sediments, and $C_{BSi,1} - C_{BSi,0}$ is subject to the Si dissolution rate of diatom frustules, which might be independent of C. Thus, the left part of Eq. 4.5 was linearly correlated with $C_{DSi,1}$; as a result, γ was determined through a regression analysis to be 0.12 by assuming that the α_0 and $C_{BSi,1} - C_{BSi,0}$ are not so different among the used sediments (**Figure 4.5**).

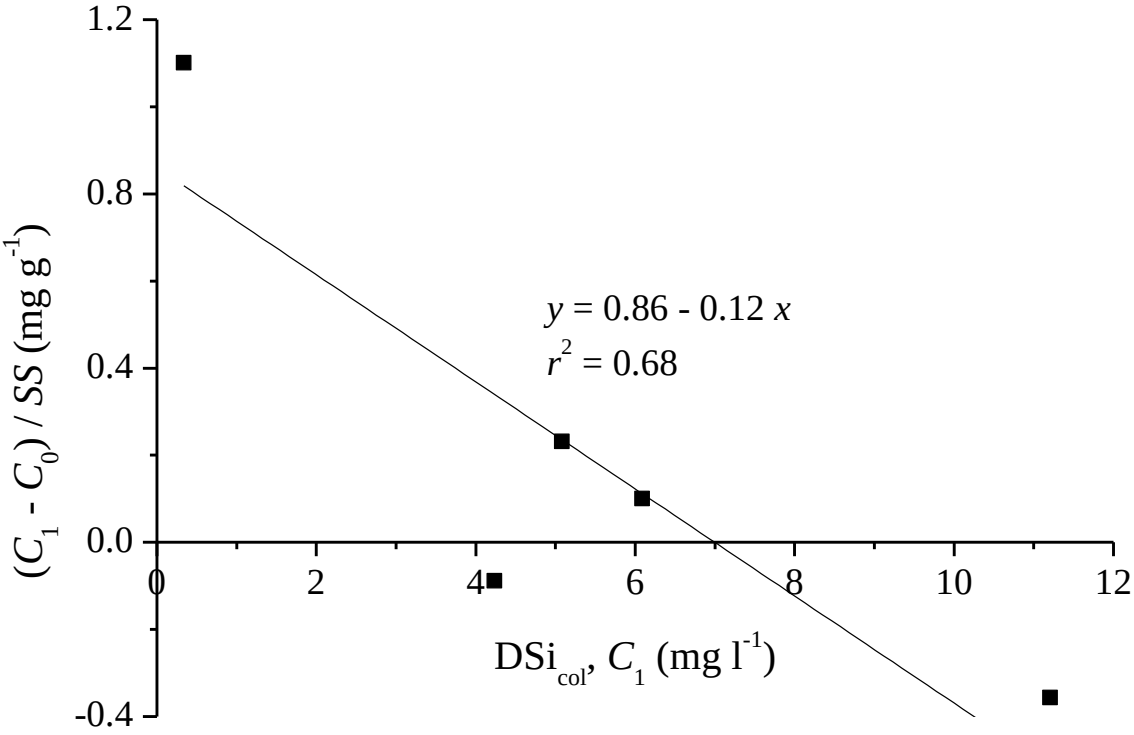

Figure 4.5 Relationship between DSi_{col} concentrations (C_1) and (C_1–C_0) / *SS* in the experiment S3 (averaged), S5-1, -2, -3, and -4

Figure 4.6 shows the changes in the Si dissolution rates, D (mg g^{-1} day^{-1}), calculated by the following equation derived from Eq. 4.4:

$$D = -\frac{1}{SS}\frac{dC_{BSi}}{dt} = \frac{1+\gamma SS}{SS}\frac{dC_{DSi}}{dt} \qquad (4.6).$$

The rates decreased exponentially, which suggests that the following reaction rate equations can be applied to the experimental results:

$$C_{BSi} = C_{BSi,0}e^{-kt} \qquad (4.7)$$

$$\frac{dC_{BSi}}{dt} = -kC_{BSi,0}e^{-kt} \qquad (4.8)$$

where k is the dissolution rate constant (day^{-1}) and the subscript indicates the initial value (t = 0). The rates decreased notably within about a first week, but were almost constant after that (**Figure 4.6**). It suggests the decrease in the BSi amount of comparatively fresh diatom frustules which is dissolved more rapidly than old diatom frustules due to alternations of the bulk structure and surface chemistry (Van Cappellen et al. 2002; Gendron-Badou et al. 2003). Now, we assumed that the BSi can be divided into two parts, contained in fresh and old diatom frustules with same temperature dependence of dissolution, and the dissolution rates of old ones were approximately constant on the time scale of this experiment. Defining β as the BSi content of SS (= C_{BSi}/SS, mg g^{-1}), the dissolution rate can be described as following equation:

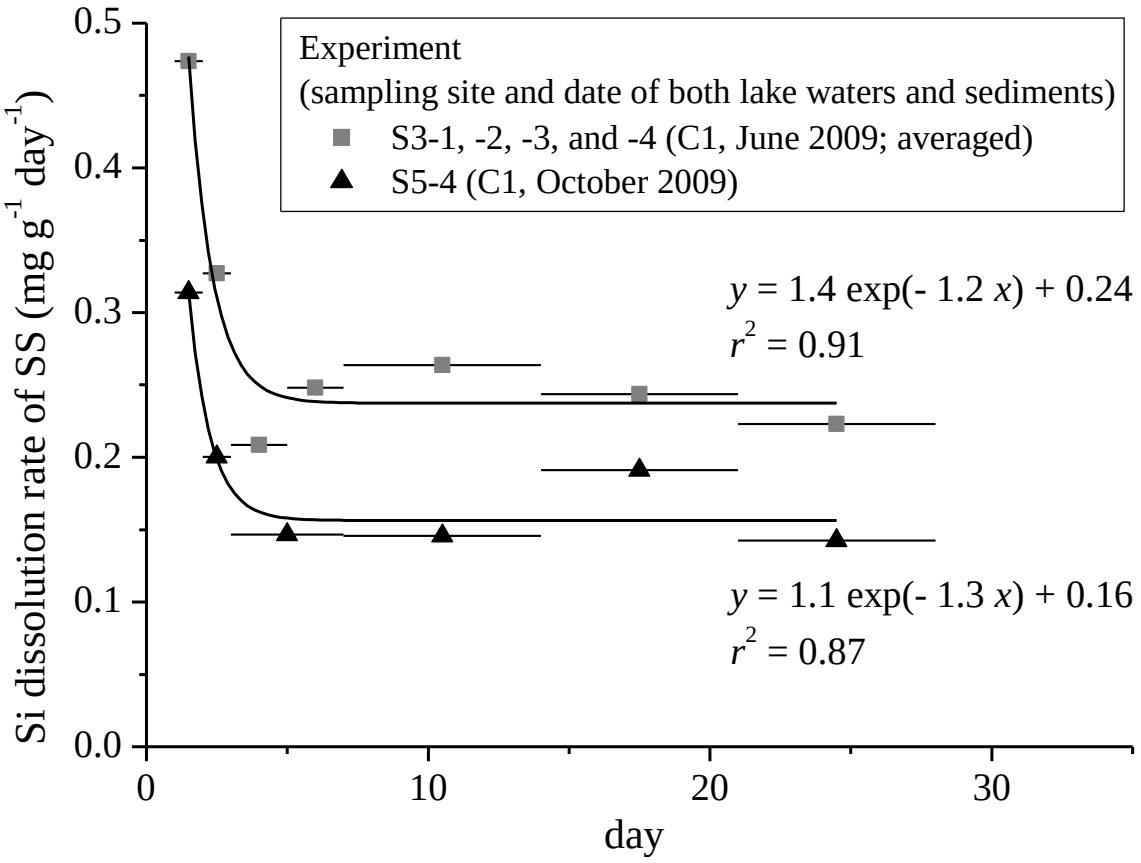

Figure 4.6 Change in Si dissolution rate of SS at 25°C in the experiment S3 (averaged) and S5-4

$$D = -\frac{\mathrm{d}\beta}{\mathrm{d}t} = k_{\mathrm{f}}\beta_{\mathrm{f}\,0}\mathrm{e}^{-k_{\mathrm{f}}t} + k_{\mathrm{o}}\beta_{\mathrm{o}\,0}\mathrm{e}^{-k_{\mathrm{o}}t} \approx k_{\mathrm{f}}\beta_{\mathrm{f}\,0}\mathrm{e}^{-k_{\mathrm{f}}t} + k_{\mathrm{o}}\beta_{\mathrm{o}\,0} \qquad (4.9)$$

where the subscripts f and o indicate the fresh and old diatom frustules, respectively ($\beta = \beta_{\mathrm{f}} + \beta_{\mathrm{o}}$, $k_{\mathrm{f}} > k_{\mathrm{o}}$). The equation could fit well to the experimental results (**Figure 4.6**). The initial BSi content, β_0 was 40 mg g^{-1} in the experiment S3 and 43 mg g^{-1} in the experiment S5-4; therefore, $\beta_{\mathrm{f}\,0}$, $\beta_{\mathrm{o}\ 0}$, k_{f}, and k_{o} were determined to be 1.2, 39, 1.2, and 6.2×10^{-3} in the experiment S3 and 0.8, 42, 1.3, and 3.8×10^{-3} in the experiment S5-4, respectively. It suggests that the dissolution rate constants, k_{f}, and k_{o}, were almost constant for the diatom frustules in the lake. In addition, the experimental period of about 30 days was sufficiently smaller than $1/k_{\mathrm{o}}$ of 160–260 days, suggesting that the assumption is reasonable. The mean values of k_{f} and k_{o} (1.3 and 5.0×10^{-3}, respectively) were used to the estimation for the field as described later. The dissolution rates also correlated positively with water temperature (**Figure 4.7**). Finally, the rates and the change in $\mathrm{DSi_{col}}$ concentration can be expressed as follows:

$$D = \left(k_{\mathrm{f}}\beta_{\mathrm{f}\,0}\mathrm{e}^{-k_{\mathrm{f}}t} + k_{\mathrm{o}}\beta_{\mathrm{o}\,0}\right)\mathrm{e}^{-\left(\frac{a}{T}-\frac{a}{\mathrm{T_a}}\right)} \qquad (4.10)$$

$$\frac{\mathrm{d}C_{\mathrm{DSi}}}{\mathrm{d}t} = \frac{SS}{1+\gamma SS}D = \frac{SS}{1+\gamma SS}\left(k_{\mathrm{f}}\beta_{\mathrm{f}\,0}\mathrm{e}^{-k_{\mathrm{f}}t} + k_{\mathrm{o}}\beta_{\mathrm{o}\,0}\right)\mathrm{e}^{-\left(\frac{a}{T}-\frac{a}{\mathrm{T_a}}\right)} \qquad (4.11)$$

where T is the water temperature (K), $\mathrm{T_a}$ is a constant (298.15 K), and a is a constant (K). The value of a was determined from the experiment of S4 to be $(4.1–4.4) \times 10^3$ (**Figure 4.7**). We applied the mean value of a of 4.2×10^3 to the estimation for the field

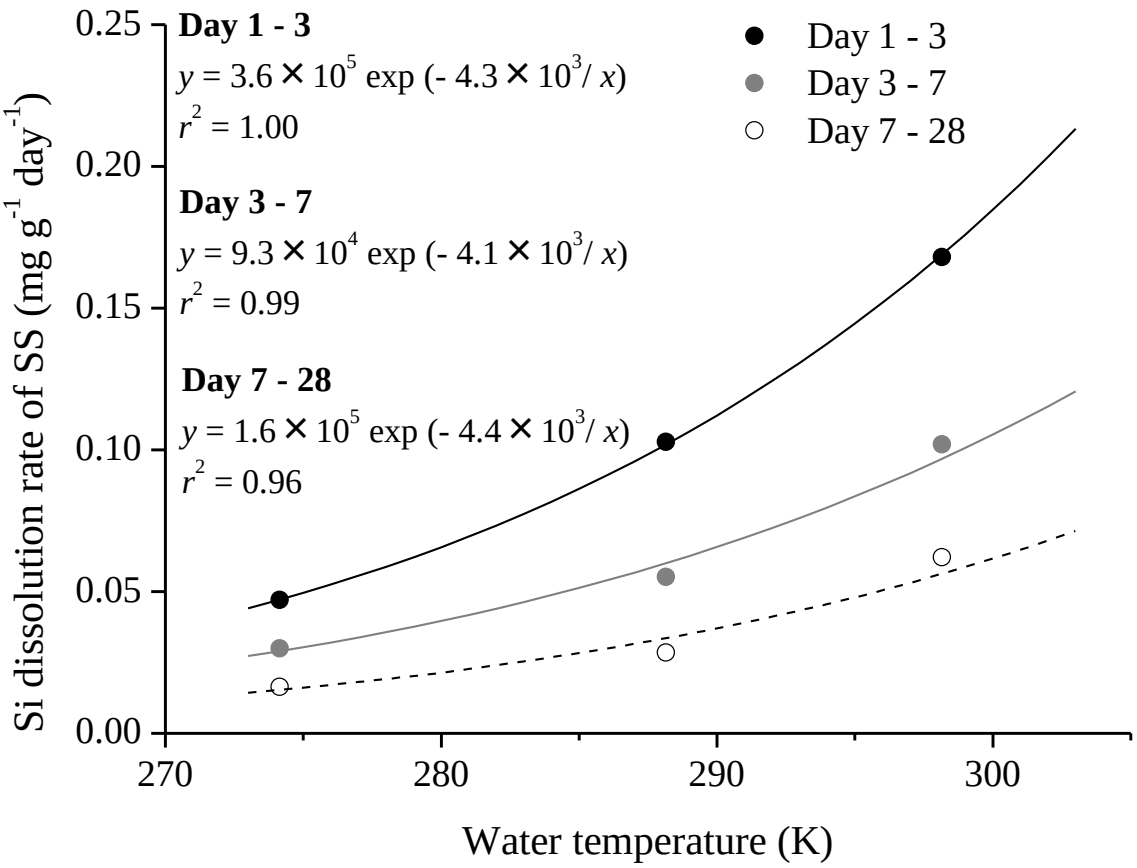

Figure 4.7 Relationship between water temperature and Si dissolution rate of SS in distilled water in the experiment S4

as described later.

4.4.2 Factors influencing the silicon release rates from bottom sediments

The results of DSi release experiment from bottom sediments fit well to the equation described in **Figure 4.4** (**a**). DSi_{col} concentrations reached constant values, which could be regarded as the equilibrium concentration, C_e. C_e was correlated with water temperature (11.7, 14.9, and 25.3 mg l^{-1} at 1, 15, and 25°C, respectively), and fit to the equation in **Figure 4.8** (r^2 = 0.86). Assuming that the concentration close to the surface of the sediments was equal to C_e, and that the concentration adequately far from the sediments was equal to the observed concentration (C_{DSi}), Si diffusion can be limited by the concentration difference, that is, the subtraction of C_{DSi} from C_e. **Figure 4.9** shows that the rates were linearly correlated with this difference, suggesting that the above assumptions could be applied to DSi release rates from bottom sediments, R_{bottom} (g m^{-2} day^{-1}) and the change in DSi concentration can be written as follows:

$$R_{bottom} = K(C_e - C_{DSi}) \quad (4.12)$$

$$\frac{dC_{DSi}}{dt} = \frac{R_{bottom}}{h} \quad (4.13)$$

where K is the rate constant (m day^{-1}) and h is the water depth (m). In this experiment, a temperature dependence of K was not clearly seen, but it was determined to be 4.9×10^{-3} (r^2 = 0.73, **Figure 4.9**). We applied this equation to the estimation for the field as

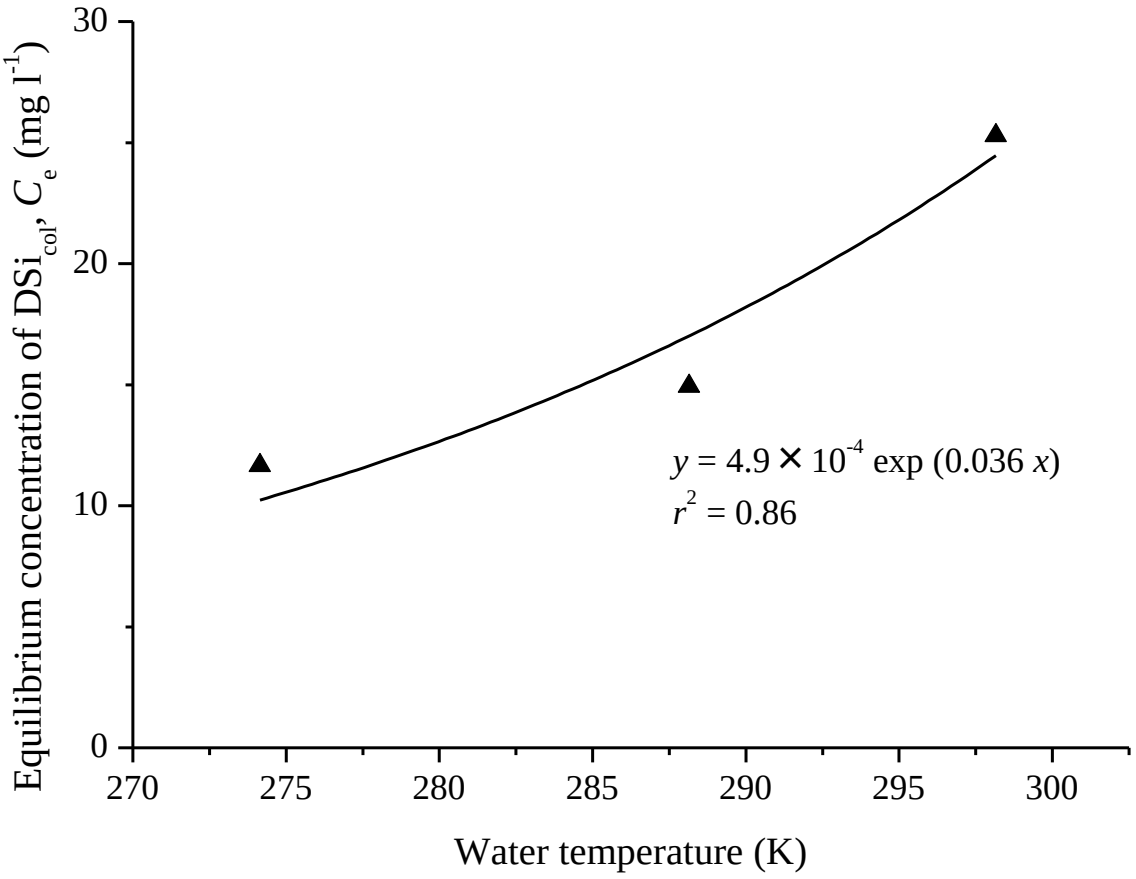

Figure 4.8 Relationship between water temperature and the equilibrium concentration of DSi_{col} (C_e) in the experiment B3

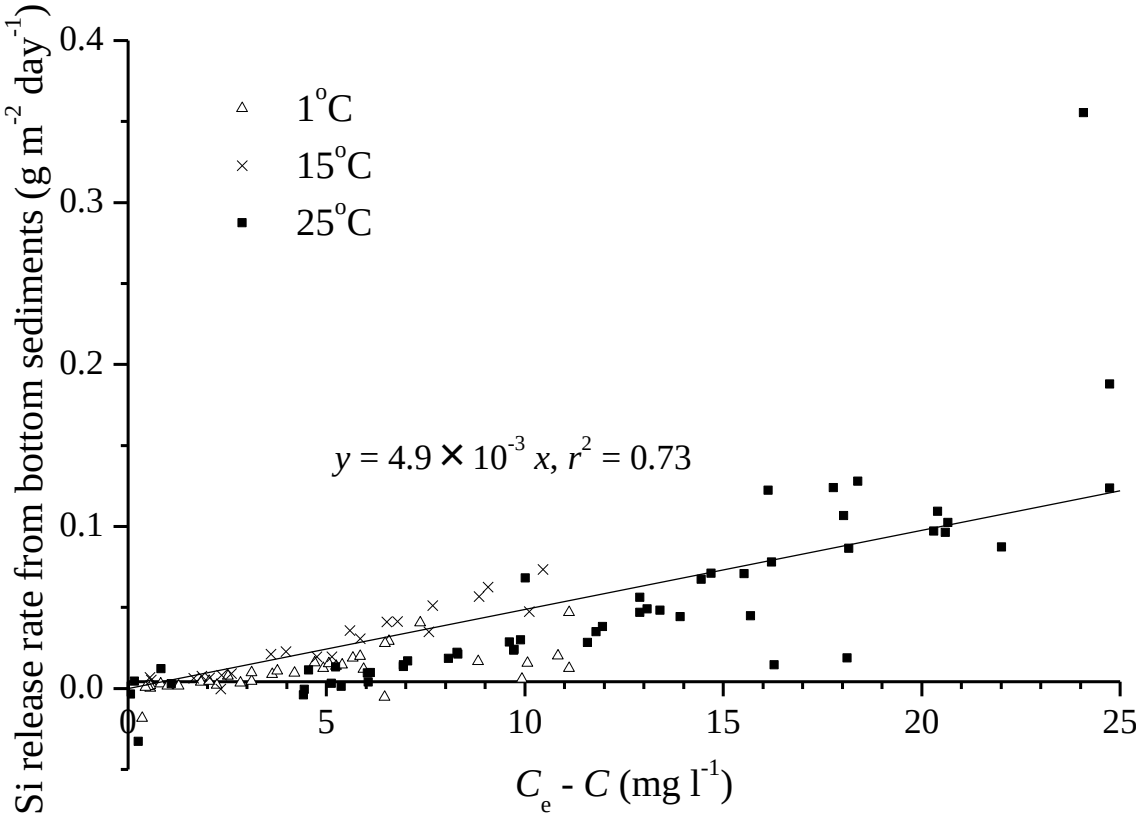

Figure 4.9 Relationship between the difference between DSi_{col} and equilibrium concentrations ($C_e - C_{DSi}$) and DSi release rate in the experiment B3

described later.

4.4.3 Estimation of silicon release rate in Lake Kasumigaura

The annual amount of DSi released from SS in Lake Kasumigaura in 2004 was estimated by assuming that: (1) the particle size distribution of SS in the entire lake is the same as that of this experiment, (2) X is constant, (3) the influence of variance in the concentrations of cations in lake water can be neglected, (4) SS concentrations contributing to the DSi release are subject to sediment resuspension driven by a critical wind, and (5) SS remaining constantly in the water column (mainly consisting of clay minerals; called as "background SS" in this study) does not affect the DSi release. Using Eq. 4.11, the amount of DSi released from SS can be estimated by following equation:

$$Y = V_{\mathrm{total}} \int \frac{\mathrm{d}C_{\mathrm{DSi}}}{\mathrm{d}t}\mathrm{d}t = V_{\mathrm{total}} \int \frac{SS}{1+\gamma SS}\left(k_{\mathrm{f}}\beta_{\mathrm{f}\,0}\mathrm{e}^{-k_{\mathrm{f}}\tau} + k_{\mathrm{o}}\beta_{\mathrm{o}\,0}\right)\mathrm{e}^{-\left(\frac{a}{T}-\frac{a}{\mathrm{T_a}}\right)}\mathrm{d}t \qquad (4.14)$$

where Y is the total amount of DSi released from SS in the entire lake (g y^{-1}), V_{total} is the water volume of the lake (6.6×10^8 m^3) and τ is the time (day). The hourly concentrations of SS derived from sediment resuspension at C1 in 2004 were simulated in the range of 10–299 mg l^{-1} by a numerical model with wind speed and sediment parameters such as the critical bottom shear stress (Seki et al. 2006). A minimum value of simulated concentrations could be regarded as "background SS". According to the assumption (2), the difference between simulated SS concentrations and background SS

concentrations was applied to *SS* in Eq. 4.14. In addition, the hourly water temperature at C1 measured by KRO was also used in Eq. 4.14. *Y* was estimated by two scenarios. The first scenario assumes that the initial BSi contents of SS were constant to be experimentally determined as the average of experiment S3 and S5-4, that is, $\beta_{f\,0} = 1.0$ and $\beta_{o\,0} = 40$. The time since the latest resuspension event (wind speed above 12 m s^{-1}) was applied to τ at each t in Eq. 4.14. This estimated value was regarded as a maximum one. The second scenario assumes that the dissolution of BSi is only of old diatom frustules, that is, $\beta_{f\,0} = 0$ and $\beta_{o\,0} = 40$. This estimated value was regarded as a minimum one. As a result, the minimum and maximum values of *Y* were 1.0×10^9 and 2.7×10^9 g y^{-1}, respectively.

The annual amount of DSi released from bottom sediments at C1 in 2004 was also estimated from Eqs. 4.12 and 4.13. DSi_{col} concentrations at C1 observed monthly by KRO were interpolated to hourly values and used in the estimation. As a result, the annual amount of DSi released from bottom sediments was estimated to be 4.3×10^9 g y^{-1}. These results suggest that the DSi released from SS accounted for about 20–40% of the total DSi amount released in the lake in 2004.

Recent DSi release rate from SS determined by the experiments in this chapter were compared with the observed increase in the DSi load through the outflow over the last three decades. The amount of DSi released from SS in 2004 was assumed to be representative of those in the 2000s. The amount of DSi released from SS in the 1980s was assumed to be zero because mean concentration of SS derived from sediment resuspension in the1980s was estimated to be 5.5 mg l^{-1} by the method of Seki et al. (2006), about half of the background SS concentration in 2004. The increases in DSi load from the 1980s to the 2000s were 3.0×10^9 g y^{-1}, based on the DSi concentration at

C1, the lake volume of 6.9×10^8 m^3, the mean water residence time of 200 days, and the mean annual precipitation of 1250 mm. The DSi release from SS could account for about 30–90% of the increases in DSi load through the outflow.

4.5 Conclusions

Laboratory experiments, suspending the sediments in filtered lake water, provided the formula of change in DSi concentration as a function of SS concentration, water temperature, and the elapsed time of dissolution of diatom frustules. The annual amount of DSi released from SS in the 2000s accounted for 30–90% of the increase in DSi load through outflow over the last three decades, as well as 20–40% of the total amount of DSi released in the lake. These findings suggest that the sediment resuspension might be the cause of the latest DSi increase.

The final publication is available at www.springerlink.com.

Chapter 5

Silicon budget in a shallow eutrophic lake

5.1 Introduction

In chapter 3, monitoring data could provide long-term trends of Si concentration in Lake Kasumigaura. To obtain the information on these historical changes, analyzing the vertical distribution of Si in sediments is also useful. In fact, BSi is commonly determined in lake sediments as an indicator of diatoms (Conley 1998).

Several paleolimnological studies have analyzed the stratigraphy of BSi in dated lake sediments to estimate long-term changes in the trophic condition (Schelske et al. 1986; Newberry and Schelske 1986; Schelske et al. 1987) and the BSi retention (Teodoru et al. 2006). Schelske et al. (1986) studied the eutrophication in the lower Great Lakes using the peaks in BSi contents and BSi:phosphorus ratios in the sediment cores from the lakes. Newberry and Schelske (1986) found that BSi contents in sediment stratigraphy corresponded to the trophic history of Little Round Lake, Ontario. The authors qualitatively indicated that the evaluation of siliceous microfossils, excluding diatoms,

and the dissolution of BSi should be considered to make a precise estimate of past diatom abundances. Teodoru et al. (2006) analyzed the sedimentary records of BSi to elucidate DSi retention in Iron Gate I Reservoir on the Danube River. The authors also compared the vertical profiles of sediment BSi with the long-term changes in DSi concentrations observed in the Black Sea coastal waters, suggesting that the construction of the Iron Gate I Reservoir was not solely responsible for decreasing the DSi loads downstream. Several researchers have also examined short sediment cores and measured water quality to calculate the annual DSi and BSi budgets from river inputs, outputs, BSi sedimentation and DSi release from sediments in lakes (Cornwell and Banahan 1992; Hoffman et al. 2002; Triplett et al. 2008). However, very few studies have assessed the long-term DSi and BSi budgets by both analyzing the sediment cores and monitoring water quality.

The purposes of this chapter are twofold: (1) to assess the DSi and BSi budgets in Lake Kasumigaura during the last three decades based on both the chronological sediment information, such as a vertical distribution of BSi content in the sediment cores, and the existing data of water quality, such as DSi concentrations and diatom abundances in the lake and DSi concentrations of the inflowing rivers, and (2) to discuss the Si cycling during the period, focusing on the recent DSi release from SS due to sediment resuspension, by comparing the historical changes of the gross sedimentation (using several diatom sinking rates), net sedimentation (by subtraction of river output from input) and apparent accumulation of BSi (based on the vertical profile of BSi in dated sediment cores). In Lake Kasumigaura, Si dynamics have been clearly changed during a last few decades; therefore, it might provide valuable findings to elucidate the long-term Si dynamics in shallow eutrophic lakes.

5.2 Materials and methods

5.2.1 Sampling of sediment cores and chemical analysis

5.2.1.1 Sampling

Multiple sediment cores were collected at the center of the lake (see **Figure 5.1**; site C) on 17 June 2005 (three cores), 19 June 2007 (two cores) and 14 July 2009 (two cores) by scuba divers using acrylic tubes of 10 cm in diameter and 100 cm long. Fukushima et al. (2010) indicated that the sedimentation process in the central basin is represented by the values obtained from the sediment taken from the center of the lake. Additional sediment cores were also collected at 2 other sites (see **Figure 5.1**; site A and B) on 19 June 2007. The sediment cores were sliced at intervals of 2 cm and those slices were composited. The water contents and apparent density were estimated from wet and dry weight (110°C, 12 hours). The mass sedimentation rates during the last 7 decades were estimated using the chronological information (such as the ^{137}Cs peak depth and the distribution of apparent density) of the sediment cores taken in 2005 and 2007, respectively. Details of dating and calculations can be found in Fukushima et al. (2010). In addition, the vertical distribution of apparent density of the cores taken in 2009 was used to calculate the mass sedimentation rate by the same method as Fukushima et al. (2010).

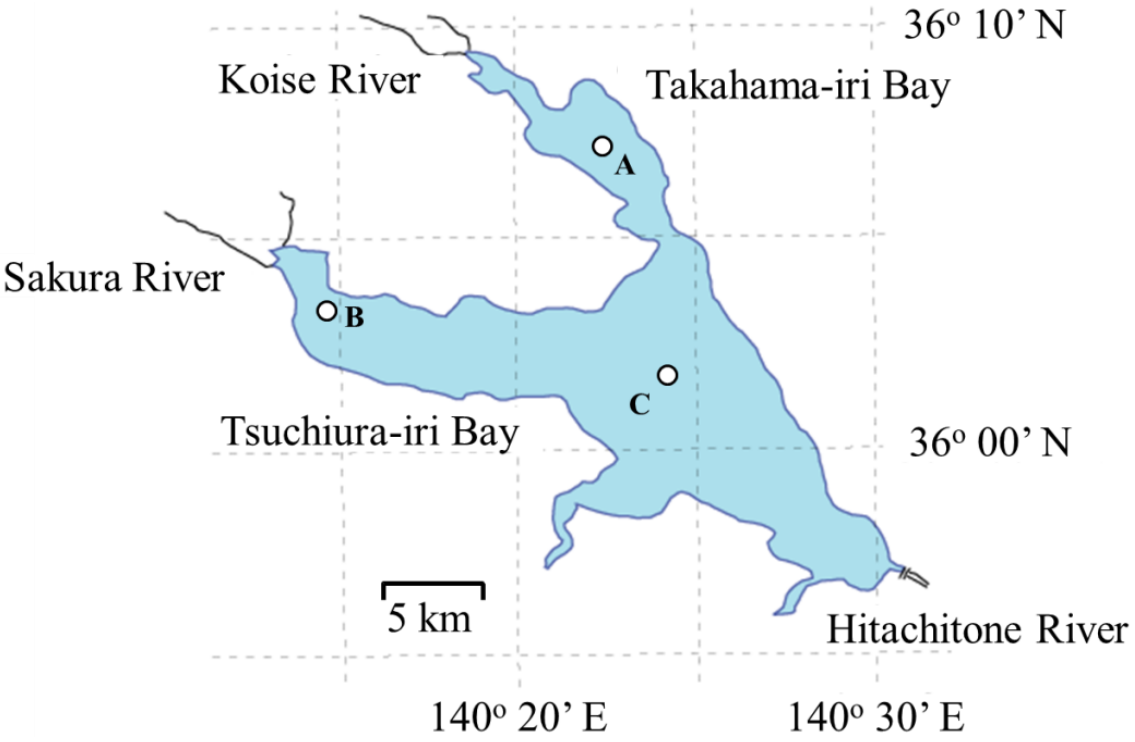

Figure 5.1 Sampling sites in Lake Kasumigaura

5.2.1.2 Chemical analysis

After freeze-drying the sediment samples, BSi was extracted for the samples taken in 2005 and 2007 by a single-step wet alkaline digestion (Mortlock and Froelich 1989). The sediments of 12–15 mg were digested in 60 ml of 1% Na_2CO_3 solution for 2 h at 85°C in an oven and the solutions were sub-sampled. These sub-samples were filtered through a 0.45-μm membrane filter. The concentrations of DSi were then analyzed by silicomolybdate blue colorimetric method JIS K 0101. However, this method has been reported to possibly overestimate BSi concentrations due to mineral dissolution; therefore, a time-step digestion (DeMaster 1981; Conley and Schelske 2001) was applied to the samples taken in 2009. Sediments of 13–19 mg were digested in 60 ml of 1% Na_2CO_3 solution for 5 h at 85°C in an oven and were sub-sampled after 3-, 4- and 5-h. These sub-samples were then filtered and analyzed following the same method as the 2005 and 2007 sub-samples. DSi concentrations at the 3-, 4- and 5-h were graphed to chart the progressive Si dissolution over time in order to correct for DSi contributed by mineral silicates. The precision of the method was 10%. The apparent accumulation rate of BSi, Z (g m^{-2} y^{-1}), was defined by the following equation:

$$Z = BSi \cdot S_{\mathrm{M}} \qquad (5.1)$$

where BSi is the BSi content in the sediments (g kg^{-1}) and S_{M} is the mass sedimentation rate (kg m^{-2} y^{-1}).

5.2.2 Budgetary calculation

5.2.2.1 Estimation of the inflows, outflow, and net sedimentation rate

Si in lake water is composed of dissolved and particulate one, and the latter consists of BSi and lithogenic Si (LSi). The dissolution of LSi is typically five orders of magnitude slower than that of BSi (Hurd 1983). Therefore, the Si budgets were calculated concentrating on DSi and BSi in the lake. The sum of DSi and BSi was expressed as (D + B) Si in this paper.

DSi concentrations and diatom abundances were observed by the Kasumigaura River office (KRO) and the National Institute for Environmental Studies (NIES), respectively, during April 1980 – March 2007. Surface waters were collected at site C and filtered through 0.45-μm glass-fiber to analyze DSi concentration by the colorimetric method (JIS K 0101). Diatom abundances were taken by a column-sampler (upper 2 m), counted on an inverted microscope, and quantified as biovolume by multiplying counted cell number by mean cell volume. BSi concentrations were estimated by multiplying the diatom abundances by the mean BSi content of freshwater diatom frustules of 1.1×10^5 g m^{-3}. The mean BSi content was determined by averaging the values found in Bailey-Watts (1976a) and Sicko-Goad et al. (1984).

Mass balances of (D + B) Si in the lake can be defined by the following equation:

$$I - O + (R - S)A = M \qquad (5.2)$$

where I is the (D + B) Si loads from the inflows (g y^{-1}), O is the (D + B) Si loads from

the outflow (g y^{-1}), R is the area-averaged DSi release rate (g m^{-2} y^{-1}), S is the area-averaged gross sedimentation rate of BSi (g m^{-2} y^{-1}), A is the lake area (m^2), and M is the rate of change in the (D + B) Si amounts in water (g y^{-1}). The DSi input through atmospheric precipitation was estimated using the annual mean precipitation and the DSi concentration of precipitation in Tsukuba, as averaged over 4 years by Hirata and Muraoka (1991). It was 2.2×10^7 g y^{-1}, two orders of magnitude lower than other fluxes; therefore, it could be neglected. The subtraction of R from S represents the area-averaged net sedimentation rate of BSi, N (g m^{-2} y^{-1}), calculated by the following equation:

$$N = S - R = (I - O - M)/A \qquad (5.3)$$

Inflows of BSi were not observed, but considered to be negligible. Temporal variation of DSi concentrations of the rivers depends mostly on the dilution by rainfall (Muraoka and Hirata 1988; Neal et al. 2005). Muraoka and Hirata (1988) measured the hydrochemistry of streams during four rainfall runoff events in the experimental forested area in the Lake Kasumigaura basin. The authors showed that the concentration of DSi decreased until the peak flow due to a dilution effect by the surface runoff water, whereas the concentration increased to approximately the same concentration around the end of the runoff period as the base flow level prior to the runoff event. Therefore, the maximum and minimum DSi loads through the inflows, I_{max} and I_{min}, respectively, were determined by the following equations:

$$I_{max} = DSi_{base} Q'_{total} \qquad (5.4)$$

$$I_{min} = [DSi_{base} q_{base}/q_{mean} + DSi_{rain}(1 - q_{base}/q_{mean})]Q'_{total} \qquad (5.5)$$

where DSi_{base} is the DSi concentration of the base flows which is the inflows when there was no rainfall (g m^{-3}), Q'_{total} is the annual total discharge of the inflows (m^3 y^{-1}), q_{base} is the daily discharge of the base flows (m^3 day^{-1}), q_{mean} is the annual mean daily discharge of the inflows (m^3 day^{-1}), and DSi_{rain} is the DSi concentration of rainwater (g m^{-3}). I_{min} was calculated by assuming the dilution effect at a maximum. DSi_{base} was determined to be 11.8 g m^{-3}, which is the mean DSi concentration of the 5–12 rivers inflowing the lake during 1994, 2007 and 2009 (details are shown in Chapter 3). There was no rainfall for 3 days before almost all samplings. Q'_{total} was estimated to be 1.0×10^9 m^3 y^{-1}, using the lake volume, the mean water residence time and the mean annual precipitation. q_{base} was estimated as the ordinary water discharge; that is, the daily discharge is not less than q_{base} for just 185 days during a year. q_{base} and q_{mean} were averaged among the main 5 rivers (Sakura, Koise, Sonobe, Ono and Seimei Rivers) inflowing the lake observed by KRO during the last decade, respectively. As a result, q_{base}/ q_{mean} was estimated to be 0.65. The DSi_{rain} value of 0.097 g m^{-3} was reported by Hirata and Muraoka (1991) as the observed value in the Lake Kasumigaura basin. Finally, I was estimated from these calculations to be $(0.8–1.2) \times 10^{10}$ g y^{-1}. The (D + B) Si loads through the outflow O were determined by multiplying (D + B) Si concentrations observed at site C by the annual discharge through the outflow (1.1×10^9 m^3 y^{-1}; estimated using the volume, water residence time and the mean annual evaporation of the lake). Assuming that the water quality at the center of the lake is representative of the whole lake, the changes in (D + B) Si concentrations at site C were used to calculate M.

5.2.2.2 Estimation of the gross sedimentation rate

The gross sedimentation rates of BSi were estimated by the following equation:

$$S = BSi_{w} \times c \times 365 \qquad (5.6)$$

where c is the diatom sinking rate (m day^{-1}) and BSi_{w} is the concentration of BSi in lake water (g m^{-3}). The diatom sinking rate is not constant but depends mostly on diatom species and their growing stages. Laboratory measurements in previous studies reported the diatom sinking rates in lake water to be 0.2–0.7 m day^{-1} (Bailey-Watts 1976b; Gibson 1984; Ferris and Lehman 2007). In this study, 0.2 and 0.7 m day^{-1} were used for the calculation as the minimum and maximum diatom sinking rate c, respectively.

5.3 Results

5.3.1 Spatial distributions of sediment BSi

Mean (min.–max.) concentrations of BSi in the dated sediments taken at site A, B and C in 2007 were 24 (19–30), 9 (6–11) and 32 (18–51) g kg^{-1}, respectively. The mass sedimentation rates at site A, B and C were estimated to be 1.5, 4.1 and 1.3 kg m^{-2} y^{-1}, respectively (Fukushima et al. 2010). Therefore, mean (min.–max.) apparent accumulation rates of BSi at site A, B and C were calculated to be 36 (29–45), 37 (25–45) and 42 (23–66) g m^{-2} y^{-1}, respectively. These rates were relatively consistent among the sites (**Figure 5.2**); therefore, the results obtained at site C were regarded as representative of the lake.

Mean (min.–max.) contents of BSi in the dated sediments taken at site C in 2005, 2007 and 2009 were 31 (22–40), 32 (18–51) and 40 (20–51) g kg^{-1}, respectively. Although the difference between these values was not large, the analytical method applied to the sediments taken in 2009 was more reliable than the others (Conley 1998);

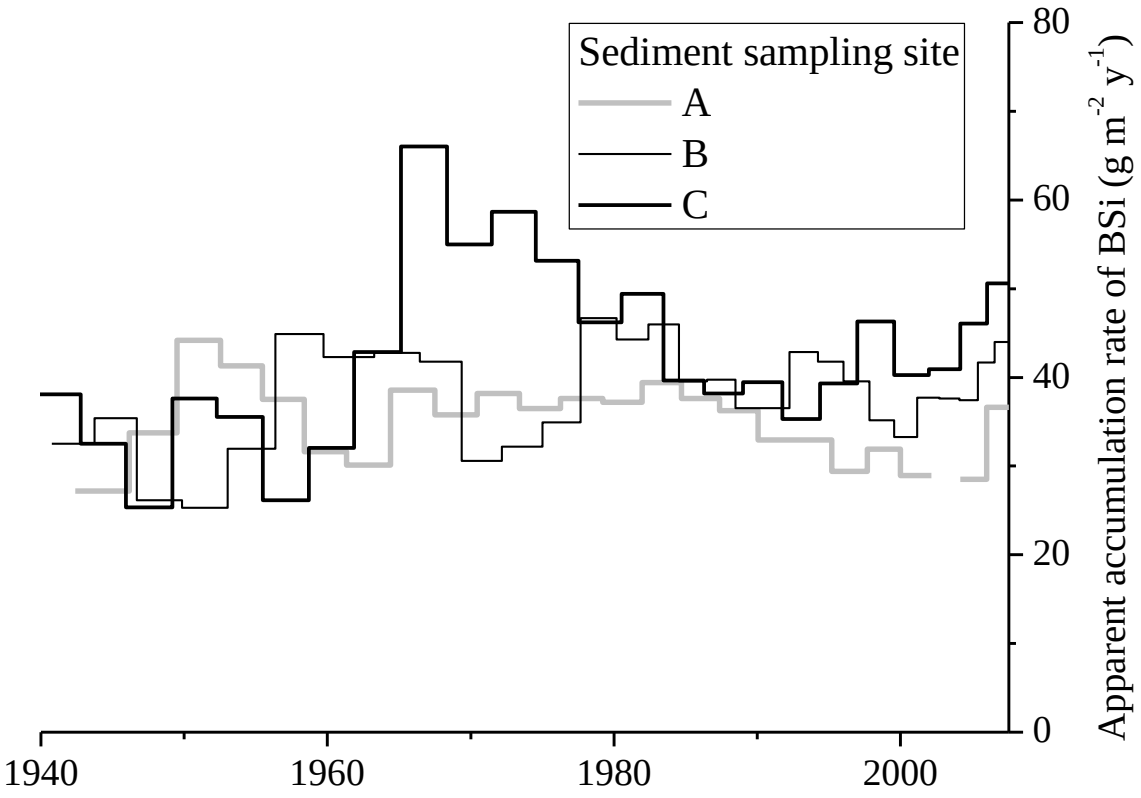

Figure 5.2 Historical plots of the apparent accumulation rate of BSi from the sediment cores taken in 2007

therefore, the contents of BSi in the sediments taken in 2009 were mainly used as described later.

5.3.2 (D + B) Si budgets over 27 years in Lake Kasumigaura

Table 5.1 shows the (D + B) Si budgets from 1980–2007 in Lake Kasumigaura. The DSi amount transported through the inflowing rivers for this 27-year time period was calculated to be (2.2–3.3) × 10^{11} g. The amounts of DSi and BSi transported through the outflow for this time period were calculated to be 0.7 × 10^{11} and 0.2 × 10^{11} g, respectively. Therefore, 60–70% of the DSi transported through the inflows was taken by diatoms and ultimately accumulated in the bottom sediments. The BSi amounts accumulated for the 27-year period in the lake were estimated to be (2.0–2.6) × 10^{11} g by analyzing the sediment cores taken in 2007 and 2009, which is slightly higher but close to the BSi amounts of (1.3–2.4) × 10^{11} g estimated by the budgetary calculation. The gross accumulated amount of BSi was estimated using Eq. 5.6 to be (2.3–8.0) × 10^{11} g, higher than the other results but of the same order of magnitude.

5.3.3 Long-term changes of net sedimentation, apparent accumulation and gross sedimentation rate of BSi

Figure 5.3 shows the changes in the net sedimentation, apparent accumulation and gross sedimentation rates of BSi in the lake. The net sedimentation rates of BSi were calculated by Eq. 5.3 to be a minimum of 6–39 g m^{-2} y^{-1} and a maximum of 31–65 g m^{-2} y^{-1} during 1980–2007, which were close to the apparent accumulation rates of BSi of 49–67 g m^{-2} y^{-1} estimated by the sediment analysis. Although a clear trend of the

Table 5.1 **(**D + B) Si budgets from 1980–2007 in Lake Kasumigaura. The rate of change in the (D + B) Si amounts in water column was not shown because those values were one order of magnitude smaller than other budgets in a decadal time scale.

(10^9 g y^{-1})	1980–2007	1980s	1990s	2000s
Input	8–12	8–12	8–12	8–12
Output	3.3	1.8	3.5	5.6
DSi	2.6	1.4	2.7	4.4
BSi	0.7	0.4	0.8	1.2
Net sedimentation	5–9	6–10	4–8	2–6
Apparent net sedimentation	10	10	10	10
Gross sedimentation	8–30	5–16	9–32	13–46
Release [a]				5.3–7.0
from bottom sediments				4.3
from SS				1.0–2.7

[a] estimated by the laboratory experiments in chapter 4

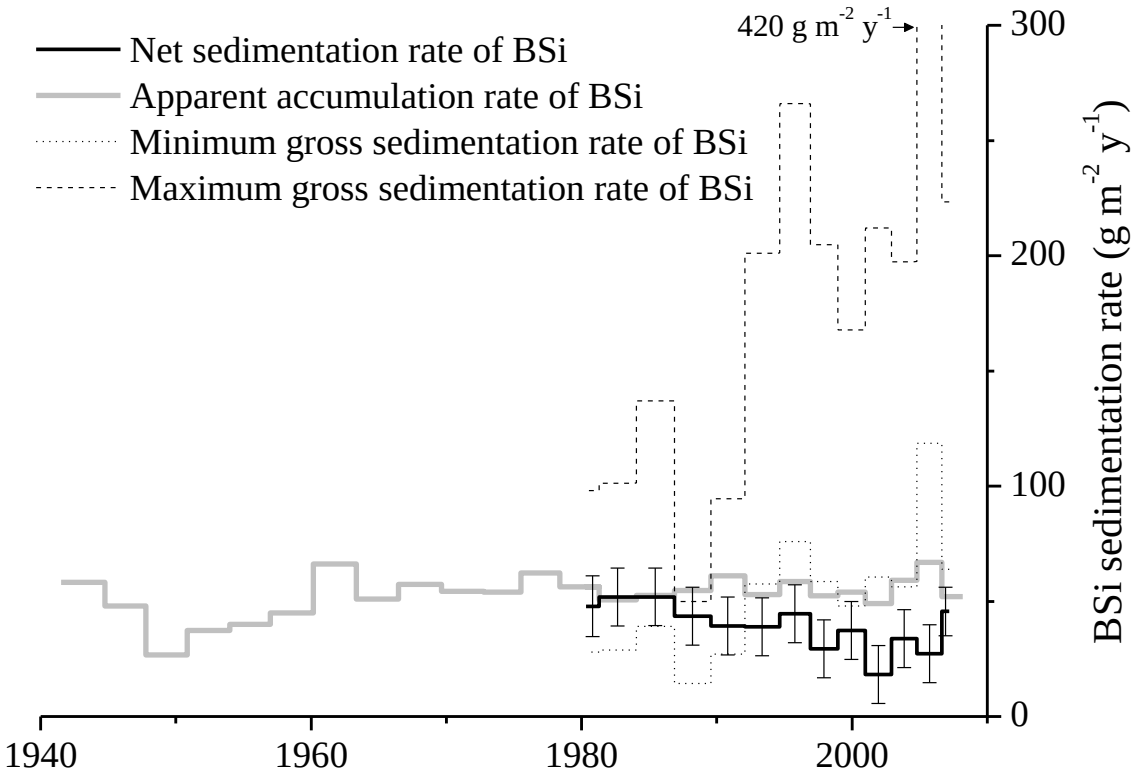

Figure 5.3 Historical plots of the net sedimentation, apparent accumulation and gross sedimentation rates of BSi. The apparent accumulation rates of BSi were estimated using the sediment cores taken at C1 in 2009. Time resolution was adjusted to the apparent accumulation rates

apparent accumulation rates was not detected, the decreasing trend of the net sedimentation rates of BSi was statistically significant ($p < 0.05$). The gross sedimentation rates of BSi were calculated by Eq. 5.6 to be a minimum of 14–120 g m^{-2} y^{-1} and a maximum of 50–420 g m^{-2} y^{-1} during the same period. The increasing trend of those rates was observed ($p < 0.05$). These rates were mostly larger than both the net sedimentation and apparent accumulation rates of BSi.

5.4 Discussion

5.4.1 Gross sedimentation rate of BSi

The gross sedimentation rates of BSi increased due to the increase in the diatom abundance in lake water during 1980–2007, which might be caused by the increase in the lake concentration of DSi (see **Figure 5.3**; **Table 5.1**). However, those rates have a large uncertainty derived from the diatom sinking rates and the BSi content of diatoms used in this study. Conley (1988) suggested that the size range and the BSi content of different diatom species make it difficult to discuss the relationship between diatom abundance and BSi contents in sediments. The diatoms observed in Lake Kasumigaura by NIES for the 27 years were mainly composed of 4 dominant species, that is, *Cyclotella* spp., *Fragilaria* spp., *Aulacoseira* spp. and *Actinocyclus* spp., accounting for about 80% of the total diatom abundance. About 60% of the increase in the diatom abundance was attributed to the increase in *Cyclotella* spp., which might influence both the diatom sinking rate and the BSi content of the diatoms in the lake. The gross sedimentation rates could be better determined using sediment traps if the exposure time is short and the traps located sufficiently above the bottom to reduce resuspension. Moreover, the resuspension may be calculated based on the difference in organic

content of the tripton and that of the re-suspended matter (Gasith 1975).

5.4.2 Net sedimentation rate of BSi

Most of the net sedimentation rates of BSi were smaller than the gross sedimentation rates of BSi (see **Figure 5.3**), indicating the dissolution of BSi comprised in diatom frustules in the water column and/or in the sediments. The net sedimentation rates of BSi decreased due to the significant increase in (D + B) Si loads through the outflow during the time period (see **Table 5.1**). Those rates were calculated by Eq. 5.3 with the assumption of constant (D + B) Si loads through the inflows, which might include an error such as a long-term increase in the DSi loads. However, a increasing trend of annual precipitation was not seen at Tsukuba meteorological weather station from 1980–2007 (http:www.jma.go.jp/jma/). In addition, there was no increasing trend of both DSi concentrations of lake water near the rivers inflowing the lake for the 27 years and those of the main inflows during 1994, 2007 and 2009, suggesting that the DSi loads through the inflows did not increase. This supports the theory of a decreasing trend of the net sedimentation rates of BSi. The decrease in those rates could be explained by a decrease in the gross sedimentation rate of BSi and/or an increase in the DSi release rate from sediments to overlying water. However, a decrease in the gross sedimentation rates of BSi is inconsistent with the trend of the gross sedimentation rates of BSi in **Figure 5.3**. On the other hand, an increase in the DSi release rates from sediments could be due to the increasing sediment resuspension from the late 1990s to mid 2000s (mean concentration of inorganic SS during the 1980s and the 2000s, estimated by the method of Seki et al. (2006) using the monthly concentrations of SS and chlorophyll *a*, was 5 and 21 mg l^{-1}, respectively). The DSi release rates from re-suspended sediment in 2004 were estimated to be (1–3) × 10^9 g y^{-1} by the laboratory experiments in Chapter 4,

which could account for about 30–80% of the decrease in the net sedimentation rate of BSi from the 1980s to the 2000s of 4×10^9 g y^{-1} (see **Table 5.1**). The DSi release rate could have also been enhanced by an increase in temperature, pH and salinity (Loucaides et al. 2008). However, increasing trends of those factors were not clearly seen in the lake.

5.4.3 Apparent accumulation rate of BSi

Although the net sedimentation rates of BSi significantly decreased, a corresponding trend of the apparent accumulation rates of BSi was not detected from 1980–2007 (see **Figure 5.3**, **Table 5.1**), suggesting that some mechanism balanced the recent higher DSi release rate derived from sediment resuspension. Those rates were determined by analyzing the BSi contents in the cores, affected by sinking and sedimentation of diatom frustules and a disappearance of BSi contained in those frustules through dissolution. The solubility and reactivity of BSi decrease with aging of diatom frustules, due mainly to alternations of the bulk structure and surface chemistry (Loucaides et al. 2008). BSi might be dissolved for a few decades after accumulation; therefore, the larger part of BSi in old sediments might already be dissolved than that in recent sediments, in the absence of an increase in the DSi release from re-suspended sediment. It suggests that the apparent accumulation rates of BSi in past years were strongly influenced by a long-term dissolution of sediment BSi and the rates in recent years were influenced by the recent higher DSi release rate derived from sediment resuspension.

5.5 Conclusions

We calculated the (D + B) Si budgets from 1980–2007 in Lake Kasumigaura, based on the chronological sediment information and the database of water quality. The BSi amount accumulated in the lake for the 27-year time period determined by analyzing the sediment cores was close to the amount based on the database of water quality, about 60–70% of DSi inputs from the inflowing rivers. Although the gross sedimentation rates of BSi might have increased during these 27 years, the net sedimentation rates of BSi decreased, suggesting the fast BSi recycling in recent years. This suggestion was consistent with the increase in the DSi release from re-suspended sediment. On the other hand, the decreasing trend could not be detected in the apparent accumulation rates of BSi based on the sediment information. Comparison between the apparent accumulation and net sedimentation rates suggested that the time scale of dissolution of sediment BSi might be a few decades. However, the apparent accumulation rates of BSi were estimated by assuming the constant mass sedimentation rate, and the errors caused by the assumption make it difficult to assess those rates quantitatively. To assess the long-term dissolution of sediment BSi, a measurement of the pore water distribution of DSi and/or analyzing the BSi content in the cores taken over a much greater time span is necessary.

The final publication is available at www.springerlink.com.

Chapter 6

Impacts of long-term increase in silicon concentrations on diatom blooms in a shallow eutrophic lake

6.1 Introduction

Diatoms, most abundant phytoplankton on Earth, play an important role in the global primary production and carbon cycling (Schelske 1999; Kristiansen and Hoell 2002; Conley et al. 2006). They take up DSi as silicate, which they mainly incorporate as BSi in their frustules. They are the dominating primary producers in the world, and Si is therefore a key factor in the ecosystem.

It was often reported that DSi acts as a factor limiting diatom growth. Kilham (1971) suggested that lake eutrophication might promote a decrease in diatom abundance due to DSi limitation. Schelske (1985) showed the decreasing trend of DSi in Lake Michigan during 1955–1970, with the increase in P load, and Barbiero et al. (2002) demonstrated the increasing trends of DSi and diatoms in summer after P load dropping

by half from the late 1970s to the 1990s in the lake. These observations indicate a shift of a factor limiting diatom growth from P to Si by eutrophication and a decline in spring diatom blooms after P emission constraint which might cause summer residual DSi. On the other hand, Takano and Hino (1994) reported that the dense water blooms of blue-green algae had been disappeared and diatoms had been dominated in Japanese hypertrophic Lake Barato during 1990–1992, suggesting that diatoms adapted to higher phosphorus limitation under conditions of low water temperature and high silicate concentration.

Following recent global trends of decline in DSi load from land to sea, a long-term influence of DSi dynamics on the phytoplankton dominance, food web and biogeochemical cycling was deeply concerned (e.g., Humborg et al. 1997; Li et al. 2007; Conley et al. 2008). However, most modeling studies simulated DSi and diatoms just in a year or few years. Ferris and Lehman (2007) reported that the spring development of diatoms in Ford Lake, Michigan, USA was markedly different in 2004 (diatom biovolume above 15 $mm^3\ l^{-1}$) from 2005 and 2006 (less than 5 $mm^3\ l^{-1}$), whereas DSi concentration fell below 0.14 mg l^{-1} in 2004 and remained above 0.84 mg l^{-1} in 2005 and 2006. Their model simulations of Si uptake, washout rates, and sinking implicated hydrologic differences among years as the cause of differential success by diatom populations in April of each year.

Chapter 3 showed the increasing trends of DSi concentration in Lake Kasumigaura during the last three decades and Chapter 4 indicated the influence of the recent sediment resuspension enhancing DSi release in the lake. Although the lake has a valuable database and showed the increasing trend of DSi concentration which is rare in the world, the influence of the DSi increase on the magnitude and seasonality of diatom

blooms was not assessed. The purposes of this chapter are threefold: (1) to detect the long-term trends of diatom abundance in Lake Kasumigaura during the last three decades, (2) to assess the relationships between diatom abundance and other items based on the long-term monitoring data, especially focusing on DSi concentration, and (3) to assess the impact of the long-term increase in DSi concentration on magnitude and seasonality of diatom blooms using a simple model.

6.2 Materials and methods

6.2.1 Observation data for statistical analysis

The database of monthly water quality used for this chapter was based on the NIES investigation at site C during 1981–2010 (**Figure 6.1**). The analytical period was coincided with the model simulation period described later. Surface waters were collected and filtered through 0.45-μm glass-fiber to analyze DSi concentration by ICP. Surface waters were also taken by a column-sampler of 2 m length, providing for analyzing NH_4-N, NO_2-N, NO_3-N, PO_4-P by auto-analyzer after filtering the collected waters through 0.45-μm glass-fiber. Dissolved inorganic nitrogen (DIN) and phosphorus (DIP) was defined as the sum of NH_4-N, NO_2-N, and NO_3-N and solely PO_4-P, respectively. Unfiltered samples were treated in an autoclave under 120^{o}C for 30 minutes after adding potassium peroxodisulfate under alkaline pH for the measurement of total nitrogen (TN) and under acidic pH for total phosphorus (TP). Filtered water samples were provided for analyzing dissolved total nitrogen (DTN) and phosphorus (DTP) by the same method of TN and TP, respectively. Phytoplankton were also taken

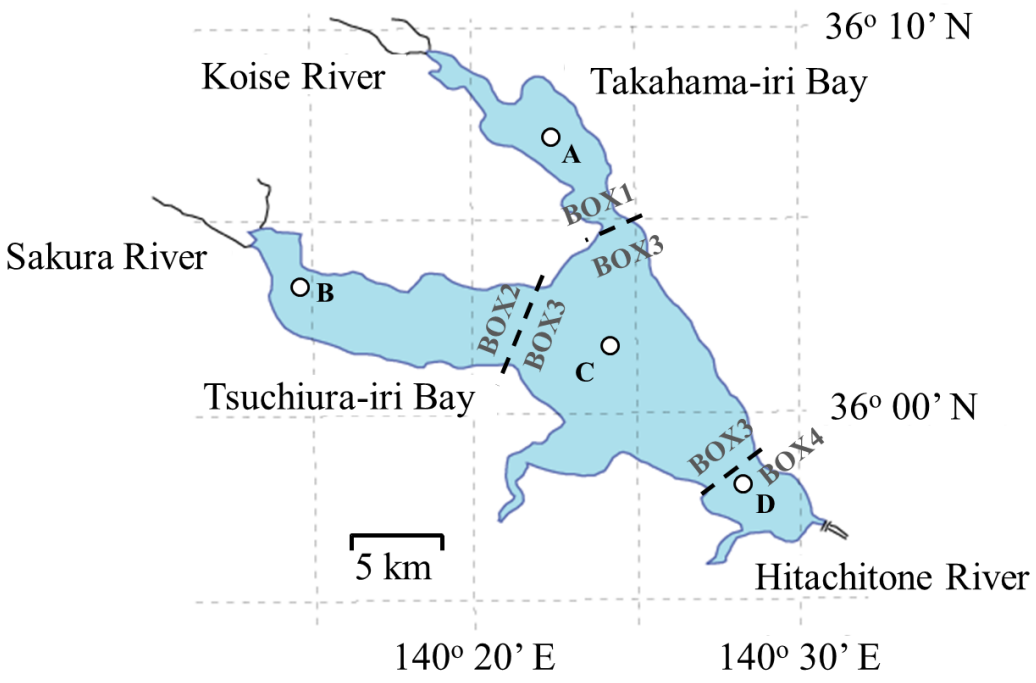

Figure 6.1 Observation sites in Lake Kasumigaura and box division on the model

by a column-sampler, counted on an inverted microscope, and quantified as biovolume by multiplying counted cell number by mean cell volume. BSi concentrations were estimated by multiplying diatom abundances by the BSi content of freshwater diatom frustules of 0.11 g cm^{-3} determined by averaging the values found in Bailey-Watts (1976a) and Sicko-Goad et al. (1984). The sum of DSi and BSi was expressed as (D + B) Si in this chapter. Monthly water temperature, pH, and DO were used also for correlation analysis.

6.2.2 Modeling

6.2.2.1 Box-model structure

The lake is so shallow that stratigraphy is easily broken by wind; therefore, it could be assumed that the water qualities are constant along water depth direction. Annual variation of both DSi concentration and diatom abundance were simultaneously simulated using the simple four-box model. The lake was divided into four which was developed by Fukushima (1984) (**Figure 6.1**; **Table 6.1**). In this study, it was assumed that each box has a constant water depth. The changes in DSi concentration and diatom abundance were simulated as following equations:

$$\frac{\mathrm{d}C_{\mathrm{DSi},j}}{\mathrm{d}t} = \frac{I_{\mathrm{DSi},j} - O_{\mathrm{DSi},j}}{V_j} + \frac{R_{\mathrm{SS},j} SS_{\mathrm{sed},j}}{1000} + \frac{R_{\mathrm{bottom},j}}{h_j} - b\mu_j C_{\mathrm{diatoms},j} \qquad (6.1)$$

$$\frac{\mathrm{d}C_{\mathrm{diatoms},j}}{\mathrm{d}t} = \frac{I_{\mathrm{diatoms},j} - O_{\mathrm{diatoms},j}}{V_j} + \left(\mu_j - \frac{c}{h_j}\right) C_{\mathrm{diatoms},j} \qquad (6.2)$$

Table 6.1 Characteristics of the each box in the model

Parameter	Symbol	Value			
		BOX1	BOX2	BOX3	BOX4
Area (km^2) [a]	A	23	49.3	86	12.7
Mean water depth (m) [a]	h	3.16	3.49	4.47	2.59
Water volume (10^6 m^3)	V	72.7	172.1	384.4	32.9
Mean ratio of river discharge inflowing to the each box to that inflowing to the entire lake [a]	r	0.28	0.32	0.17	0.22
BSi concentration of SS (mg g^{-1}) [b]	β_0	23	29	41	10

[a] Fukushima (1984)

[b] BSi concentrations of surface sediments determined in Chapter 4 were used.

where C is the concentration in the water column (DSi amount in g m^{-3}; diatom cell volume in cm^3 m^{-2}), t is the time (day), I and O are the inflow and outflow, respectively (DSi in g day^{-1}; diatoms in cm^3 day^{-1}), V is the lake volume (m^3), R_{SS} is the DSi release rate from SS (mg g^{-1} day^{-1}), SS_{sed} is the concentration of SS derived from sediment resuspension (g m^{-3}), R_{bottom} is the DSi release rate from bottom sediments (g m^{-2} day^{-1}), h is the water depth (m), b is the BSi content of freshwater diatom frustules (g cm^{-3}, calibrated), μ is the growth rate of freshwater diatoms (day^{-1}), and c is the diatom sinking rate (m day^{-1}, calibrated). The subscript j indicates the box number. The values of h and V in each box are shown in **Table 6.1**.

Inflow

The loads flowing to the box j were expressed by:

$$I_j = \left(L_{\text{river},j} + L_{\text{piston},j} + L_{\text{exch},j}\right) \times 60 \times 60 \times 24 \qquad (6.3)$$

where L_{river} is the load from the inflowing rivers (DSi amount in g s^{-1}; diatom cell volume in cm^3 s^{-1}), L_{piston} is the load by extrusion flows from the upper boxes, and L_{exch} is the load by exchange flows from the adjacent boxes. The loads by groundwater input and precipitation could be negligible. L_{river} for diatoms was also regarded as zero. L_{river} for DSi was calculated by the following formula:

$$L_{\text{river},j} = \frac{Q_{\text{total}}\left(L_{\text{Sakura}} + L_{\text{Ono}}\right)}{\left(Q_{\text{Sakura}} + Q_{\text{Ono}}\right)} r_j \qquad (6.4)$$

$$Q_{\text{total}} = \frac{A'_{\text{total}}\left(Q_{\text{Sakura}} + Q_{\text{Seimei}} + Q_{\text{Ono}}\right)}{\left(A'_{\text{Sakura}} + A'_{\text{Seimei}} + A'_{\text{Ono}}\right)} \qquad (6.5)$$

where Q is the river discharge ($m^3\ s^{-1}$) and A' is the watershed area (km^2). Q_{total} is the total river discharge inflowing to the entire lake and A'_{total} is the watershed area of Lake Kasumigaura of 1426 km^2. r_j is the mean ratio of the river discharge inflowing to the box j to the total river discharge inflowing to the entire lake which determined by water budgets in the lake investigated by Fukushima (1984). Q_{Sakura}, Q_{Seimei}, Q_{Ono} were hourly observed discharge at the monitoring station on R. Sakura, Seimei, and Ono by KRO, respectively (**Table 6.2**). L_{sakura} and L_{Ono} were estimated by L-Q equation based on the monitoring data in 6 rainfall events taken by KRO in 2007 ($L_{sakura} = 8.9\ Q_{sakura}^{0.88}$, $r^2 = 0.98$, $N = 50$; $L_{Ono} = 8.4\ Q_{Ono}^{0.80}$, $r^2 = 0.94$, $N = 50$). L_{piston} was calculated by multiplying the concentration C of the upper box by the flow rate determined on the assumption of steady state of water level. L_{exch} was calculated by multiplying M of the adjacent box and exchange flow discharge Q_{exch} (3.0 $m^3\ s^{-1}$ between BOX 1 and BOX 3, 21.4 $m^3\ s^{-1}$ between BOX 2 and BOX 3, and 13.9 $m^3\ s^{-1}$ between BOX 3 and BOX 4; Fukushima 1984).

Outflow

The outflow load was calculated by multiplying the mass in the water column M by the flow rate on the assumption of steady state of water level on each box.

DSi release

The DSi release rate R was determined by laboratory experiments (see Chapter 4). The rate could be divided into two processes; DSi release from re-suspended sediments and that from bottom sediments. R_{SS} was expressed as the following equation:

Table 6.2 Model input variables

Hourly input variables	Symbol	Used data	How to estimate
River discharge (m^3 s^{-1})	Q	Hourly discharge at the sites in R. Sakura, Ono, and Koise during 1981–2010 (KRO)	directly used
Solar irradiation (MJ m^{-2} h^{-1})	IRR	(i) Daily irradiation at Tsukuba weather station during 1981-2010 (JMA) (ii) Hourly irradiation at Kasumigaura Water Research Station during 1998–2010 (NIES)	multiplying the daily irradiation by α to estimate hourly values (α was the ratio of hourly to daily irradiation averaged during 1998–2010 using data by NIES; CV of RMSE is 42%)
Water temperature (^oC)	WT	Monthly water temperatures at the depth of 0.5 m at site A, B, C, and D during 1981–2010 (NIES)	linearly-interpolating the monthly water temperatures to hourly values
SS concentration derived from sediment resuspension (g m^{-3})	SS_{sed}	(i) Automatic-monitored hourly turbidity and chlorophyll *a* concentration at site A, B, C, and D during 1998–2010 (KRO) (ii) Monthly SS and chlorophyll *a* concentrations at site A, B, C, and D during 1998–2010 (NIES)	1981–1997: simulated by Seki et al. (2006) at site C in 1997 1998–2010: Hourly SS and chlorophyll *a* concentration were estimated from the data (i) and the linear regression model between the monthly-sorted data (i) and (ii) in each year (CV of RMSE for SS, 29–38%; chlorophyll *a*, 33–42%). Hourly SS_{sed} was calculated by the method in Seki et al. (2006) using SS and chlorophyll *a*.
Light attenuation coefficient (m^{-1})	K_d	(i) Monthly light intensity in water at the depth of 0, 0.25, 0.50, 0.75, 1.0, 1.5, 2.0, 3.0, and 4.0 m at site A, B, and C during 1981–2010 (NIES) (ii) Hourly NPSS concentration estimated as seen above	except site D: Monthly K_d was calculated by the Lambert-Beer's law using the light intensity profiles. Hourly K_d was estimated from *NPSS* and the linear regression model of monthly *NPSS* and K_d (r^2 = 0.36 –0.50). site D: estimated from K_d at site C and the linear regression model of K_d at site C and D

$$R_{\mathrm{SS},j} = \frac{1}{1+\gamma \cdot SS_{\mathrm{sed},j}} \left[k_{\mathrm{f}} \beta_{0\mathrm{f},j} \exp\left(-k_{\mathrm{f}} \tau_j\right) + k_{\mathrm{o}} \beta_{0\mathrm{o},j} \right] \exp\left[-\left(\frac{a_1}{WT_j + 273.15} - \frac{a_1}{298.15} \right) \right] \quad (6.6)$$

where γ is a constant ($m^3\ g^{-1}$), k is the dissolution rate constant of diatom frustules (day^{-1}), β_0 is the initial BSi content of SS ($mg\ g^{-1}$), τ is the elapsed time of dissolution of diatom frustules (day), a_1 is a constant (K), and WT is the water temperature (^oC). The subscripts f and o indicate the fresh and old diatom frustules, respectively ($k_f > k_o$). The laboratory experiments determined the values of γ, k_f, k_o, and a_1 to be $1.2 \times 10^{-4}\ m^3\ g^{-1}$, $1.3\ day^{-1}$, $5.0 \times 10^{-3}\ day^{-1}$, and 4.2×10^3 K, respectively (see chapter 4). The ratios β_{0f}/β_0 and β_{0f}/β_0 were found to be 0.024 and 0.98, respectively. Therefore, those ratios were multiplied by β_0 determined in chapter 4 (**Table 6.1**) to calculate β_{0f} and β_{0o}, respectively. Method for estimating SS_{sed} was different between before 1997 and since 1998. Before 1997, no trend of inorganic SS concentration was obtained, based on the estimation technique of Seki et al. (2006) using monthly observed SS and chlorophyll *a*. Therefore, I assumed that SS_{sed} did not change among the years during the period. The concentrations of resuspended sediments in 1997 were simulated by sediment resuspension model driven by wind developed by Seki et al. (2006), and they were applied to SS_{sed} before 1997. On the other hand, SS_{sed} was estimated by method of Seki et al. (2006) using the automatically-monitored hourly turbidity and chlorophyll *a* concentrations by KRO and monthly SS and chlorophyll *a* concentrations taken by NIES at site A, B, C, and D since 1998 (details are shown in **Table 6.2**). A minimum value of the SS concentrations in 2004 simulated by Seki et al. (2006), $10\ g\ m^{-3}$, were subtracted from estimated SS_{sed} by assuming that SS remaining constantly in the water column (mainly consisting of clay minerals) might not attribute to DSi release.

R_{bottom} was also determined by:

$$R_{\mathrm{bottom},j} = k_{\mathrm{bottom}} \left\lfloor a_2 \exp\left(a_3 WT_j\right) - C_{\mathrm{DSi},j} \right\rfloor \qquad (6.7)$$

where k_{bottom} is the rate constant (m day^{-1}), a_1 is a constant (g m^{-3}), and a_2 is a constant (K^{-1}). The parameters k_{bottom}, a_1 and a_2 were experimentally determined to be 4.9×10^{-3} m day^{-1},4.9×10^{-4} g m^{-3} and 3.6×10^{-2} K^{-1}, respectively. *WT* was estimated by linear-interpolation of the monthly water temperature at the depth of 0.5 m at site A, B, C, and D observed by NIES (**Table 6.2**).

Diatom growth

Assuming that the limiting factors of growth of diatoms are light condition, water temperature or DSi concentration in the lake, the growth rate of diatoms μ was calculated by the following equation:

$$\mu_j = \mu_{\max} f_{\mathrm{I},j} f_{\mathrm{T},j} f_{\mathrm{Si},j} \qquad (6.8)$$

where $\mu_{\max}$ is the maximum growth rate of freshwater diatoms (day^{-1}, calibrated) and f_{I}, f_{T}, and f_{Si} are the function representing the influence of irradiance, temperature, and DSi concentration on the growth of diatoms, respectively.

In this model, f_{I} at a certain depth was expressed as the following equation:

$$f_{\mathrm{I},j} = \frac{IRR_j}{K_\mathrm{I} + IRR_j} \qquad (6.9)$$

where *IRR* is the irradiance in water at a certain depth (MJ m^{-2} h^{-1}) and K_I is the half-saturation constant of irradiance (MJ m^{-2} h^{-1}, calibrated). *IRR* was subject to the Lambert-Beer's law as the following equation:

$$IRR = IRR_0 \exp\left(-K_\mathrm{d} z\right) \quad (6.10)$$

where IRR_0 is the solar irradiance at the water surface, K_d is the vertically-averaged light attenuation coefficient (m^{-1}) and *z* is the water depth (m). Using Eq.6.9 and 6.10, the vertically-averaged light influence function f_I' could be expressed by:

$$f_{\mathrm{I},j}' = \frac{1}{h_j}\int_{h_j}^{0} f_{\mathrm{I},j}\,\mathrm{d}z = \frac{1}{K_{\mathrm{d}j}\cdot h_j}\ln\left[\frac{IRR_0 + K_\mathrm{I}}{IRR_0\exp\left(-K_{\mathrm{d}j}\cdot h_j\right) + K_\mathrm{I}}\right] \qquad (6.11).$$

The hourly *IRR* was estimated by multiplying the daily *IRR* at Tsukuba weather station by the ratio of hourly to daily irradiance averaged during 1998–2010 using data at Kasumigaura Water Research Station by NIES (details are shown in **Table 6.2**). The hourly K_d was estimated from SS_{sed} using the relationships between SS_{sed} and monthly-observed K_d in all sites except site D where the correlation coefficient was low (**Figure 6.2**). Therefore, K_d at sited D was estimated from that at site C ($y = 1.06\,x$, $r^2 = 0.36$). Monthly K_d shown in **Figure 6.2** was determined by the Lambert-Beer's law applying to the profiles of light intensity in water column taken by NIES (**Table 6.2**).

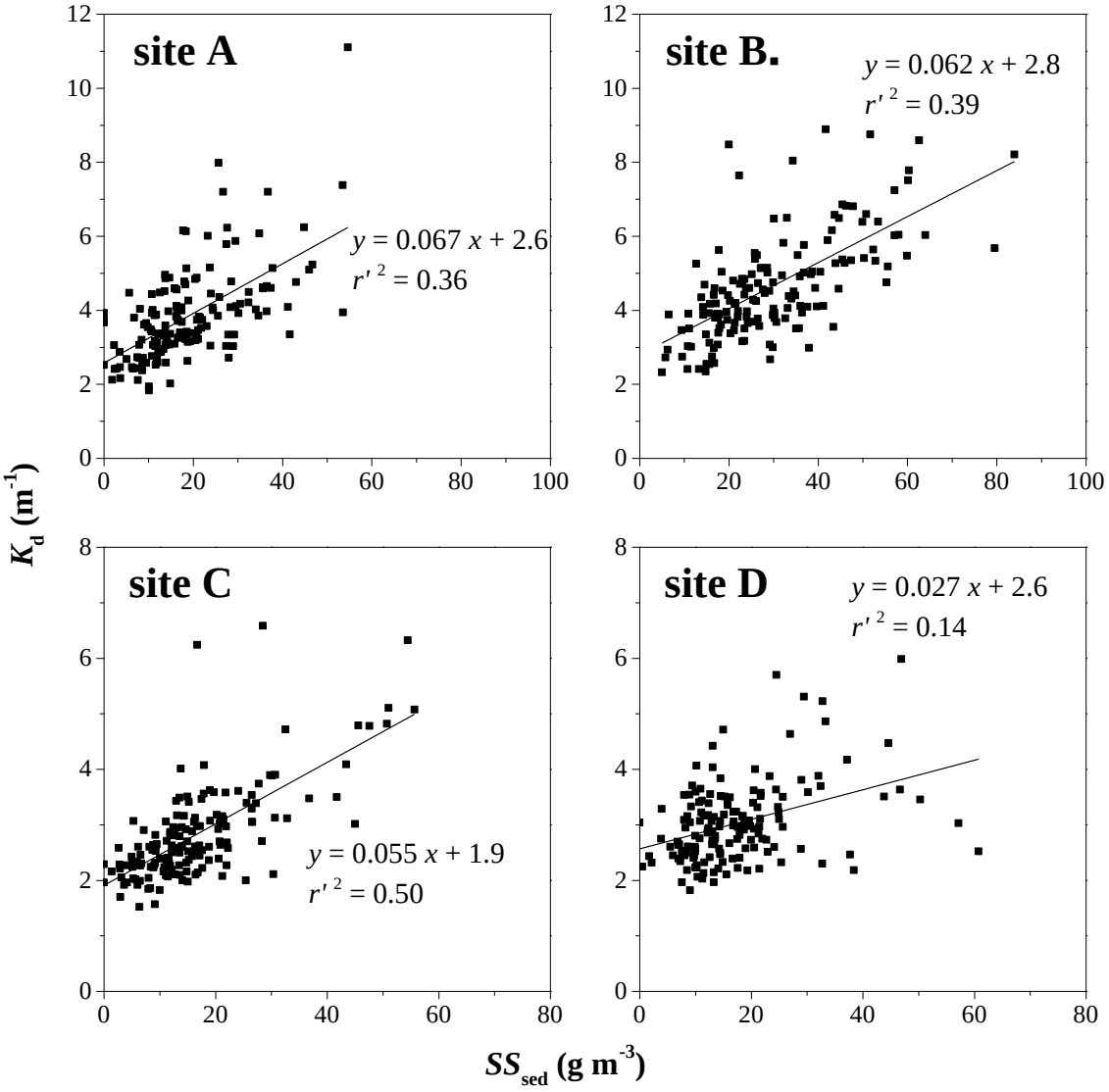

Figure 6.2 Relationships between SS_{sed} and K_d at each site during 1998–2010 in Lake Kasumigaura. K_d was determined using the monthly profiles of light intensity in water column observed by NIES

The temperature influence function f_T was expressed as the following formula by reference to Matsuoka (1984):

$$f_{T,j} = \begin{cases} \left(WT_j - d_{WT}\right)/14 & (WT_j < 14 + d_{WT}) \\ 1 & (14 + d_{WT} \le WT_j < 20 + d_{WT}) \\ 2 - \left(WT_j - d_{WT}\right)/20 & (20 + d_{WT} \le WT_j) \end{cases} \quad (6.12)$$

where d_{WT} is constant (^{o}C, calibrated).

The influence function of DSi concentration f_{Si} was expressed as the Monod equation as the following equation:

$$f_{Si,j} = \frac{C_{DSi,j}}{K_{Si} + C_{DSi,j}} \quad (6.13)$$

where K_{Si} is the half-saturation constant of DSi concentration for diatoms (g m^{-3}, calibrated).

6.2.2.2 Parameter calibration

The BSi content of freshwater diatom frustules b, the maximum growth rate of diatoms μ_{max}, the half-saturation constant of irradiance K_I, the water temperature constant d_{WT}, the half-saturation constant of DSi concentration for diatoms K_{Si}, and the diatom sinking rate c were calibrated in every 5 year (1981, 1986, 1991, 1996, 2001, and 2006). The parameter sets were determined by random sampling and the least squares method

(Komatsu et al. 2006). For random sampling, the ranges of b, μ_{max}, and K_{Si} were assigned based on the literature values (**Table 6.3**). The sufficient ranges of K_I, d_{WT}, and K_{Si} were determined after sensitive analysis.

The object function *OFUNC* was calculated as following equations:

$$OFUNC = \overline{E}_{DSi}\overline{E}_{diatoms} \qquad (6.14)$$

$$\overline{E} = \frac{\sum_j E_j V_j}{\sum_j V_j} \qquad (6.15)$$

where $\overline{E}$ is the volume-weighted root mean squared error (RMSE; DSi in g m^{-3}, diatoms in cm^3 m^{-3}), E is the RMSE, and V is the water volume of the box (m^3; **Table 6.1)**. DSi concentrations were calibrated in all boxes using the observation data at sites A, B, C, and D. On the other hand, diatom abundances were just monitored at sites A and C; therefore, parameters were calibrated in BOX 1 and 3. While E_{DSi} was determined as RMSE of monthly DSi concentration, $E_{diatoms}$ was calculated by 3 different methods as: (1) RMSE of monthly diatom abundance (N = 12 months × 6 years), (2) RMSE of annual maximum diatom abundance (N = 6), and (3) average of RMSE of annual maximum diatom abundance and RMSE of annual minimum diatom abundance (N = 6). In this study, the above 3 calibration methods were called as CM1, CM2, and CM3, respectively.

Calibrated parameters were shown in **Table 6.4**. After parameter identification, the parameter sets were not changed during model validation for the whole period. Half

Table 6.3 Values of the model parameters in the previous studies

Paper	Mean (min.–max.)	Diatom species
BSi content of diatom frustules, *b* (g cm^{-3})		
Bailey-Watts (1976a)	0.10 (0.08–0.12)	*Asterionella formosa*, *Cyclotella pseudostelligera*, *C. pseudostelligera*, *C. comta*, and *S. rotula*
Sicko-Goad et al. (1984)	0.10 (0.07–0.41)	*Cyclotella* spp., *Fragilaria* spp., *Melosira* spp., and *Stephanodiscus* spp.
Takano and Hino (1996)	0.07	*Cyclotella meneghiniana* mostly
Conley et al. (1989)	0.13 (0.10–0.15)	nano- and netplanktonic diatoms
Range	*0.07–0.13*	
Maximum growing rate of diatoms, μ (day^{-1})		
Matsuoka (1984)	1.7	*Asterionella formasa*
	2.5	*Cyclotella* spp.
	1.9	*Skeletonema costatum*
	1.6	*Synedra* spp.
Range	*1.6–2.5*	
Sinking rate of diatoms, *c* (m day^{-1})		
Bailey-Watts (1976b)	0.25	diatoms existed in lake water
Gibson (1984)	0.3 (0.2[a]–0.4[b])	Fitting an exponential regression to observatins
Ferris and Lehman (2007)	0.66	diatoms existed in lake water, mainly of *Asterionella*, *Cyclotella*, *Fragilaria*, *Aulacoseira*, and *Synedra* spp.
Range	*0.20–0.66*	

[a] growing period, [b] depletion period

Table 6.4 Values of the parameters calibrated by the various methods

Parameter	**Values**		
	CM1	CM2	CM3
BSi content of diatom frustules, b (g cm^{-3})	0.13	0.068	0.067
Maximum growth rate of diatoms, μ (day^{-1})	2.3	1.8	2.2
Half-saturation constant of irradiance, K_I (MJ m^{-2} h^{-1})	0.071	0.021	0.028
Water temperature constant, d_{WT} (^{o}C)	-3.8	-4.6	-4.7
Half-saturation constant of DSi, K_{Si} (g m^{-3})	6.5	4.8	3.1
Sinking rate of diatoms, c (m day^{-1})	0.20	0.29	0.42

saturation constant of DSi K_{Si} was larger than the experimental value of about 0.9 at 20^{o}C reported by Takano and Hino (1996).

6.3 Results

6.3.1 Field observations

6.3.1.1 Dominant phytoplankton species

In Lake Kasumigaura, diatoms and cyanobacteria were most dominant during the last three decades. They occupied about 80% of all phytoplankton cell volume on average. Although the trends of chlorophyll *a* concentration and total phytoplankton abundance were not significantly detected (**Figure 6.3a**), dominant phytoplankton species changed remarkably (**Figure 6.3b**). Mean proportion of diatom abundance was increased from less than 40% during 1981–2000 to 66% during 2001–2010, with the decrease in mean proportion of cyanobacteria abundance from over 40% to about 20%.

Dominant diatom species in the lake, *Actinocyclus* spp., *Aulacoseira* spp., *Cyclotella* spp., *Fragilaria* spp., and *Synedra* spp., occupied about 90% of all diatom cell volume on average. Shift of dominant diatom species was also observed during the last three decades (**Figure 6.4**). *Actinocyclus* spp., blooming often in autumn before 1991, vanished and *Cyclotella* spp. was remarkably dominant during the 2000s.

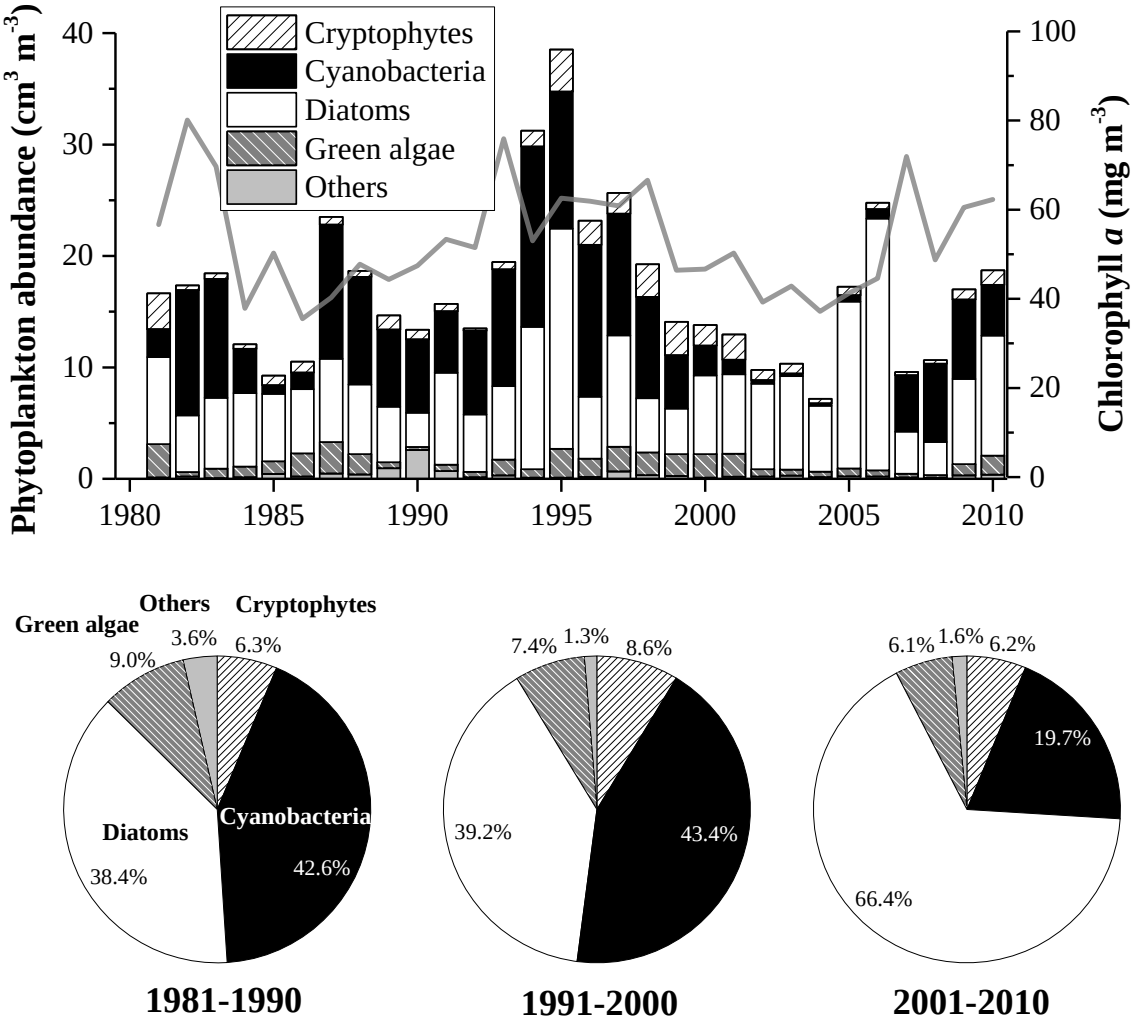

Figure 6.3 Long-term change in phytoplankton abundances and chlorophyll *a* concentrations (**a**) and mean proportion of cell volumes of the respective phytoplankton groups during 1981–1990, 1991–2000, and 2001–2010 (**b**) at site C in Lake Kasumigaura

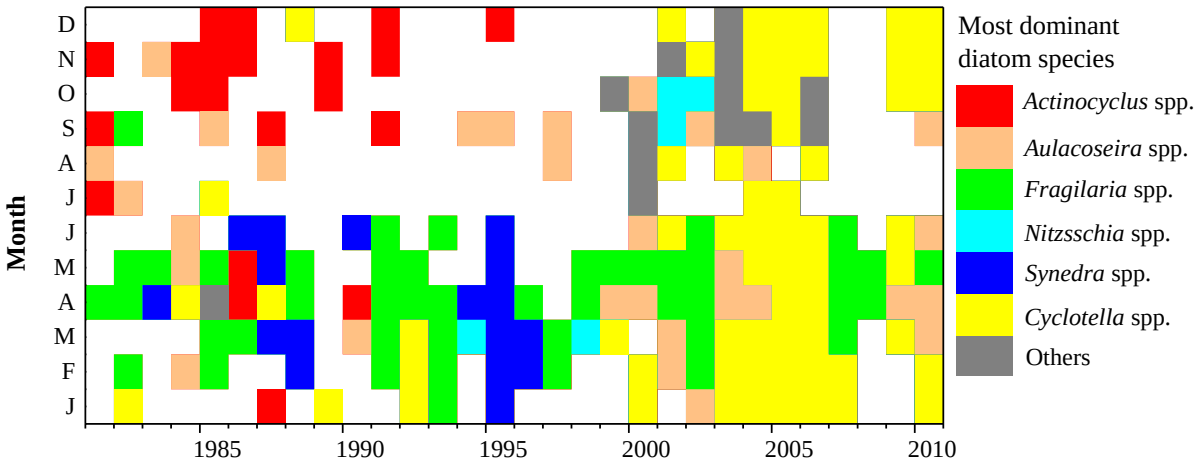

Figure 6.4 Long-term and seasonal change in the most dominant diatom species at site C in Lake Kasumigaura. Open area indicate the period when the phytoplankton except diatoms were dominant

6.3.1.2 Nutrient limitation

Marine diatoms take up N, P, and Si in an atomic ratio of 1 for Si/N and 16 for Si/P which is well known as Redfield ratio (Redfield et al. 1963; Brzezinski 1985). On the other hand, freshwater diatoms usually need more Si than marine diatoms. Nagai et al. (2001) reported that the Si/N and Si/P atomic ratios of diatoms collected in Japanese Lake Biwa were 3–14 times higher than Redfield ratio. These ratios could be used for analyzing a limiting nutrient for diatoms. Therefore, Si:N:P atomic ratios were investigated in the lake during the last three decades (**Figure 6.5**). (D + B)Si was compared with TP and TN since LSi was not attribute to nutrient for diatoms. DSi/DTP, (D + B)Si/TP, DSi/DTN, and (D + B)Si/TN atomic ratios mostly declined to below those ratios of freshwater diatoms and occasionally less than the ratios of marine diatoms when annual maximum diatom abundance was observed. DSi/DIP atomic ratios were often more than Si/P ratio of freshwater diatoms, but in the range of it at few years when a blooming occurred. DSi/DIN atomic ratios were frequently less than Si/N ratio of freshwater diatoms, but significantly increased during the last three decades ($p < 0.01$). However, usually N might not limit diatom growth compared with P from the viewpoint of N/P ratios. These findings suggest that DSi might be one of the main factors limiting growth of diatoms in the lake during a bloom season.

6.3.1.3 Long-term trends of diatom abundance

Increasing trend of diatom abundances was detected during 1981–2010 (12 months moving average, $p < 0.001$; **Figure 6.6**). Mean abundance of diatoms during 1981–

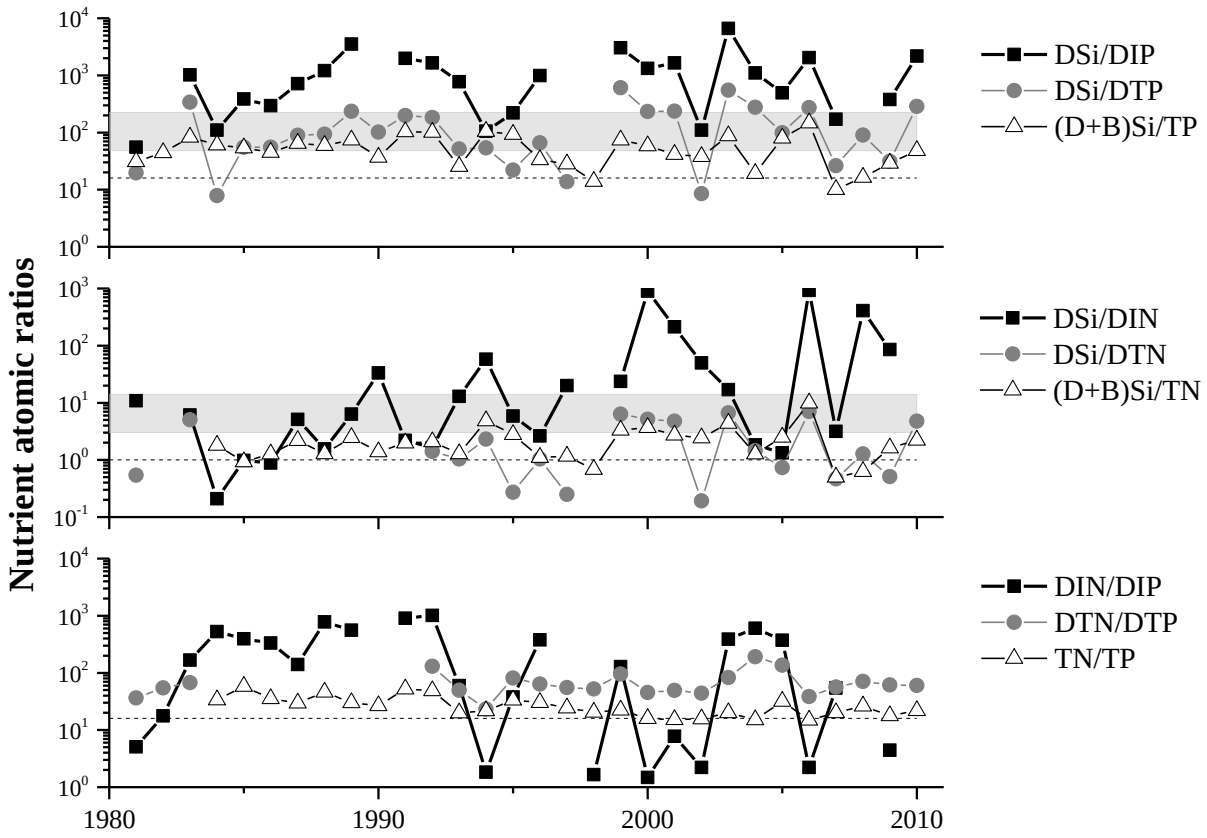

Figure 6.5 Long-term changes in the nutrient atomic ratios when annual maximum diatom abundance was observed at site C during 1981–2010. The gray zone and broken line indicates the nutrient atomic ratios of freshwater diatoms reported by Nagai et al. (2001) and of marine diatoms (Redfield ratio), respectively

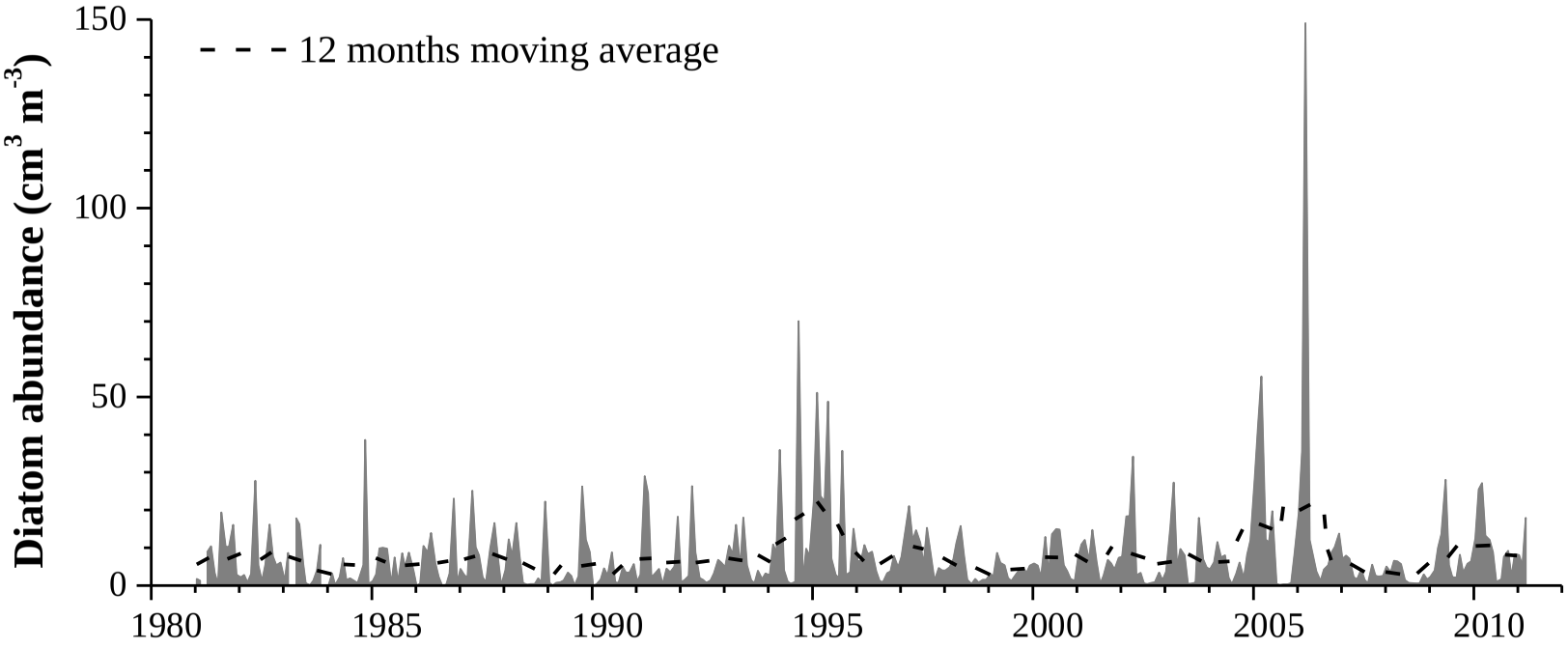

Figure 6.6 Long-term change in diatom abundances at site C in Lake Kasumigaura

1990, 1991–2000, and 2001–2010 was 6.0, 8.4, and 9.2 cm^3 m^{-3}, respectively. Massive blooming was seen during 1994–1995 and 2005–2006, which consists mainly of *Synedra* spp. and *Cyclotella* spp., respectively.

Mean seasonal changes of diatom abundances in **Figure 6.7** showed that spring and autumn diatom blooms were confirmed during 1981–1990, but autumn blooms decreased and spring blooms were beginning since last winter during 2001–2010. As results of monthly t-test, diatom abundance significantly increased in January ($p < 0.01$), February, and March ($p < 0.05$) and decreased in in November ($p < 0.01$). The characteristics of periodic blooms were clearly shown by Fourier analysis (**Figure 6.8**).

Seasonal relationships between DSi and diatoms were investigated due to the role of DSi as a factor limiting diatom growth. Many relationships between DSi concentration and diatom abundance during the last three decades showed a counterclockwise loop (**Figure 6.9**). These hysteresis loops represent as follows: (i) diatom growth by uptake of DSi under preferable condition (e.g., at optimal temperature), (ii) rapid sinking of diatoms after DSi depletion, and (iii) almost no diatom with DSi supply by inflowing DSi-rich river water and release from sediments. The relationships were mostly characterized as a two-round loop during the 1980s with spring and autumn diatom blooms (e.g., 1983, 1986, and 1987), while a one-round big loop during the 2000s with extensive winter–spring blooms (e.g., 2002, 2003 and 2005).

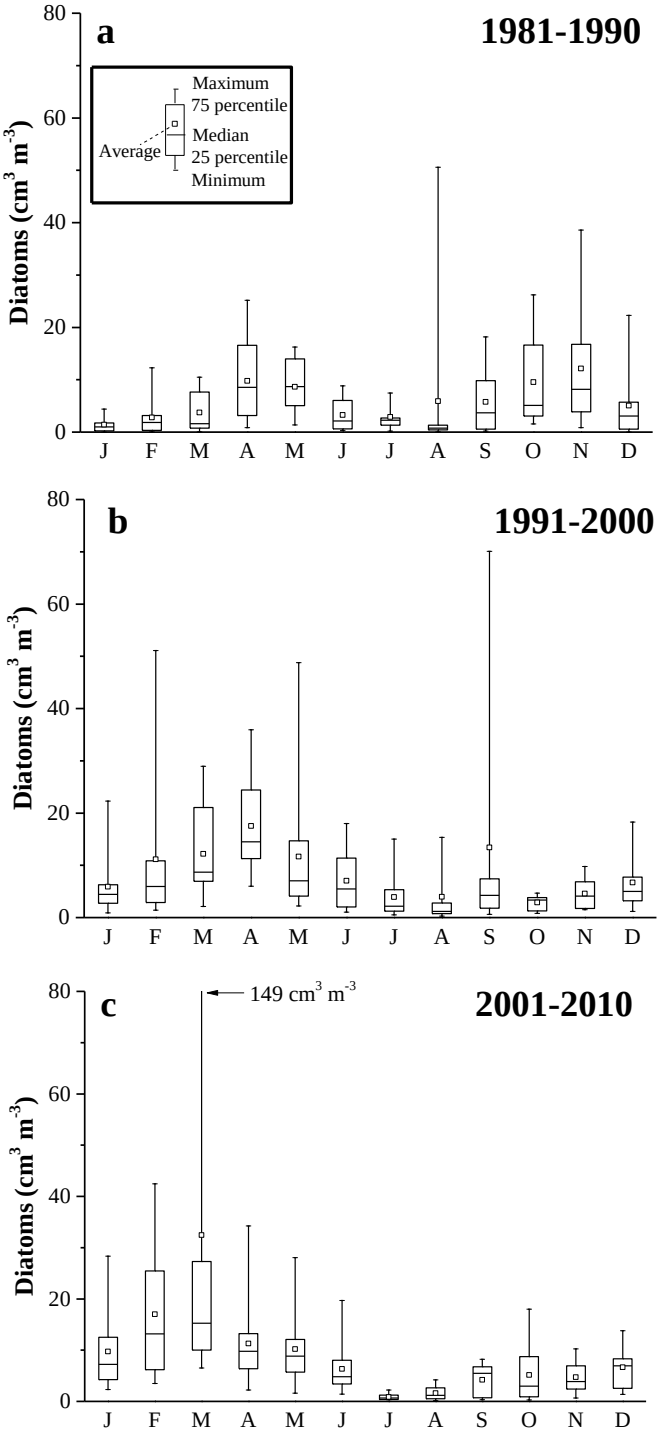

Figure 6.7 Monthly change in decadal statistics of diatom abundances at site C during 1981–1990 (**a**), 1991–2000 (**b**), and 2001–2010 (**c**)

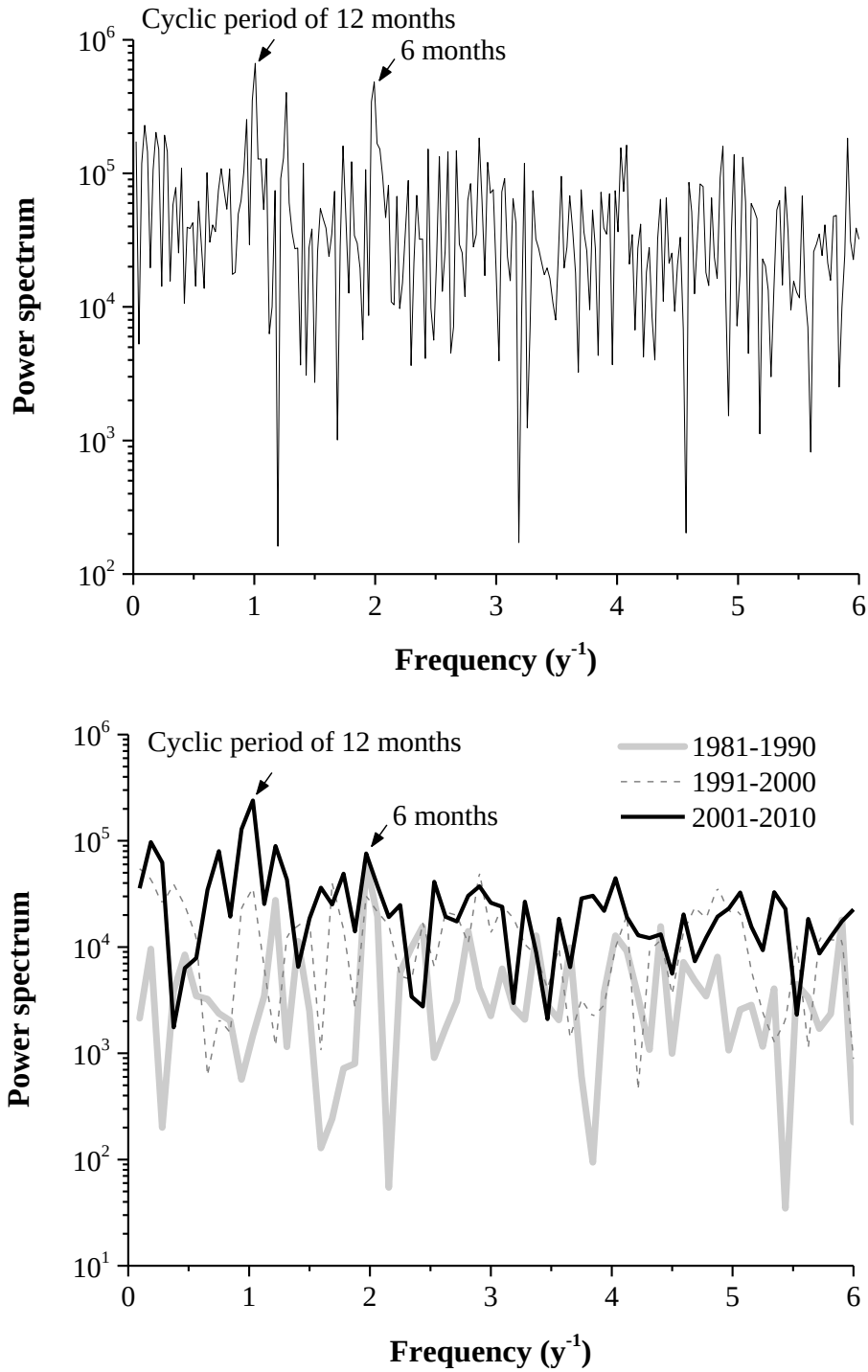

Figure 6.8 Power spectrums of diatom abundance at site C during 1981–2010 (**a**) and 1981–1990, 1991–2000, and 2001–2010 (**b**)

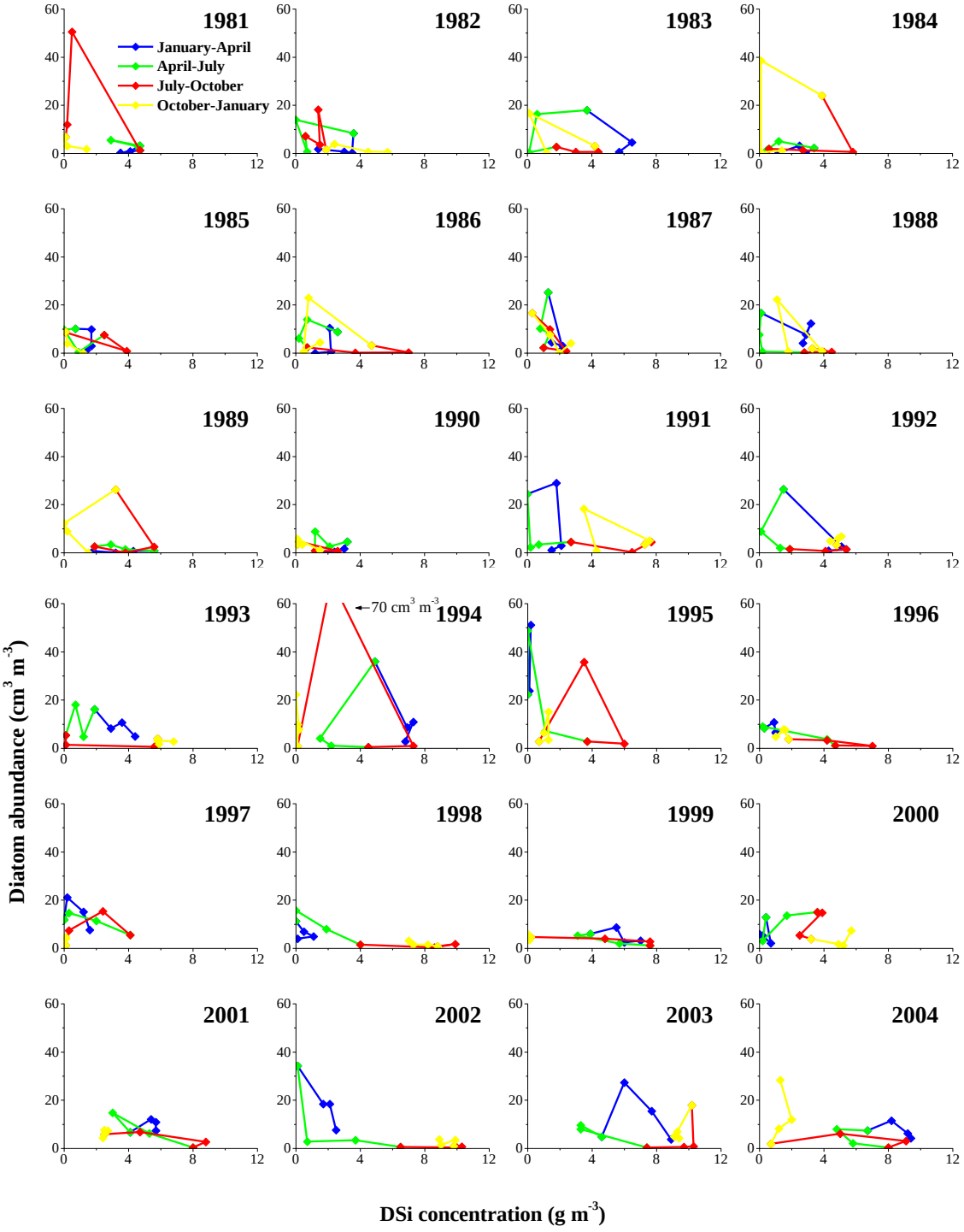

Figure 6.9 Seasonal changes of DSi concentration and diatom abundance at site C during 1981 –2010

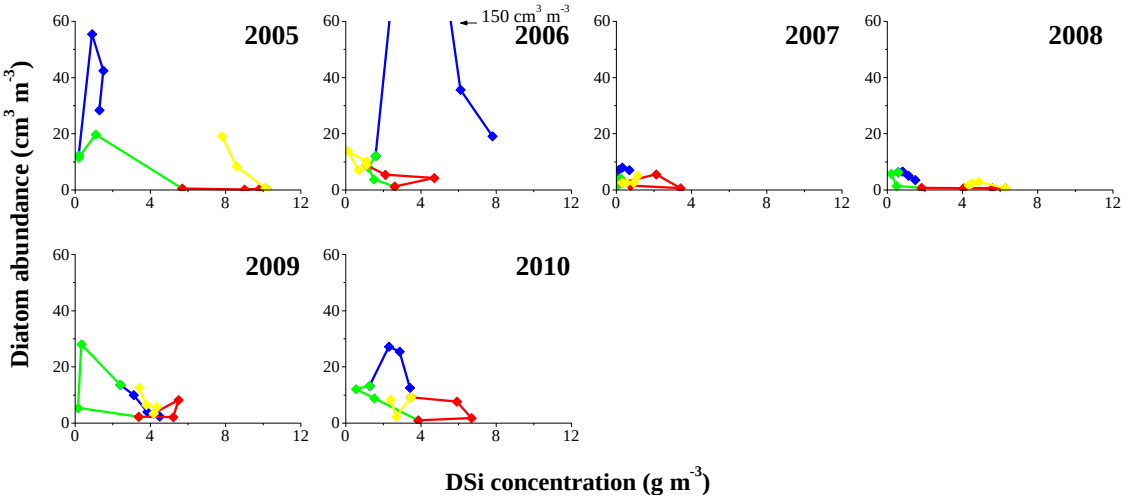

Figure 6.9 (continued)

6.3.1.4 Long-term relationships between DSi concentration and diatom abundance

DSi concentration significantly increased at the center of the lake (see Chapter 3). Long-term change in DSi concentration was compared with diatom abundance (**Figure 6.10**). Annual statistics were calculated for the year from August to July because recent diatom blooms often occurred in winter and because about 60% of annual minimum diatom abundance was observed in July and August during the period. Annual maximum diatom abundance was significantly related to annual maximum DSi concentration (r^2 = 0.16, p < 0.05) and (D + B)Si concentration (r^2 = 0.59, p < 0.001; **Figure 6.10a, b**). Significant correlation was also detected between DSi concentration and two year-lagged diatom abundance, but a correlation coefficient was lower than no lagged diatom abundance (p < 0.05; **Figure 6.10c**). Correlation coefficient between DSi concentration and diatom abundance was not so high, which might be caused by daily fluctuation of diatom abundance and other factors influencing diatom growth such as N and P concentrations, light condition, and water temperature. However, annual maximum diatom abundance was not significantly related to annual mean values of other nutrients such as DIP, TP, DIN, and TN (r^2 < 0.07) and those of potential factors influencing diatom blooms such as water temperature, pH, DO (r^2 < 0.01), and transparency (r^2 = 0.07).

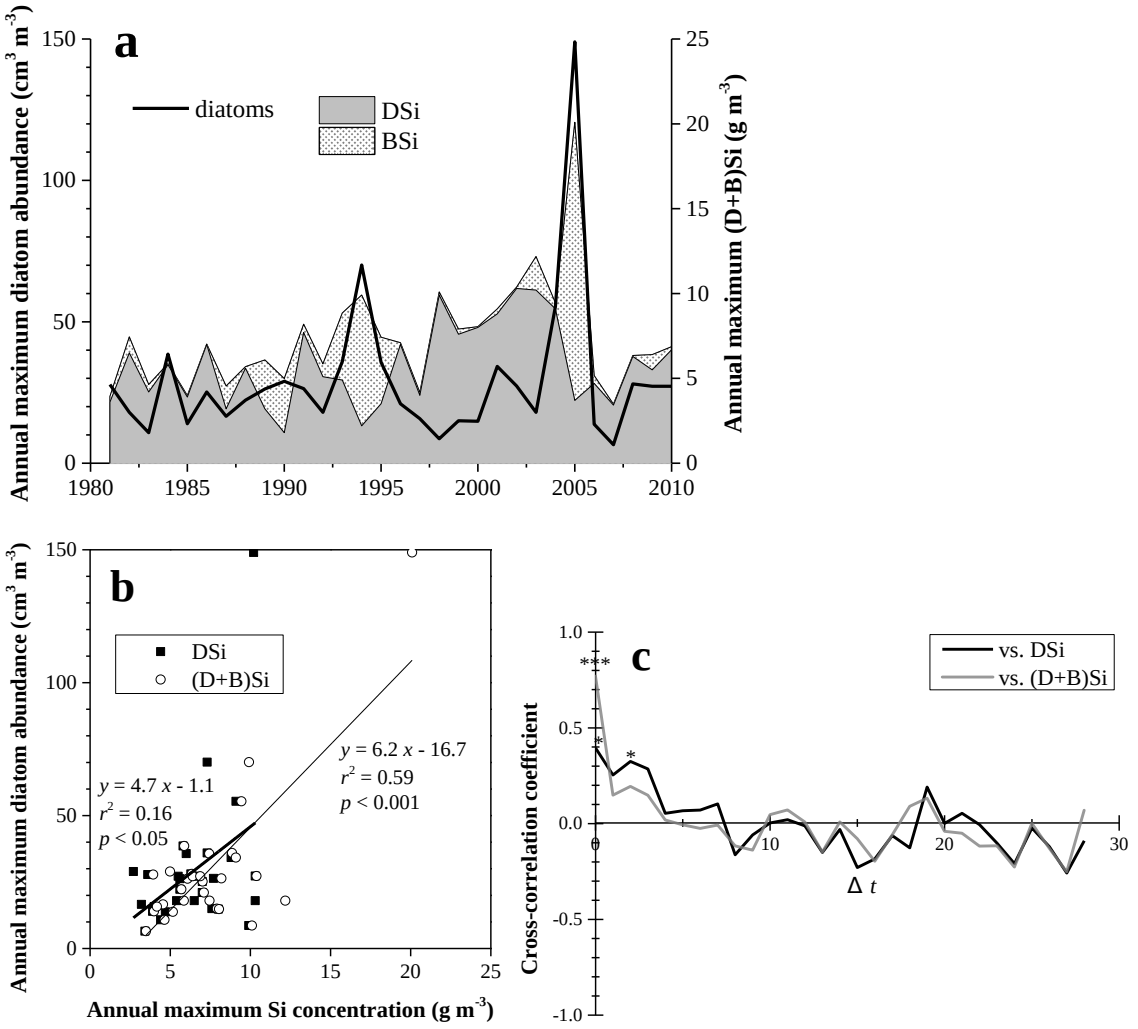

Figure 6.10 Long-term changes in annual maximum diatom abundance (left axis) and annual maximum (D + B)Si concentration (right axis) at site C in Lake Kasumigaura (**a**), comparisons of annual maximum DSi or (D + B)Si concentration with diatom abundance (**b**), and distributions of cross-correlation coefficient between annual maximum DSi or (D + B)Si concentration and diatom abundance lagging Δ*t* years behind DSi or (D + B)Si concentration (**c**). Annual maximum values were determined for the period from August to July. * and *** indicate a significant level $p < 0.05$ and 0.001, respectively in (**c**)

6.3.2 Simulation

6.3.2.1 Comparison of different calibration methods

Different shapes of diatom bloom patterns were obtained among the various calibration methods (**Figure 6.11**). Some model predictions by CM1 and 2 represented relatively flat peaks of diatom blooms which were different from field observations (e.g., in 2003 and 2004). On the other hand, predictions calibrated by CM3 showed sharp peaks of blooms which were similar to observations. Therefore, the results calibrated by CM3 were used as described later.

6.3.2.2 Accuracy of the model

Model predictions for DSi and diatoms were shown in **Figure 6.12** and **6.13**. Focusing on BOX 3, including the center of the lake, the validation results showed that RMSE was 2.6 g m^{-3} for DSi and 13 cm^3 m^{-3} for diatoms, respectively (**Figure 6.14**). The coefficient of variation (CV) of RMSE was calculated as the ratio of RMSE to the mean of the observation values, to be 85% for DSi and 170% for diatoms. The coefficient of determination R^2 was also calculated to be 0.22 ($p < 0.001$) for DSi and 0.0061 ($p = 0.14$) for diatoms.

Annual statistics of DSi and diatoms observed at site C were compared with model predictions in BOX 3 (**Figure 6.15, 6.16**). CV of annual mean, standard deviation, and maximum DSi concentration was less than 50%. In addition, model predictions of annual mean and maximum DSi concentration were significantly related to the observed

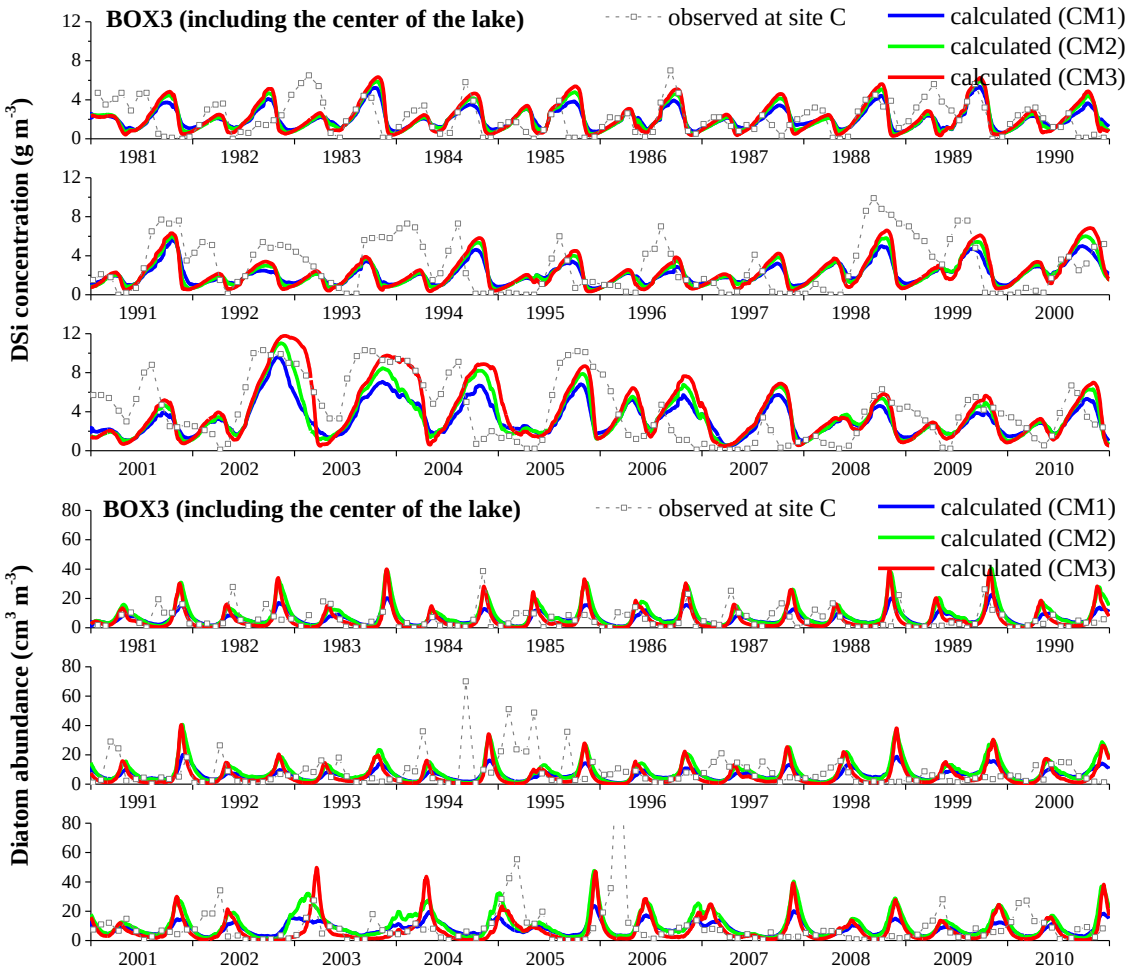

Figure 6.11 Long-term changes in DSi concentration and diatom abundance calculated by the model whose parameters were calibrated by the various methods (CM1, 2, and 3) in BOX 3 and observed at site C in Lake Kasumigaura during 1981–2010

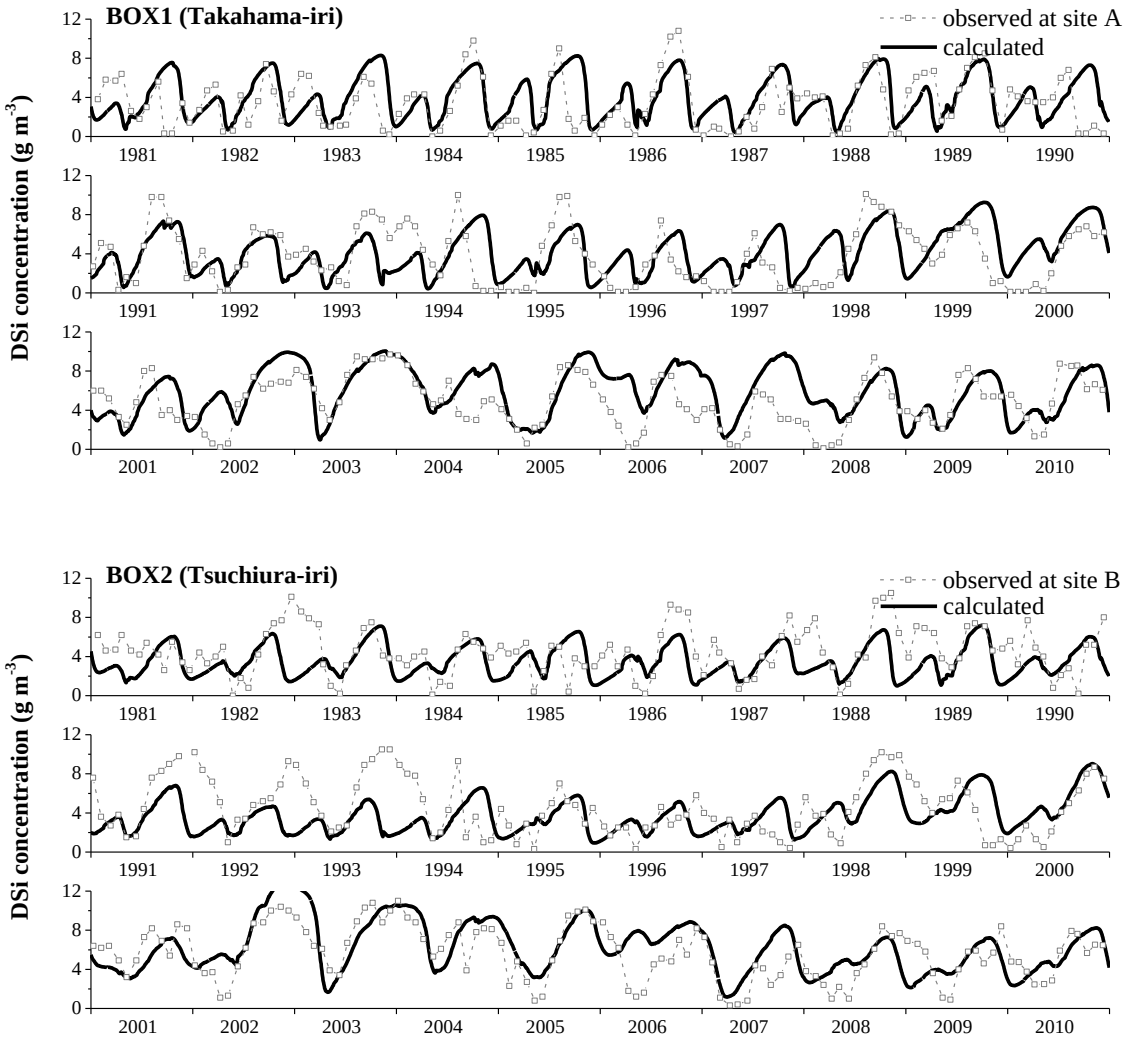

Figure 6.12 Model predictions in BOX 1, 2, 3, and 4 (solid lines) and observed data at site A, B, C, and D (broken lines and points) for DSi in Lake Kasumigaura during 1981–2010. The model was calibrated by CM3

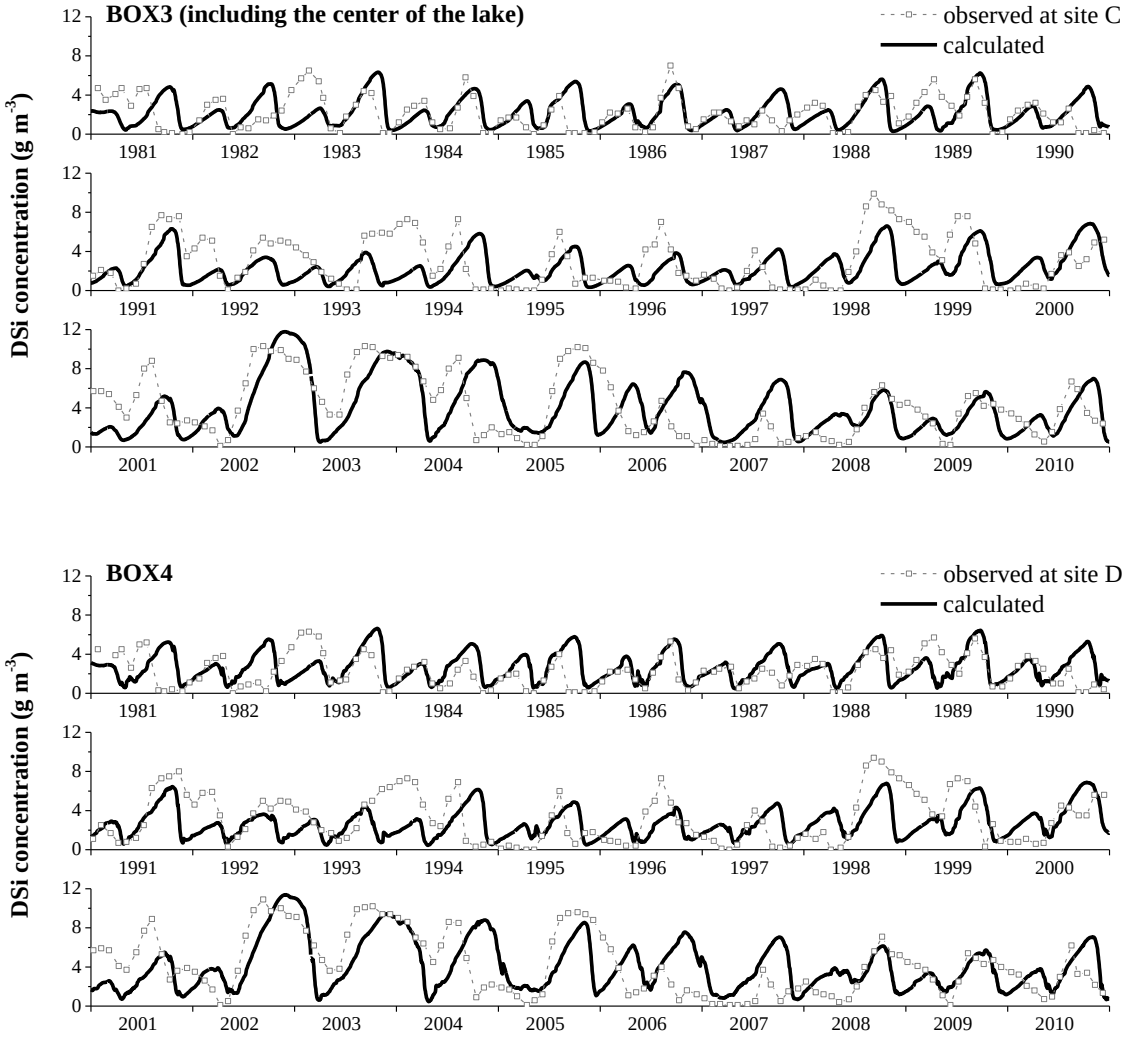

Figure 6.12 (continued)

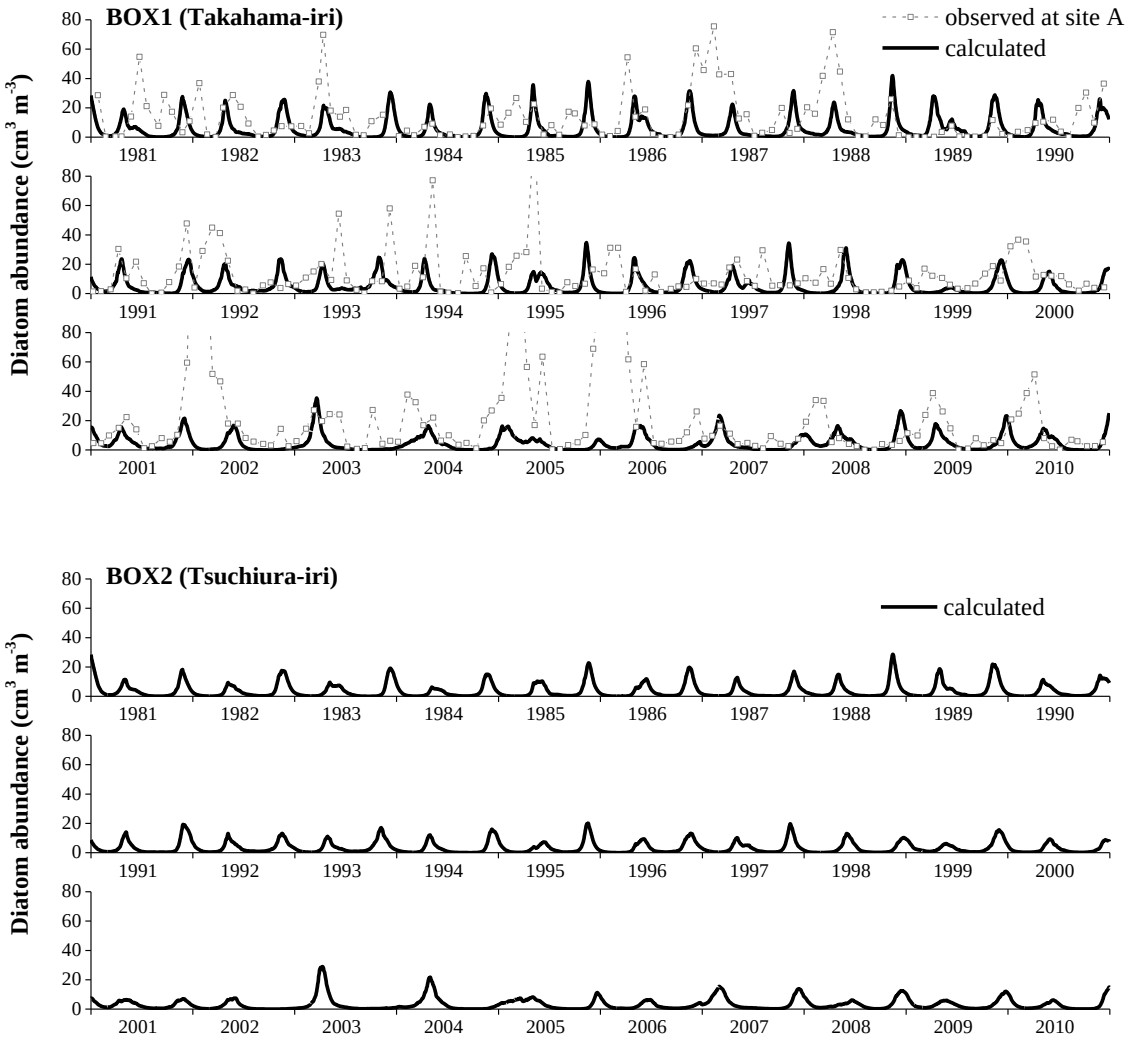

Figure 6.13 Model predictions in BOX 1, 2, 3, and 4 (solid lines) and observed data at site A, B, C, and D (broken lines and points) for diatoms in Lake Kasumigaura during 1981–2010. The model was calibrated by CM3

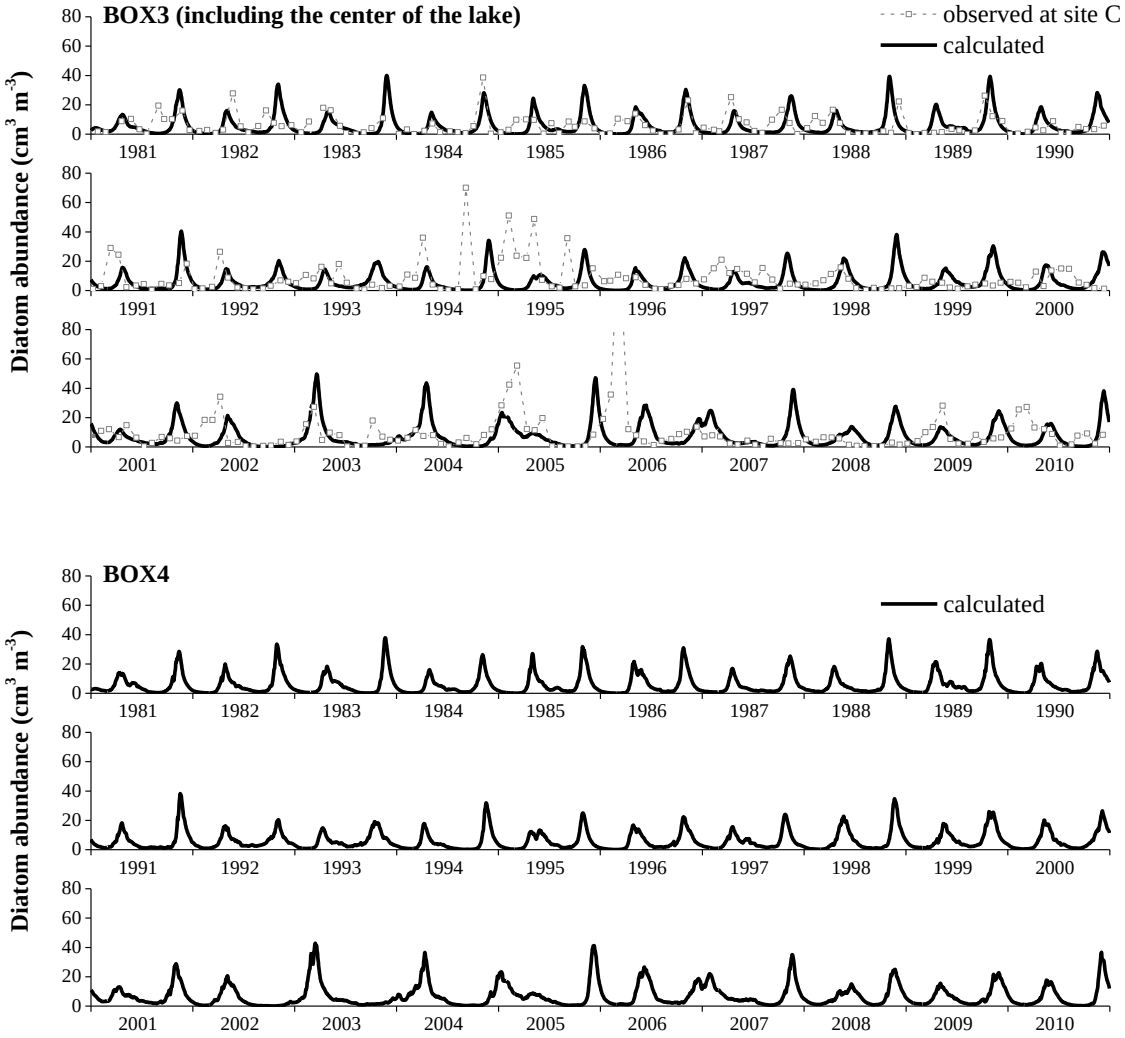

Figure 6.13 (continued)

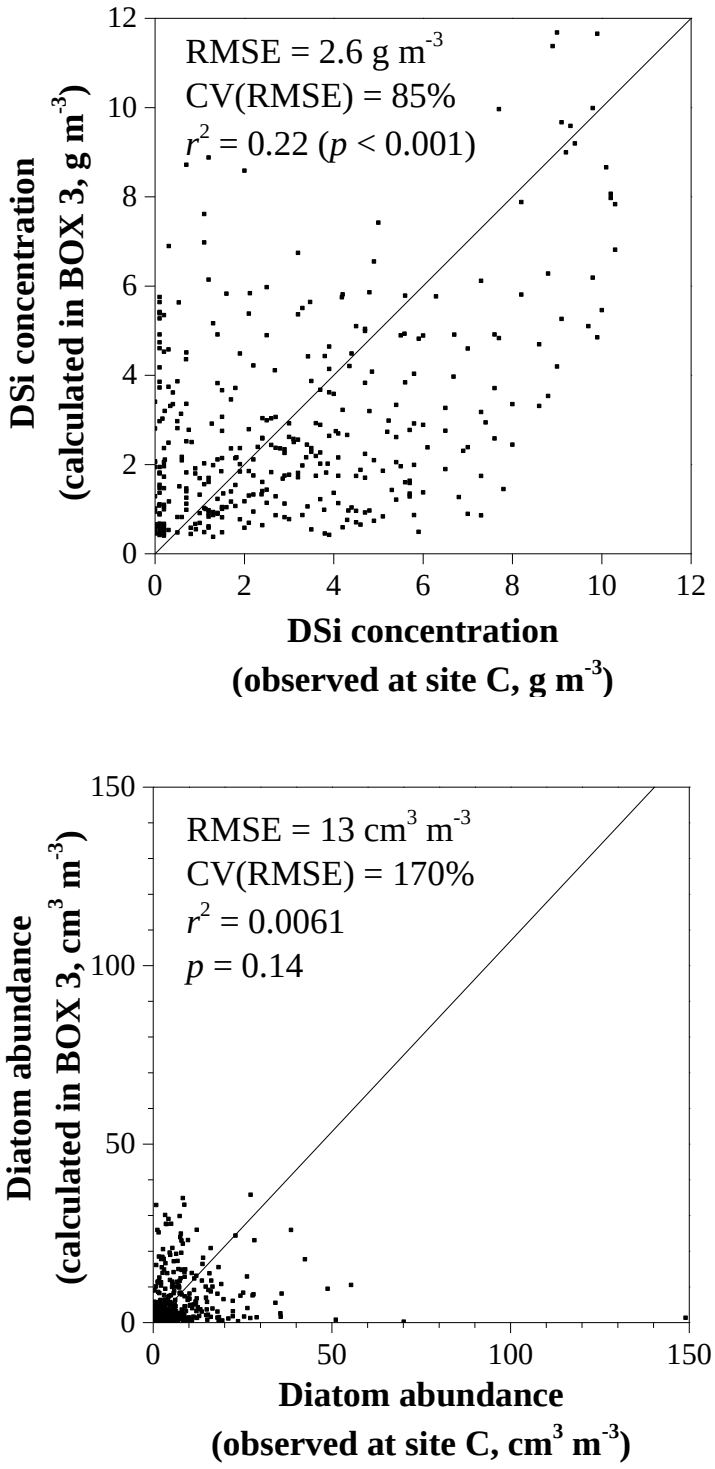

Figure 6.14 Comparisons of monthly observation data at site C with model predictions in BOX3 for DSi (**a**) and diatoms (**b**) during 1981–2010

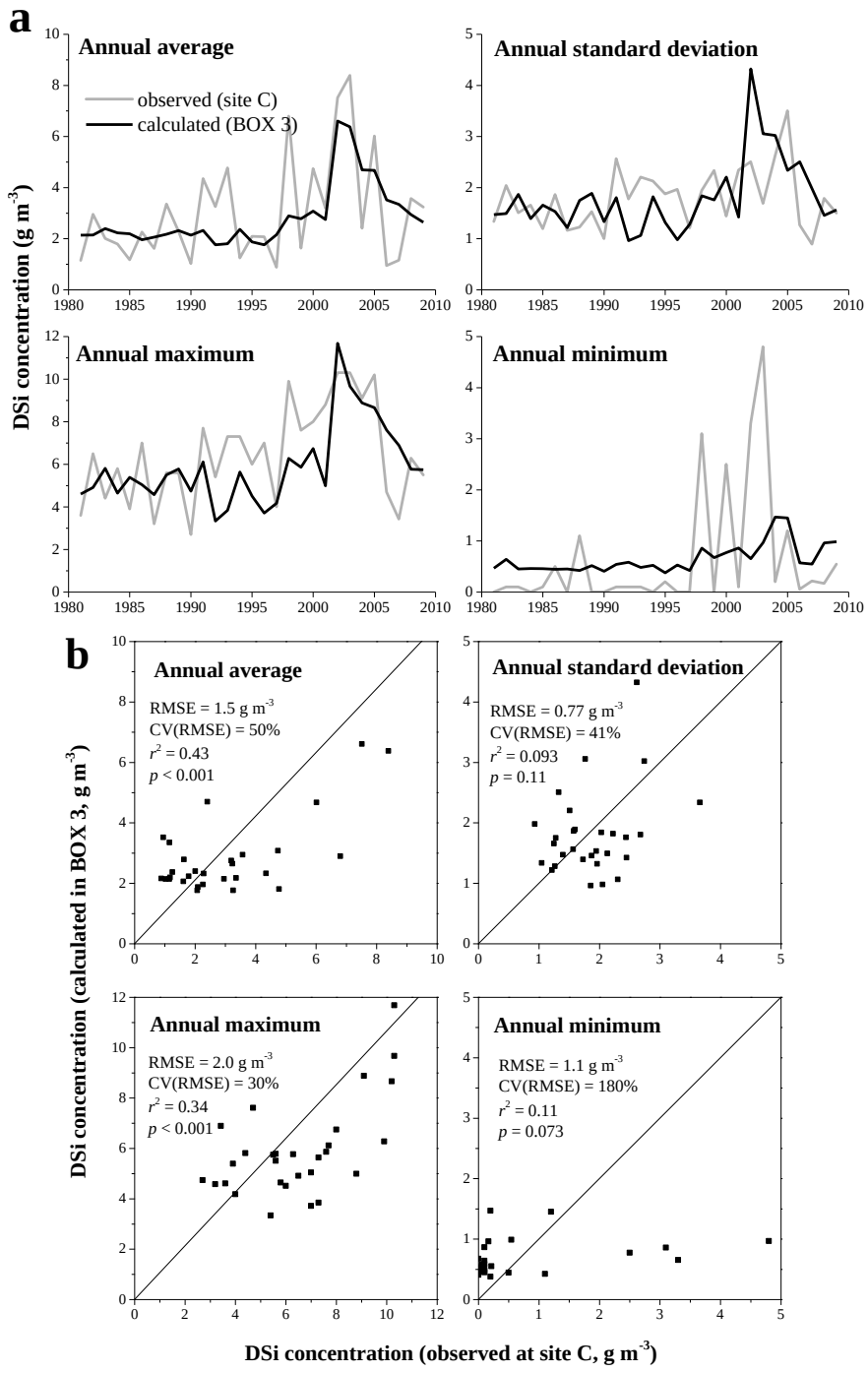

Figure 6.15 Long-term changes in annual statistics of DSi concentration calculated by model simulation in BOX 3 and observed at site C (**a**) and comparisons of them (**b**) during 1981–2010. Annual statistics were calculated for the year from August to July. Model predictions on the observation date were used to calculate annual statistics

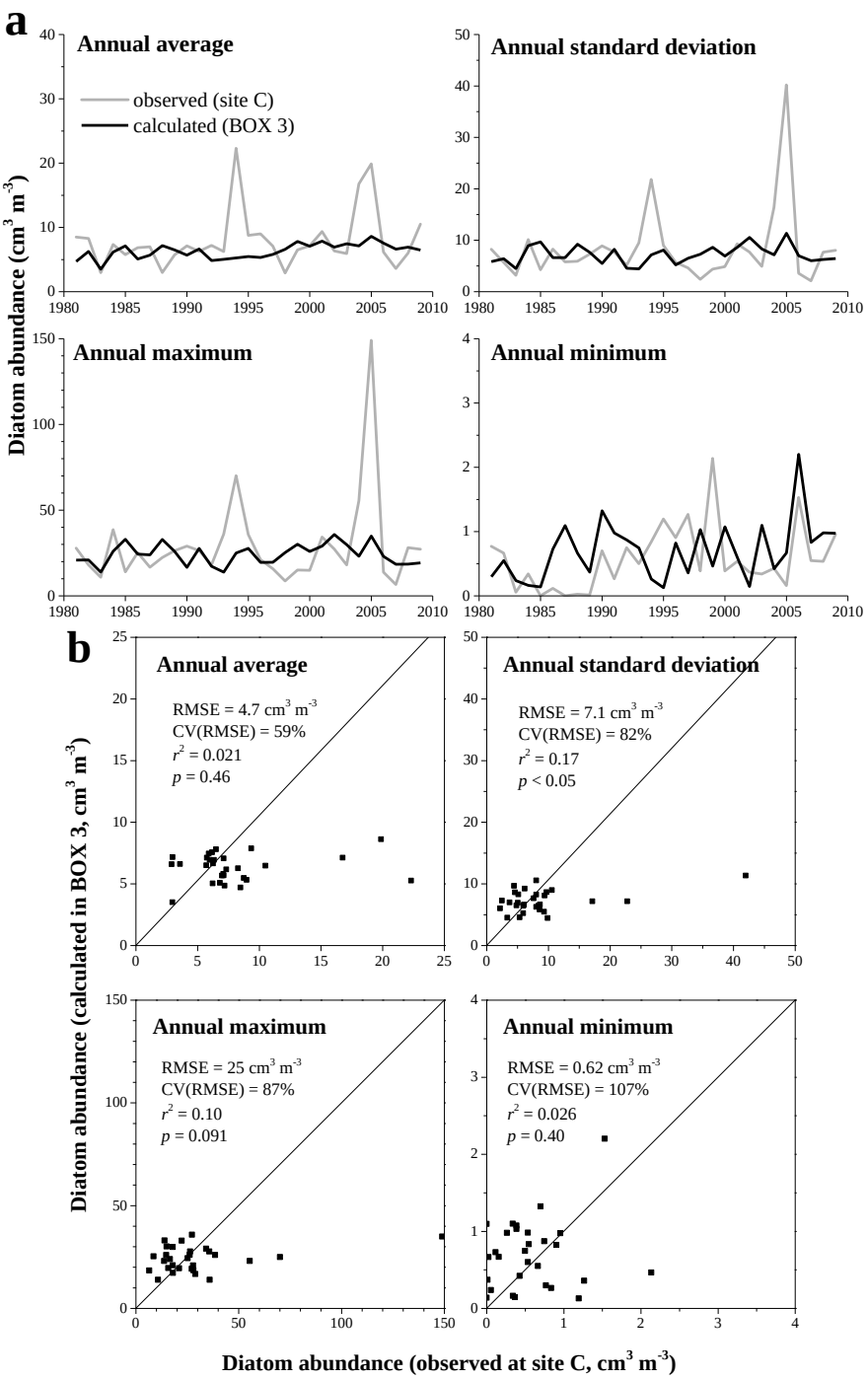

Figure 6.16 Long-term changes in annual statistics of diatom abundance of model predictions in BOX 3 and observed data at site C (**a**) and comparisons of them (**b**) during 1981–2010. Annual statistics were calculated for the year from August to July. Model predictions on the observation date were used to calculate annual statistics

data ($p < 0.001$). On the other hand, CV of annual standard deviation, maximum, and minimum diatom abundance was more than 80%, while CV of annual mean diatom abundance was 59%. Model prediction was not significantly related to the observation data except annual standard deviation ($p < 0.05$). These results suggest that the long-term changes in DSi concentrations were reproduced with more sufficient accuracy than diatom abundances. Although peaks of diatom blooms were underestimated in some years (e.g., 1994, 2005, and 2006), long-term increasing trends of both DSi and diatoms were detected for model predictions as well as observed data (12 month moving average; $p < 0.001$).

Seasonal changes in DSi concentration were relatively well-simulated (**Figure 6.17**). RMSE (CV) of decadal average during 1981–1990, 1981–1990, and 2001–2010 were 1.2 g m^{-3} (56%), 1.4 g m^{-3} (46%), and 1.4 g m^{-3} (34%), respectively. In addition, decadal average of model predictions were significantly related to observation data during 2001–2010 ($r^2 = 0.37$, $p < 0.05$) and close to significant level during 1981–1990 ($r^2 = 0.30$, $p = 0.063$) and 1991–2000 ($r^2 = 0.30$, $p = 0.064$).

Seasonal changes in diatom abundance were shown in **Figure 6.18**. RMSE (CV) of decadal average during 1981–1990, 1981–1990, and 2001–2010 were 3.9 cm^3 m^{-3} (65%), 8.1 cm^3 m^{-3} (96%), and 8.5 cm^3 m^{-3} (92%), respectively. Decadal averages of model predictions were significantly related to observation data during 1981–1990 ($r^2 = 0.71$, $p < 0.001$), but no significant correlation during 1991–2000 ($r^2 = 0.063$, $p = 0.43$) and 2001–2010 ($r^2 = 0.048$, $p = 0.49$). In spring, model predictions of diatom blooms might have a lag time of a month compared to observation data during 1991–2000. Although the peak of diatom blooms were underestimated in some years, observed change in a seasonality of diatom blooms, from spring and autumn during 1981–1990 to

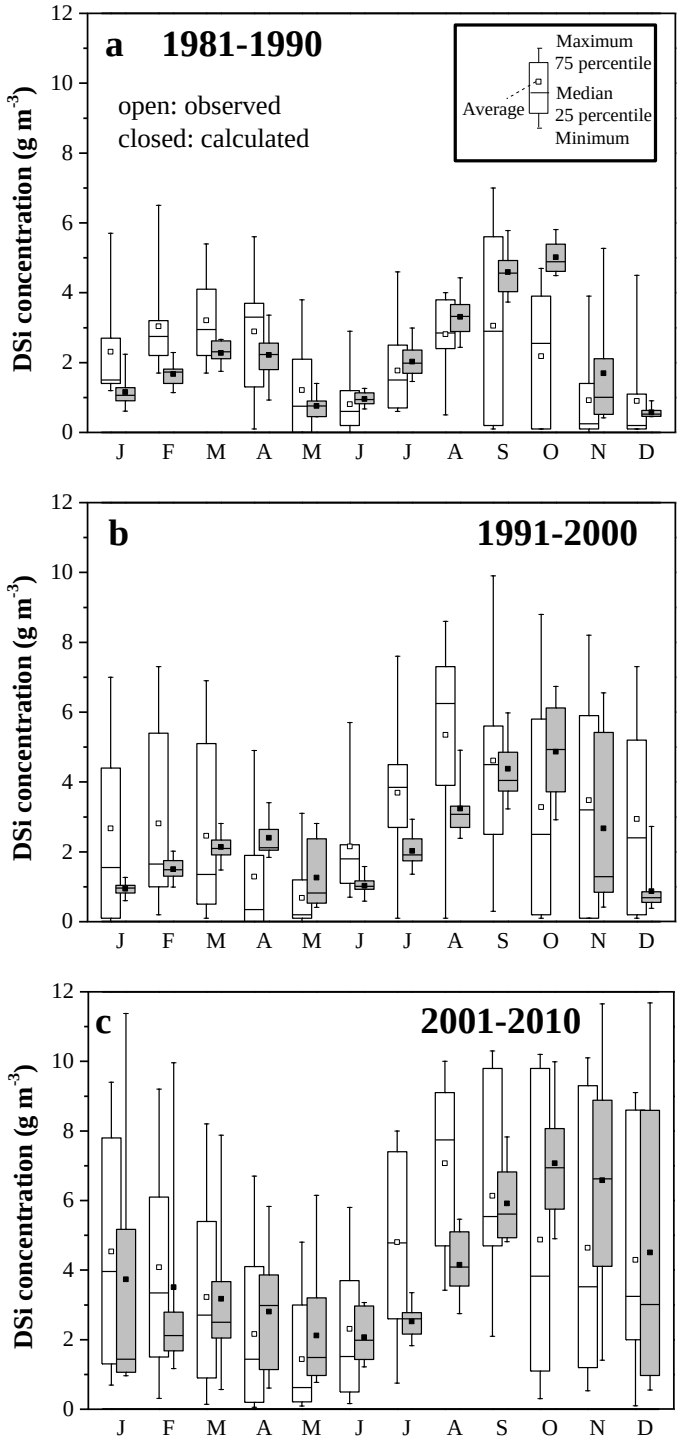

Figure 6.17 Monthly changes in decadal statistics of DSi concentration calculated in BOX 3 and observed at site C during 1981–1990 (**a**), 1981–1990 (**b**), and 2001–2010 (**c**). Model predictions on the observation date were used to calculate decadal statistics

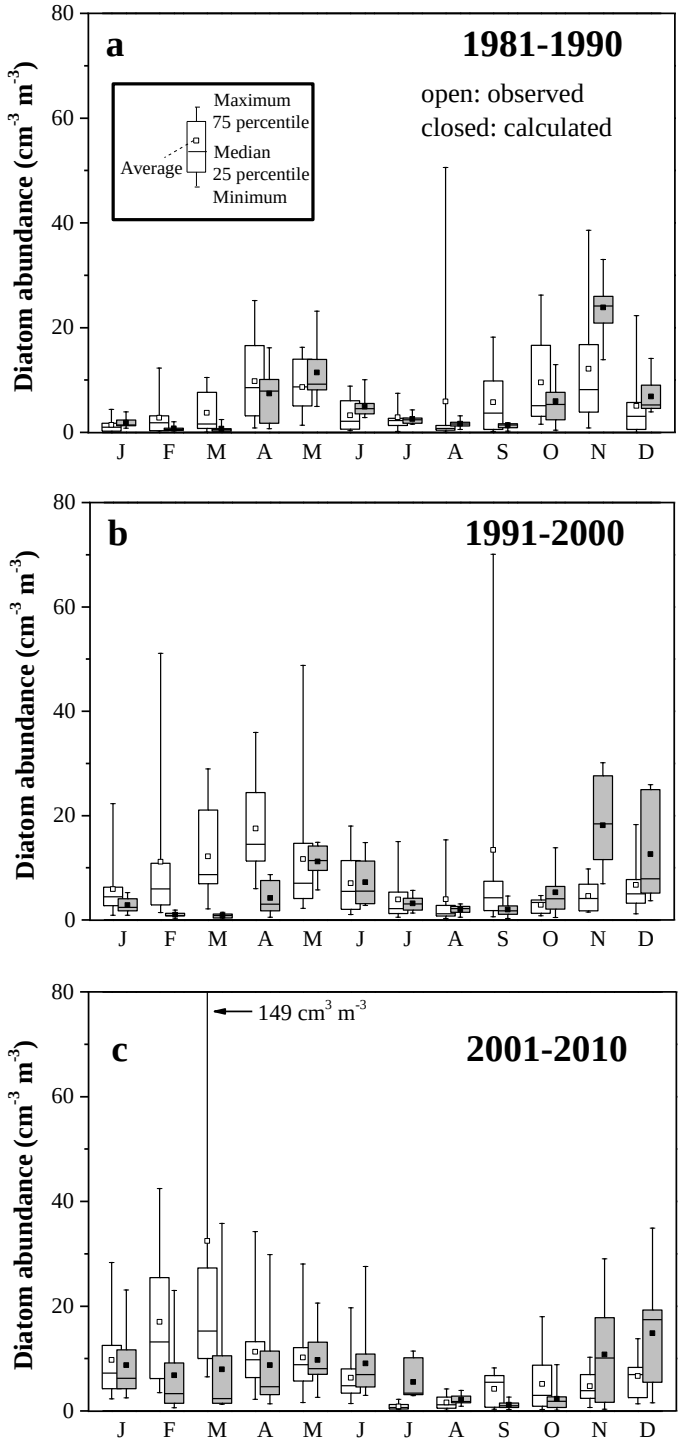

Figure 6.18 Monthly changes in decadal statistics of diatom abundance calculated in BOX 3 and observed at site C during 1981–1990 (**a**), 1981–1990 (**b**), and 2001–2010 (**c**). Model predictions on the observation date were used to calculate decadal statistics

winter–spring period during 2001–2010, was comparatively reproduced by the model. Moreover, Fourier analysis showed that model predictions of diatom abundance had a cyclic period of 6 and 12 months, same as observation data (**Figure 6.19a**). Change in frequency of diatom blooms, twice a year during 1981–1990 and once a year during 2001–2010, was also obtained by model simulation (**Figure 6.19b**, **c**, **d**).

The shift of seasonal relationships between DSi concentration and diatom abundance, from two-round loop during 1981–1990 with spring and autumn diatom blooms to one-round big loop during the 2001–2010 with extensive winter–spring blooms, was nearly reproduced by model simulation (**Figure 6.20**).

6.4 Discussion

6.4.1 Causes for error of simulation

Most high peaks of diatom blooms were underestimated by model simulation (**Figure 6.13**, **6.16**), which might be attributed in part by time intervals of observation data used in calibration. Monthly observation data was used for parameter calibration in the model; however, diatom abundance varied enormously in a month (e.g., 5.0 cm^3 m^{-3} on 20th September 1984, 24 cm^3 m^{-3} on 4th October 1984, and 5.5 cm^3 m^{-3} on 24th October 1984; NIES observation at site C). Moreover, constant diatom parameters might cause an error due to several species existing in the field. For example, diatom abundance was not simulated well during 1994 and 1995 (**Figure 6.13**), when significant blooms consisting of *Synedra* spp. were observed transiently (**Figure 6.3, 6.4**). Additionally, peaks of diatom abundance were lower than observed ones in the first half of 2005 and

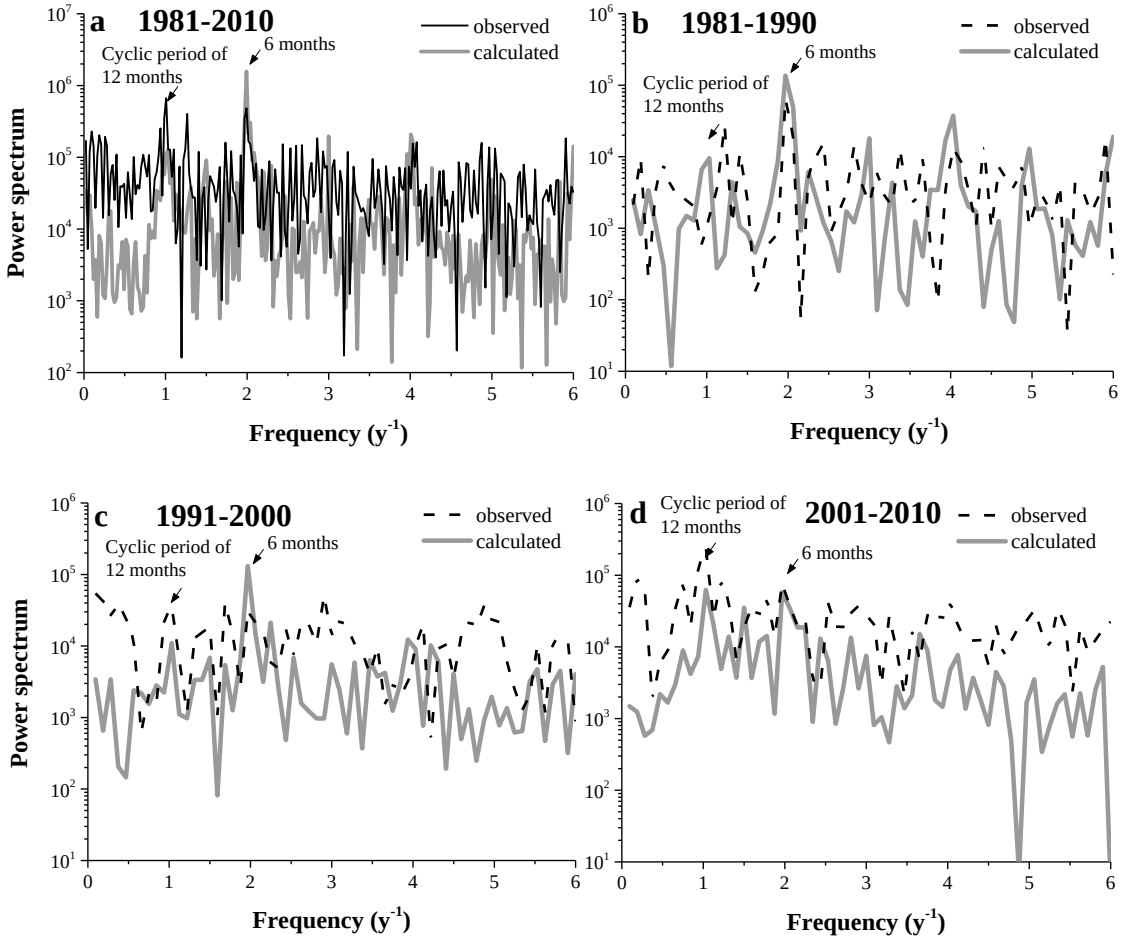

Figure 6.19 Power spectrums of model predictions of diatom abundance in BOX 3 during the entire period (**a**), 1981–2010 (**b**), 1991–2000 (**c**), and 2001–2010 (**d**). Model predictions on the observation date were used for Fourier analysis

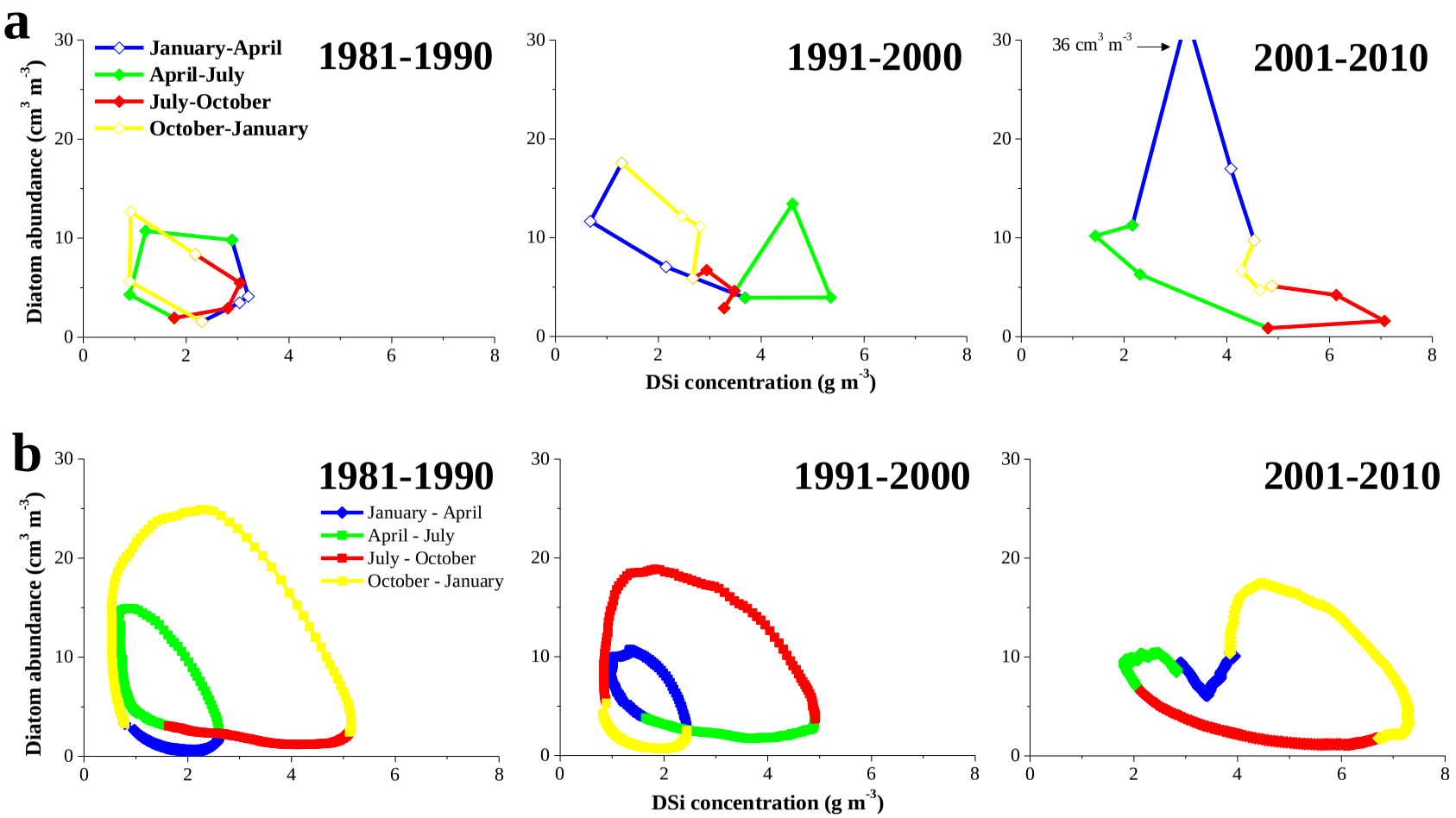

Figure 6.20 Mean seasonal changes of DSi concentration and diatom abundance observed at site C (**a**) and calculated in BOX 3 (**b**) during 1981–1990, 1991–2000, and 2001–2010

2006 even though beginning of blooms was relatively well simulated (**Figure 6.13**, BOX 3). Several studies indicated that diatom sinking rate was different between growing season and depletion season; that is, rapid sinking of diatoms occurs under nutrient limitation in fresh water (Titman and Kilham 1976; Sommer and Stabel 1983; Conley et al. 1989) and in physically stable water columns (Reynolds 1973; Scavia and Fahnenstiel 1987). These reports suggest that the model with constant sinking rate of diatoms could not reproduce the observed peaks in these years.

6.4.2 Influence of DSi release and degradation of light condition on long-term changes in diatom blooms

Among the input variables of the model, increasing trend was detected only for SS concentration derived from sediment resuspensin SS_{sed} (**Figure 6.21**). Sediment resuspension, pronouncedly increased in the early 2000s, probably caused not only an increase in DSi release amount but also degradation of light condition. For investigating those impacts on diatom blooms, DSi concentration and diatom abundance were calculated by assuming no recent intense resuspension of bottom sediments (**Table 6.5**, *Case-1*) to be compared with the results of the simulation shown in **Figure 6.12** and **6.13**. Now, the simulation shown in **Figure 6.12** and **6.13** is called as "standard simulation". The calculated DSi concentrations and diatom abundances of *Case-1* were usually lower than the "standard simulation" during the 2000s (**Figure 6.22**). In fact, there was no significant trend for DSi concentration and diatom abundance of *Case-1* during 1981–2010. Seasonal relationships between DSi and diatoms of *Case-1* showed two-round loop on average during 2001–2010 (**Figure 6.23b**), being difference from the "standard simulation" (**Figure 6.23a**). On the other hand, DSi concentration and diatom

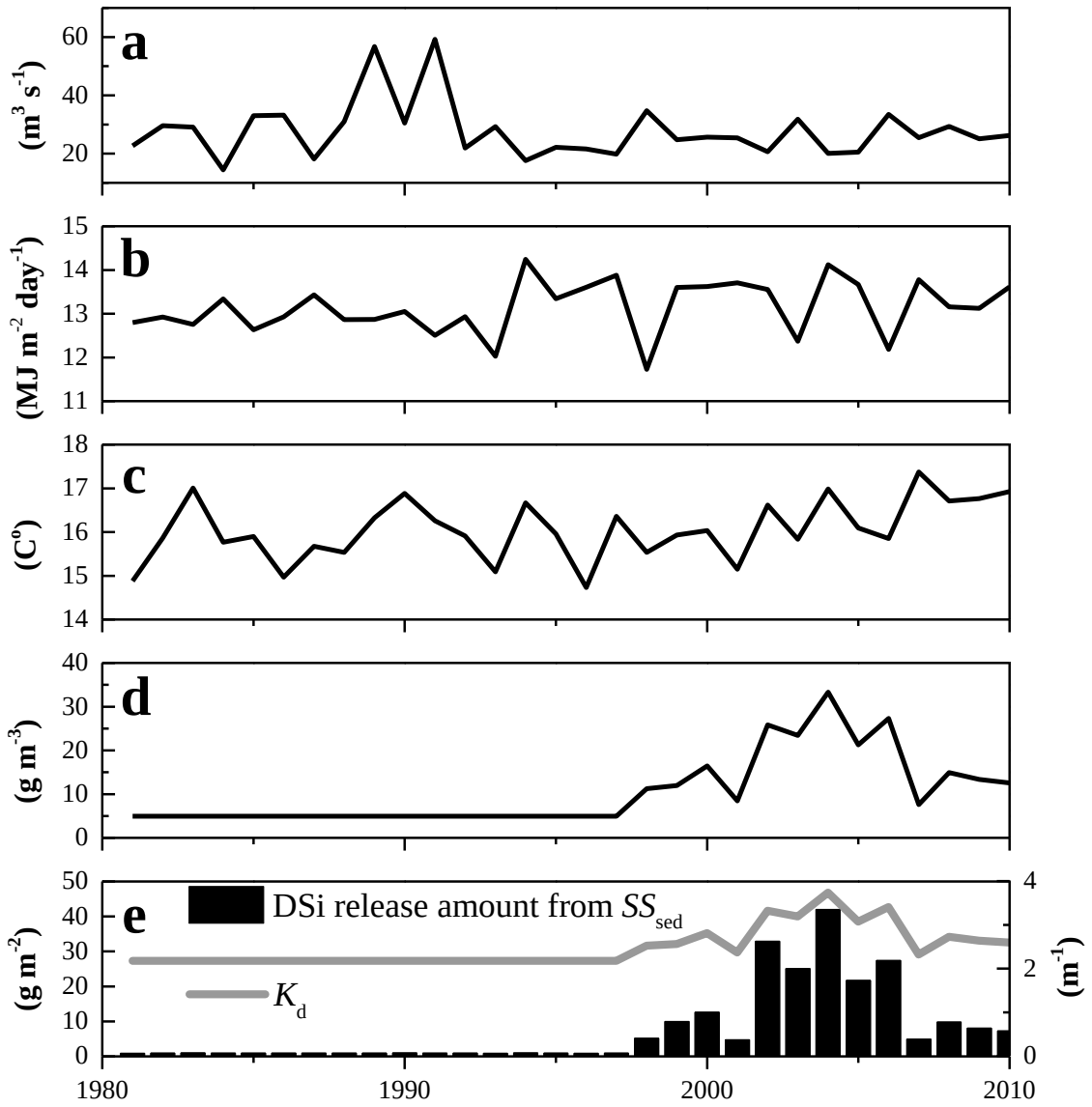

Figure 6.21 Annual averages of model input variables such as discharge of the rivers inflowing the entire lake (**a**), daily solar irradiance (**b**), water temperature in BOX 3 (**c**), and SS concentration derived from sediment resuspensin SS_{sed} in BOX 3 (**d**) and annual total amount of DSi released from SS_{sed} and annual mean light attenuation coefficient in water K_d estimated from SS_{sed} in BOX 3 (**e**)

Table 6.5 Difference of the input variables and parameters between the "standard simulation", simulation of *Case-1*, and of *Case-2*

Input variables or parameters	Symbol	"standard simulation" (simulation in Figure 6.12 and 6.13)	*Case-1* (no recent intense sediment resuspension)	*Case-2* (no DSi release from SS)
SS derived from sediments	SS_{sed}			
1981–1997		simulated values in 1997 [a]		
1998–2010		estimates from monitoring data in each year [b]	simulated values in 1997 [a]	estimates from monitoring data in each year [b]
Dissolution rate constant (day^{-1})				
Fresh diatom frustules	k_f	1.3	1.3	0
Old diatom frustules	k_o	5×10^{-3}	5×10^{-3}	0
Change from the period 1981–1990 to 2001–2010 [c]				
DSi amount released from SS_{sed}		↑	→	→
Light attenuation coefficient K_d		↑	→	↑
Diatom abundance		↑	→	↓
Frequency of blooms per year during 2001–2010		1	2	approximately 1

[a] Seki et al. (2006)

[b] see Table 6.2

[c] ↑, increase; ↓, decrease; →, no trend

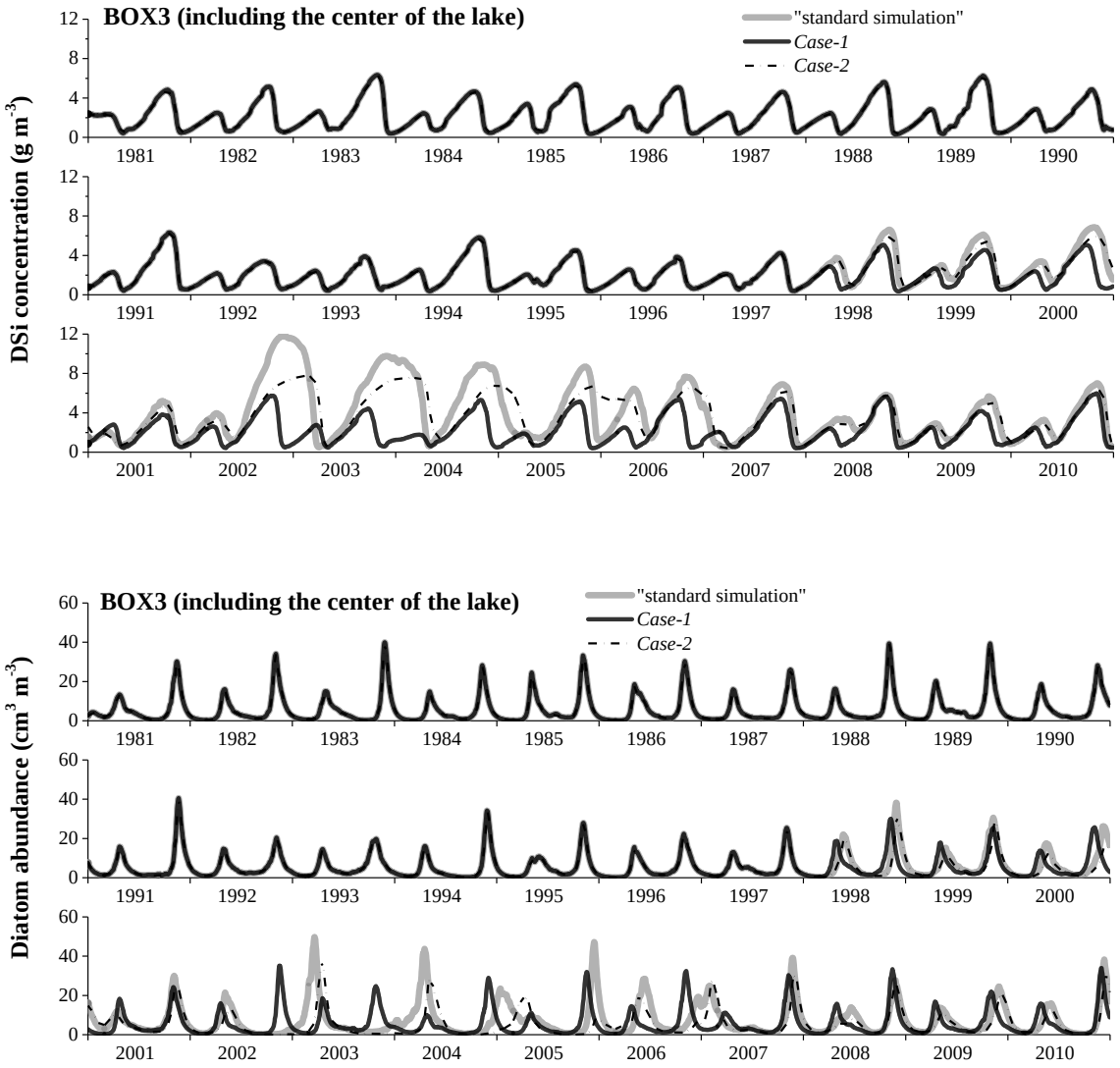

Figure 6.22 Model predictions for DSi and diatoms in BOX 3 calculated by the "standard simulation", simulation of *Case-1*, and of *Case-2*

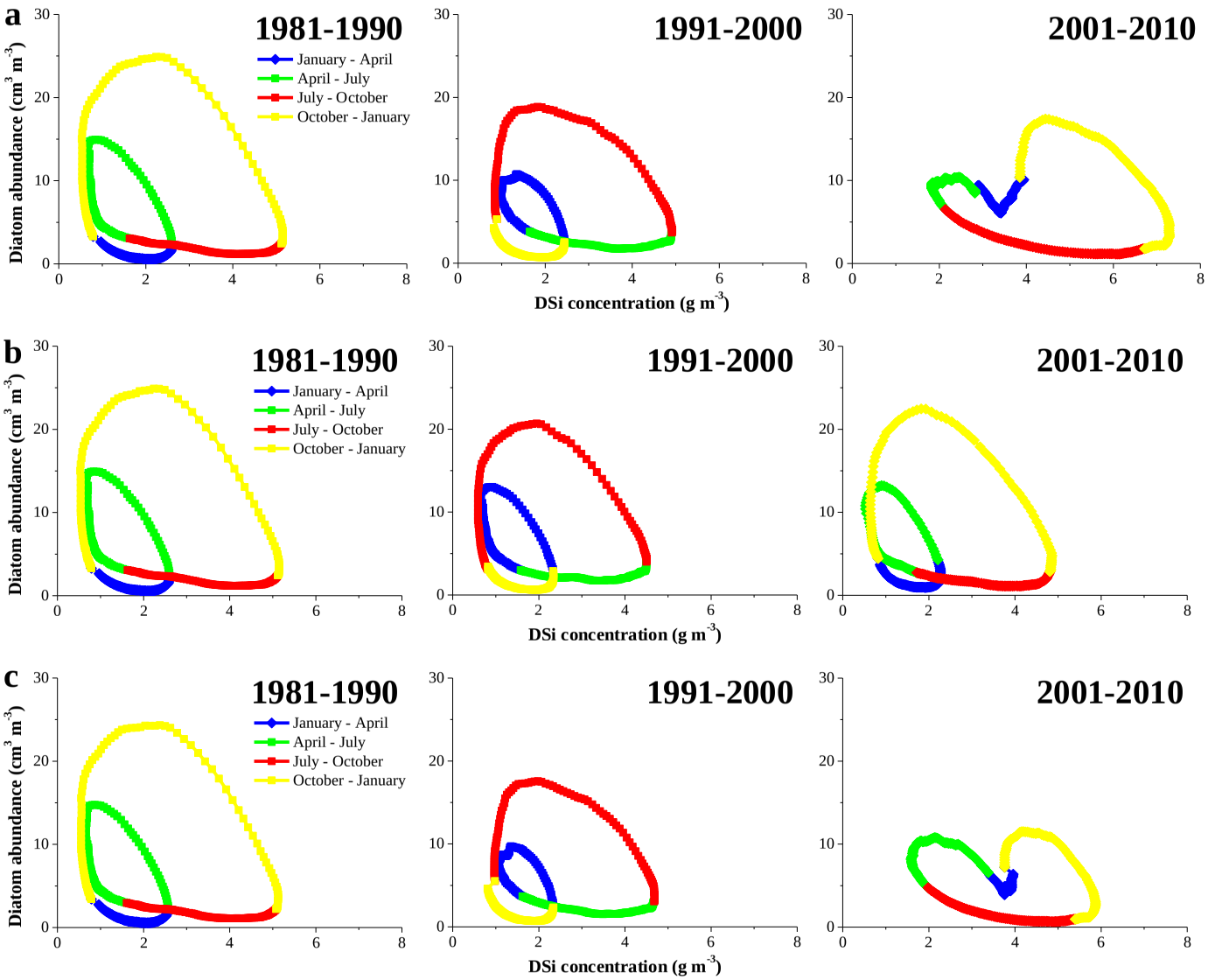

Figure 6.23 Mean seasonal changes of DSi concentration and diatom abundance in BOX 3 calculated by the "standard simulation" (**a**), simulation of *Case-1* (**b**), and of *Case-2* (**c**) during 1981–1990, 1991–2000, and 2001–2010

abundance were calculated by assuming that the recent sediment resuspension occurred but DSi release rate from SS was zero during the entire period (**Table 6.5**, *Case-2*). The results of *Case-2* represented diatom blooms at once a year during some years (e.g., 2003 and 2004) (**Figure 6.22, 6.23c**). Therefore, DSi release from SS_{sed} alone could never explain the observed change in seasonality of diatom blooms. These results suggested that degradation of light condition by resuspension might play an important role in the changes of a seasonality of diatom blooms. As a result of *Case-2*, annual maximum diatom abundance in BOX 3 were 20–50% lower than those by the "standard simulation" for 2002–2006 (**Figure 6.22**), nearly same as *Case-1*, indicating the impacts of the recent release on diatom blooms in the lake. Although annual maximum DSi concentrations of *Case-2* were about 20–30% lower than those by the "standard simulation" for the same period, an increasing trend of DSi concentration was detected ($p < 0.001$), suggesting the impacts of a weakening of diatom blooms due to degradation of light condition on DSi concentration.

6.4.3 Comparison among budgetary calculations

(D + B) Si budgets calculated by the "standard simulation" and simulation of *Case-1* were compared with those by budgetary analysis based on the long-term database shown in chapter 5 (**Table 6.6**). The values of the "standard simulation" were close to those described in chapter 5, on average during the last three decades. Based on the simulation the "standard simulation", the river input and release account for about 60% and 40% of total (D + B) Si inputs, which are close to the percentages 70% and 30% estimated in chapter 5, respectively. In addition, the river output and BSi gross sedimentation account for 30% and 70% of total output, which are within to the ranges 70–90% and 10–30% estimated by the budgetary analysis in chapter 5, respectively.

Table 6.6 **(**D + B) Si budgets in Lake Kasumigaura estimated by budgetary analysis based on the long-term database (see chapter 5) and calculated by the "standard simulation" and the simulation of *Case-1*

(10^9 g $year^{-1}$)	**Budgetary analysis**			**"standard simulation"**			***Case-1***		
	1980–2007	1980s	2000s	All period	1981–1990	2001–2010	All period	1981–1990	2001–2010
Input	**12–17**	**12–16**	**13–19**	**13**	**13**	**14**	**12**	**13**	**12**
River input of DSi	8–12	8–12	8–12	8	8	7	8	8	7
DSi release	4–5	4	5–7	5	5	7	5	5	5
from bottom sediments	4.3	4.3	4.3	4.1	4.3	3.8	4.4	4.3	4.4
from SS	0.3–0.9	0?	1.0–2.7	1.3	0.2	3.1	0.2	0.2	0.2
Output	**11–33**	**7–18**	**19–52**	**13**	**13**	**14**	**12**	**13**	**12**
River output	3	2	6	4	3	4	3	3	3
DSi	2.6	1.4	4.4	3.2	3.0	3.6	2.7	3.0	2.4
BSi	0.7	0.4	1.2	0.3	0.4	0.4	0.3	0.4	0.3
BSi gross sedimentation	8–30	5–16	13–46	10	10	10	9	10	9
Apparent accumulation (determined by core analysis)	10	10	10						

Although the recent amount of DSi released from SS by the “standard simulation” was close to the maximum estimation by budgetary analysis during the 2000s, the increase in river output of (D + B) Si was not so much as the results of budgetary analysis. It might be caused by DSi uptake by diatoms and their rapid sinking in the model. The BSi gross sedimentation by the “standard simulation” was lower than that by budgetary analysis; however, close to BSi apparent accumulation rate calculated by analyzing sediment cores (**Table 6.6**). It suggests the underestimation of gross sedimentation by the “standard simulation” due to inaccuracy in peaks of diatom blooms and/or overestimation of that by budgetary analysis in chapter 5 due to an incompatibility of the parameters such as diatom sinking rate.

6.4.4 Factors influencing seasonality of diatom blooms

Although only physical environment was considered for estimating diatom abundances in the model, daily changes in diatom abundance were probably influenced by physiological and/or ecological factors such as other phytoplankton appearance and predation pressure. Laboratory experiments by Bienfang et al. (1982) demonstrated the rapid sinking of some diatom species after DSi depletion, and they did not come back soon in water column after addition of nutrients. This report was consistent with the hysteresis loop of DSi and diatoms seasonally observed in Lake Kasumigaura (**Figure 6.9**). However, the typical seasonality could be nearly simulated by the box model with only considering physical condition and constant diatom parameters such as sinking rate (**Figure 6.20**). This result suggests that physical condition is one of the causes for the observed hysteresis loop.

The influence function of irradiance f_I, temperature f_T, and DSi concentration f_{Si} on diatom growth are shown for 1982–1984 (**Figure 6.24**) and 2002–2004 (**Figure 6.25**),

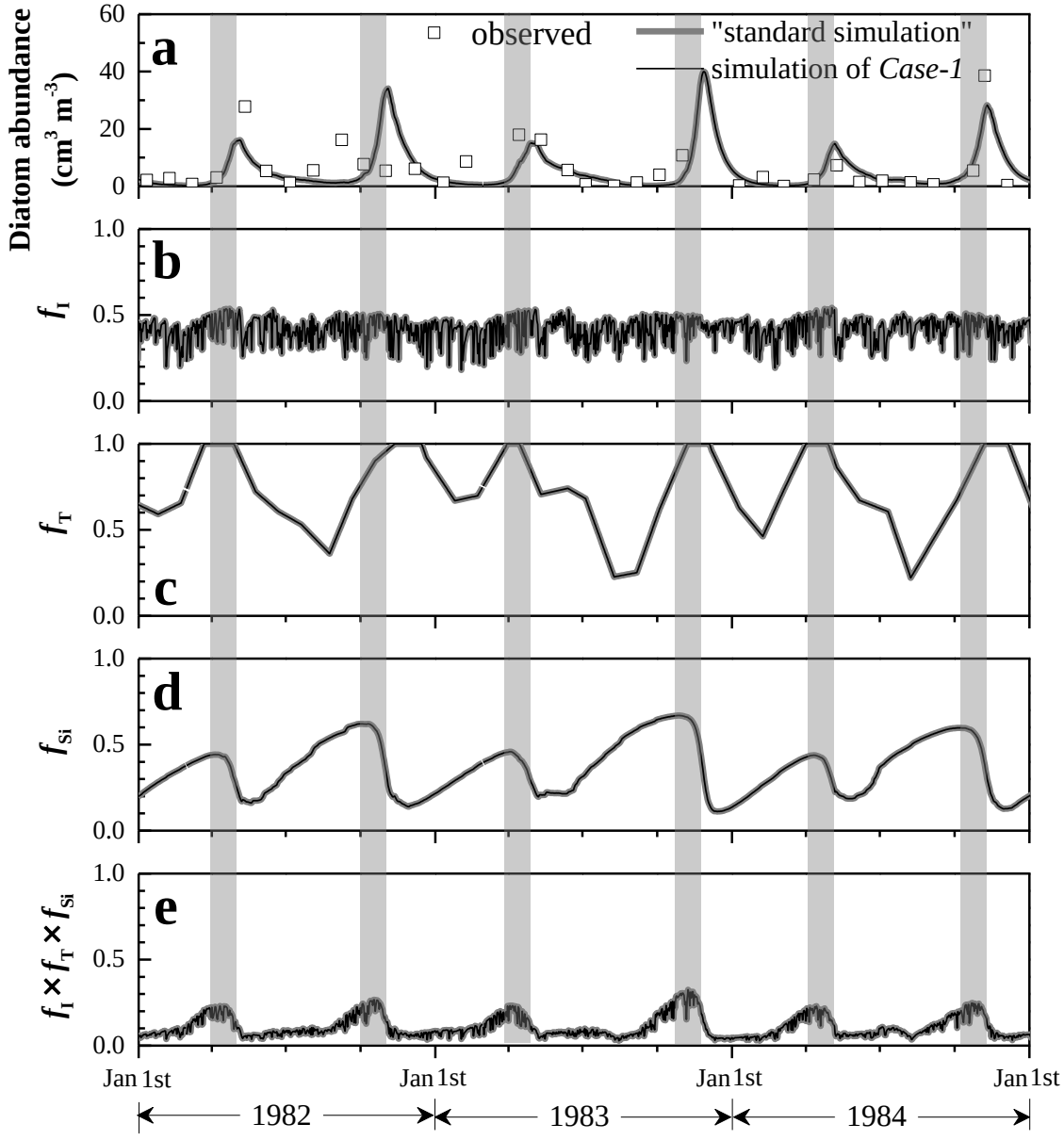

Figure 6.24 Model predictions and observation data for diatoms (**a**), influence functions of irradiance f_I (**b**), temperature f_T **(c)**, and DSi concentration f_{Si} (**d**) on diatom growth at 12:00 noon, and products of multiplication of f_I, f_T, and f_{Si} (**e**) in BOX 3 during 1982–1984. They were calculated by the "standard simulation" or simulation of *Case-1*. The gray zones through (**a**) to (**e**) indicate the growing season of diatoms in the "standard simulation". Observation was missing in March and December 1983

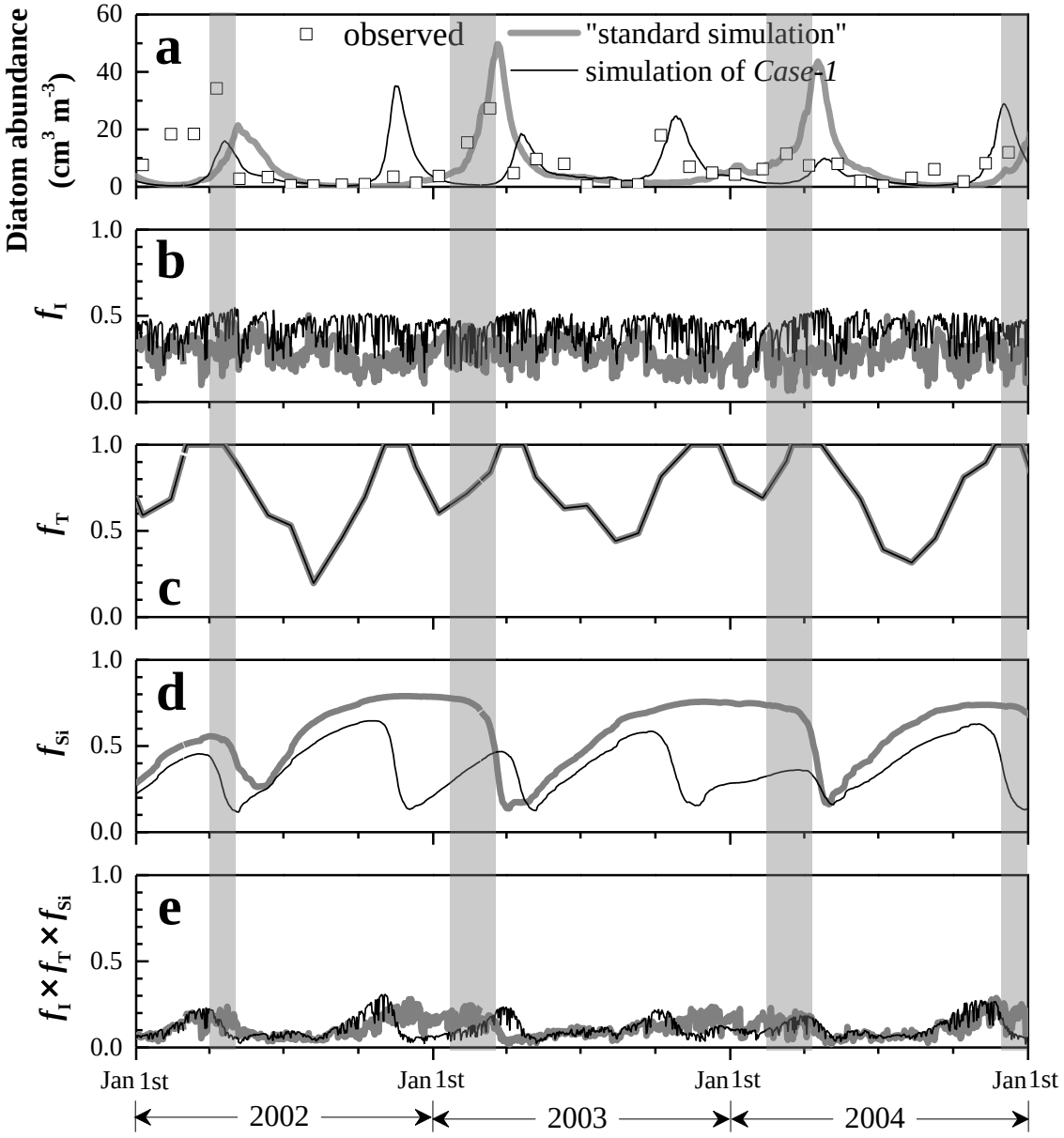

Figure 6.25 Model predictions and observation data for diatoms (**a**), influence functions of irradiance f_I (**b**), temperature f_T **(c)**, and DSi concentration f_{Si} (**d**) on diatom growth at 12:00 noon, and products of multiplication of f_I, f_T, and f_{Si} (**e**) in BOX 3 during 2002–2004. The gray zones through (**a**) to (**e**) indicate the growing season of diatoms in the "standard simulation". They were calculated by the "standard simulation" or simulation of *Case-1*

as a representative of the year spring and autumn blooms and winter–spring blooms observed, respectively. During each period, while short fluctuation range of f_I in a year, f_T and f_{Si} changed substantially. During 1982–1984, an increase in diatom abundance was not obtained during the increase in f_{Si}, but obtained when f_T approaching optimal temperatures (e.g., in the second half of 1982). Therefore, timing of the beginning of diatom blooms probably depends mainly on water temperature. On the other hand, a timing of the ending of diatom blooms probably depends mainly on DSi concentration due to radical decline of f_{Si} during blooming. Seasonal patterns of f_{Si} in 1982–1984 were similar to those of *Case-1* during 2002–2004, but not of the "standard simulation". For instance, autumn blooms were not observed in 2002 and winter–spring blooms were observed in the first half of 2003, which was well reproduced by the "standard simulation" but not the simulation of *Case-1*. During autumn in 2002, the products of multiplication of f_I, f_T, and f_{Si} of the "standard simulation" were less than those of *Case-1* in spite of larger f_{Si} of the "standard simulation" than the simulation of *Case-1*. During the same period, f_I of the "standard simulation" was less than that of *Case-1*; therefore, degradation of light condition might prevent autumn diatom blooms. Peaks of diatom blooms of the "standard simulation" were higher than that of *Case-1*. It could be derived from high f_{Si} which lasted a long time until bloom ending, probably caused by high DSi concentration at the beginning of blooms.

As results, I propose the following scenario about winter–spring blooms observed in recent years; (1) beginning of autumn blooms got delay due to degradation of light condition, (2) blooms lasted for several months due to DSi concentration which were sufficient for diatom growth. Diatom blooms were observed during winter–spring

period but not in summer–autumn, which might be related to lower f_T remaining for several months during summer than winter.

6.4.5 Other factors influencing long-term trends in diatom abundance

In Lake Kasumigaura, a shift of dominant diatom species was observed during the last three decades (**Figure 6.4**). During the 2000s, *Cyclotella* spp., especially *C. meneghiniana*, was most dominant. Their growth rate is relatively fast (**Table 6.3**); therefore, they could form extend blooms under better condition for them such as high DSi concentration. It might be related the underestimation of peaks of recent diatom abundance based on the model simulated (**Figure 6.13**, **6.16**).

In the light of nutrient for diatoms, the increase in phosphorus (P) concentration, observed in the lake during the last three decades, might also be related to diatom blooms. However, nutrient atomic ratios indicated that Si is one of the most crucial factors limiting diatom growth (**Figure 6.5**).

6.5 Conclusions

In Lake Kasumigaura, diatom abundance significantly increased during the last three decades. Seasonality of diatom blooms shifted from spring and autumn to winter–spring period; therefore, the relationships between DSi and diatoms changed from two-round during the 1980s to one-round during the 2000s. Nutrient limitation for diatoms was analyzed by nutrient atomic ratios N:P:Si, which provided a suggestion of Si limitation during blooms in most years. Modeling and simulation of major processes involved in

DSi and diatoms reproduced spring and autumn blooms during the 1980s and winter–spring blooms during the 2000s. Peaks of diatom blooms were underestimated in some years, suggesting an influence of the observed shift of diatom species and other physiological and/or ecological factors. Peaks of diatom blooms declined by removal of DSi release from resuspended sediments removed, which indicated the impacts of the recent release on diatom blooms in the lake. Seasonality of diatom blooms did not changed by removal of DSi release from SS; however, it changed by removal of sediment resuspension causing both DSi release and degradation of light condition, suggesting the contribution of degradation of light condition by resuspension to the observed change of the loop from two-round to one-round. These findings implicate the significance of the interactions between sediments and water to phytoplankton blooms.

Chapter 7

General Conclusions

7.1 Significance of Si regeneration by sediment resuspension in a shallow eutrophic lake

In shallow lakes, sediment resuspension had been often observed (Amano et al. 2002; Seki et al. 2006). Regeneration of N and P was indicated in several studies (Amano et al. 2002). On the other hand, Si was focused only on release from bottom sediments in the previous studies. In this dissertation, I found a significance of DSi release from SS in a shallow lake, which explained the increasing trend of DSi in Lake Kasumigaura during the last three decades.

In Lake Kasumigaura, the amount of DSi released from SS was 20–40% of the total amount of DSi released during high sediment resuspension period. Total amount of DSi released from SS and bottom sediments for this period might be about two-third of the loads from inflows. These results suggested that DSi release from SS might not be neglected for budgetary analysis of Si in some shallow lakes where sediments are resuspended by wind easily and contains BSi plentifully.

7.2 Application of information of Si dynamics on management of water quality in a shallow eutrophic lake

Diatoms form a major part of the aquatic food web. From the viewpoint of prevention of harmful algal blooms (HABs), diatom species have been preferred. In addition, diatoms play a critical role in marine biogeochemical cycles, especially in the sequestration of carbon dioxide from the atmosphere via the biological pump (Schelske 1999; Ittekkot et al. 2006). Therefore, management and prediction of diatom blooms were important, especially in lakes and estuaries subjected by intense human activities.

In Lake Kasumigaura, cyanobacteria abundance declined when diatoms were dominant during the 2000s (**Figure 6.3**). Although other factors might cause a decrease in cyanobacteria abundance, small-scale blooms remained for the last decade, indicating that a possibility of preventing harmful algae by regulating diatom blooms. Tsunogai (1979) suggested that diatoms could be predominant under an ideal environmental condition for growth of phytoplankton in the ocean. Figueiras (2003) also indicated that diatoms have faster growth rate than others with adequate nutrient supply, but upward advection or turbulent mixing is required. These suggestions imply that shallow lakes suffering HABs have potentiality of occurrence of diatom blooms due to high nutrient loads from inflows and high turbulence condition by a wind.

The statistical analysis of observation data (**Figure 6.10**) and model simulations (**Figure 6.22**) in chapter 6 suggested that the scale of diatom blooms were mainly dependent on DSi concentration before blooms starting in Lake Kasumigaura. The significance of Si for diatoms was suggested both in marine and freshwater ecosystems

(Koszelnik and Tomaszek 2008); however, evidence for significant effects of Si dynamics on aquatic ecosystems in stagnant waters is sparse in the world (Humborg et al. 1997; Harashima 2007). In addition, the long-term changes in the dominant season of diatoms could be explained by model simulation with considering an effect of resuspension of bottom sediments, which promoted DSi release and degraded light condition in water column (**Figure 6.24, 6.25**). The results of this study suggested that not only N and P but also Si should be monitored regularly for management of algal occurrence in eutrophic lakes. N: P: Si stoichiometric ratio should also be investigated. In shallow lakes, the variance of turbidity is usually large; therefore, light condition should also be taken consideration for predicting diatom blooms.

7.3 Summary

Si dynamics and its impacts on diatom blooms were assessed in Lake Kasumigaura as a representative of shallow lakes, using various biogeochemical methods such as statistical analysis, laboratory experiment, budgetary analysis comparing with sediment core information, and simulation by a numerical model. Knowledge and information obtained by this dissertation was summarized as follows:

(i) Previous studies indicated an importance of Si cycling through release from bottom sediments. However, in a shallow lake, a significance of Si release from resuspended sediment was suggested in this study.

(ii) Long-term budgets of Si were calculated in a shallow lake and got consistency with the recent increase in a release amount from resuspended sediments

determined by laboratory experiments.

(iii) Model simulation suggested that DSi supply rate to lake water could be a crucial factor determining a scale of diatom blooms in a eutrophic lake. On the other hand, a seasonality of blooms might be influenced by a degradation of light condition in water column caused by sediment resuspension.

(iv) Significance of water-sediment interaction and its impacts on ecosystems were implied in a shallow eutrophic lake.

The above information suggested a complexity of Si dynamics in inland waters. Importance of taking considerable care in Si was implied for management in a shallow eutrophic lake, especially focusing on Si cycling and its influence on diatom blooms.

7.4 Further research

This dissertation focused on Si dynamics and relationships with diatom blooms in a shallow eutrophic lake. However, a part of role of Si for aquatic ecosystems remains poorly understood, such as effects of bacteria on BSi dissolution, long-term dissolution of sediment BSi, and impacts of Si dynamics on shift of dominant phytoplankton species. Especially, the last problem is intricately related to biogeochemistry and physiology. Global decreasing trend of DSi load from land to coastal area may become more acute in the near future, especially around a developing county such as in South East Asia where dam construction is active. For this reason, a continuous monitoring may be of more significance. For interpreting a long-term change, analyzing sediment cores can also bring useful information; however, still accumulated sediments should be

preferred for analyzing stratigraphy of BSi.

As for Lake Kasumigaura, the causes for sediment resuspension observed during the early 2000s are still unclear. Wind speed did not increase in that region. The sediment properties might become susceptible to resuspending by a wind, such as an increase in water content and a decrease in organic content (Seki et al. 2006); however, the external factors were not elucidated. In this study, the influence of sediment resuspension on Si dynamics and phytoplankton dominance was suggested. Therefore, the detailed studies approaching the mechanisms of intense sediment resuspension in the lake during the early 2000s is needed in future.

Acknowledgements

I would like to acknowledge my academic advisor, Professor Takehiko FUKUSHIMA, Environmental Modeling and Creation, Integrative Environmental Sciences, Graduate School of Life and Environmental Sciences, University of Tsukuba. This dissertation would not have been completed without his valuable guidance and encouragement.

I would like to sincerely thank Professor Yuichi ONDA, Associate Professor Bunkei MATSUSHITA, and Associate Professor Tsutomu YAMANAKA for their helpful discussions and corrections for this dissertation. I also thank Associate Professor Teruyuki MARUOKA and Lector Ryo ANMA for their constructive comments at seminars.

This research would not have been possible without the long-term field data; for this reason I would like express my thanks to the National Institute for Enviromnental Studies (NIES) and Kasumigaura River Office. I really thank Dr. Akio IMAI and Dr. Kazuhiro KOMATSU at NIES for their comments on my presentation, published papers, and so on.

The part of this dissertation was written based on my two published papers (Arai et al. 2012; Arai and Fukushima 2012). Therefore, I appreciate the anonymous reviewers for the constructive comments on these papers. I also thank to the participants in the domestic or international academic forum commenting to my presentation.

I spent about six worthwhile years in my laboratory, and thank every member for

their direct or indirect contribution to the entire research. I am grateful to Dr. Yoichi OYAMA, Dr. Eiji KOMATSU, and Dr. Kazuya YOSHIMURA for their productive advice, especially relevant to technics for research such as field observation, laboratory experiment, and model simulation.

Finally, I would like to express my heartful gratitude to my parents and my wife for their support throughout the research period.

References

Alexander GB, Heston WM, Iler RK (1954) The solubility of amorphous silica in water. J Phys Chem 58:453–455

Amano K, Yasuda Y, Suzuki H (2002) Modeling of water quality change due to resuspension of bottom sediments in a shallow reservoir (in Japanese with English abstract). Mizu Kougaku Ronbunshuu 46: 1085–1090

Arai H, Fukushima T (2012) Silicon budget of eutrophic Lake Kasumigaura, Japan. J Soils Sediments 12:1501–1507

Arai H, Fukushima T, Komatsu K (2012) Increase in silicon concentrations and release from suspended solids and bottom sediments in Lake Kasumigaura, Japan. Limnol 13:81–95

Bailey-Watts AE (1976a) Planktonic diatoms and some diatom-silica relations in a shallow eutrophic Scottish loch. Freshw Biol 6:69–80

Bailey-Watts AE (1976b) Planktonic diatoms and silica in Loch Leven, Kinross, Scotland: a one month silica budget. Freshw Biol 6:203–213

Barbiero RP, Tuchman ML, Warren GJ, Rockwell DC (2002) Evidence of recovery from phosphorus enrichment in Lake Michigan. Can J Fish Aquat Sci 59:1639–1647

Bienfang PK, Harrison PJ, Quarmby LM (1982) Sinking rate response to depletion of nitrate phosphate and silicate in four marine diatoms. Mar Biol 67:295–302

Brzezinski MA (1985) The Si:C:N ratio of marine diatoms: Interspecific variability and the effect of some environmental variables. J Phycol 21:347–357

Conley DJ (1988) Biogenic silica as an estimate of siliceous microfossil abundance in Great Lakes sediments. Biogeochemistry 6:161–179

Conley DJ (1998) An interlaboratory comparison for the measurement of biogenic silica in sediments. Mar Chem 63:39–48

Conley DJ, Kilham SS, Theriot E (1989) Differences in silica content between marine and freshwater diatoms. Limnol Oceanogr 34:205–213

Conley DJ, Schelske CL, Stoermer EF (1993) Modification of the biogeochemical cycle of silica with eutrophication. Mar Ecol Prog Ser 101:179–192

Conley DJ, Stalnacke P, Pitkanen H, Wilander A (2000) The transport and retention of dissolved silicate by rivers in Sweden and Finland. Limnol Oceanogr 45:1850–1853

Conley DJ, Schelske CL (2001) Biogenic silica. In: Smol JP, Birks HB, Last WM (eds) Tracking environmental change using lake sediments. Kluwer Academic Publishers, Dordrecht

Conley DJ, Sommer M, Meunier JD, Kaczorek D, Saccone L (2006) Silicon in the terrestrial biogeosphere. In: Ittekkot V, Unger D, Humborg C, Tac An N (eds) The silicon cycle: human perturbations and impacts on aquatic systems. Island, Washington DC, pp 13–28

Cornwell JC, Banahan S (1992) A silicon budget for an Alaskan arctic lake. Hydrobiologia 240:37–44

DeMaster DJ (1981) The supply and accumulation of silica in the marine environment. Geochim Cosmochim Acta 45:1715–1732

Derry LA, Kurtz AC, Ziegler K, Chadwick OA (2005) Biological control of terrestrial silica cycling and export fluxes to watersheds. Nature 433:728–731

Duan S, Xu F, Wang LJ (2007) Long-term changes in nutrient concentrations of the Changjiang River and principal tributaries. Biogeochemistry 85:215–234

Ferris JA, Lehman JT (2007) Interannual variation in diatom bloom dynamics: Roles of hydrology, nutrient limitation, sinking, and whole lake manipulation. Water Res 41:2551–2562

Figueiras FG, Pitcher GC, Estrada M (2003) Harmful Algal Bloom Dynamics in Relation to Physical Processes. In: Graneli E, Turner JT (eds) Ecology of Harmful Algae. Springer Berlin Heidelberg, Berlin, pp 127–138

Foundation of River & Watershed Environment Management (2007) Research of the runoff mechanism for silicate and other dissolved inorganic matters in rivers (in Japanese).

Fukushima T (1984) Studies on the change characteristics and management of water quality in a shallow lake (in Japanese).

Fukushima T, Kawamura S, Seki T, Onda Y, Imai A, Matsushige K (2005) Why has Lake Kasumigaura become turbid? Verh Internat Verein Limnol 29 (2):732–737

Fukushima T, Kamiya K, Onda Y, Imai A, Matsushige K (2010) Long-term changes in lake sediments and their influences on lake water quality in Japanese shallow lakes. Fundam Appl Limnol, Arch Hydrobiol 177:177–188

Ferris JA, Lehman JT (2007) Interannual variation in diatom bloom dynamics: Roles of hydrology, nutrient limitation, sinking, and whole lake manipulation. Water Res 41:2551–2562

Gasith A (1975) Tripton sedimentation in eutrophic lakes – simple correction for the

resuspended matter. Verh Internat Verein Limnol 19:116–122

Gendron-Badou A, Coradin T, Maquet J, Frohlich F, Livage J (2003) Spectroscopic characterization of biogenic silica. J Non-Cryst Solids 316:331–337

Gibson CE (1984) Sinking rates of planktonic diatoms in an unstratified lake; a comparison of field and laboratory observations. Freshw Biol 14:507–515

Gibson CE, Wang G, Foy RH (2000) Silica and diatom growth in Lough Neagh: the importance of internal recycling. Freshw Biol 45:285–293

Harashima A (2007) Evaluating the effects of change in input ratio of N-P-Si to coastal marine ecosystem. J Envoron Sci Sustainable Society 1:33–38

Harashima A, Kimoto T, Wakabayashi T, Toshiyasu T (2006) Verification of the silica deficiency hypothesis based on biogeochemical trends in the aquatic continuum of Lake Biwa – Yodo River – Seto Inland Sea, Japan. Ambio 35:36–42

Harashima A, Iseki K, Tarutani K (2007) Possibility of the deterioration of Coastal and Shelf Ecosystem due to the Change in the Nutrient Input Ratio (in Japanese with English abstract). Umi To Sora 82:61–71

Hirata T, Muraoka K (1991) Seasonal change of soilwater and streamwater chemistries in the Tsukuba experimental forest basin (in Japanese with English abstract). Mizu Kougaku Ronbunshuu 35:105–110

Hoagland KD, Rosowski JR, Gretz MR, Roemer SC (1993) Diatom extracellular polymeric substances: function, fine structure, chemistry, and physiology. J Phycol 29:537–566

Hoffman A, Roussy D, Filella M (2002) Dissolved silica budget in the North basin of Lake Lugano. Chem Geol 182:35–55

Humborg C, Ittekkot V, Cociasu A, Bodungen B (1997) Effect of Danube river dam on

Black sea biogeochemistry and ecosystem structure. Nature 386:385–388

Hurd DC (1983) Physical and chemical properties of siliceous skeletons. In: Aston SR (eds) Silicon Geochemistry and Biogeochemistry. Academic, London, pp 187–244

Ittekkot V, Humborg C, Schafer P (2000) Hydrological alterations and marine biogeochemistry: A silicate issue?. Bioscience 50:776–782

Ittekkot V, Unger D, Humborg C, Tac An N (2006) Introduction. In: Ittekkot V, Unger D, Humborg C, Tac An N (eds) The Silicon Cycle: Human Perturbations and Impacts on Aquatic Systems. Island, Washington DC, pp 1–2

Kilham P (1971) A hypothesis concerning silica and the freshwater planktonic diatoms. Limnol Oceanogr 16:10–18

Komatsu E, Fukushima T, Shiraishi H (2006) Modeling of P-dynamics and algal growth in a stratified reservoir—mechanisms of P-cycle in water and interaction between overlying water and sediment. Ecol Model 197:331–349

Koszelnik P, Tomaszek JA (2008) Dissolved silica retention and its impact on eutrophication in a complex of mountain reservoirs. Water Air Soil Pollut 189:189–198

Kristiansen S, Hoell EE (2002) The importance of silicon for marine production. Hydrobiologia 484:21–31

Lewin JC (1962) Silicification. In: Lewin RA (ed) Physiology and Biochemistry of Algae. Academic, New York, pp 445–455

Li M, Xu K, Watanabe M, Chen Z (2007) Long-term variations in dissolved silicate, nitrogen, and phosphorus flux from the Yangtze River into the East China Sea and impacts on estuarine ecosystem. Estuar Coast Shelf Sci 71:3–12

Loucaides S, Van Cappellen P, Behrends T (2008) Dissolution of biogenic silica from

land to ocean: Role of salinity and pH. Limnol Oceanogr 53:1614–1621

Matsuoka Y (1984) An eutrophication model of Lake Kasumigaura (in Japanese with English abstract). Res Rep Natl Inst Environ Stud Jpn 54:53–242

Miretzky P, Cirelli AF (2004) Silica dynamics in a pamean lake (Lake Chascomus, Argentina). Chem Geol 203:109–122

Mortlock RA, Froelich PN (1989) A simple method for the rapid determination of biogenic opal in pelagic marine sediments. Deep-Sea Res 36:1415–1426

Muraoka K, Hirata T (1988) Streamwater chemistry during rainfall events in a forested basin. J Hydrol 102:235–253

Nagai M, Sugiyama M, Hori T (2001) Environmental chemistry of rivers and lakes, Part VII. Fractionation by calculation of suspended particulate matter in Lake Biwa into three types of particles of different origins. Jpn J Limnol 2:147–155

Neal C, Neal M, Reynolds B, Maberly SC, May L, Ferrier RC, Smith J, Parker JE (2005) Silicon concentrations in UK surface waters. J Hydrol 304:75–93

Newberry TL, Schelske CL (1986) Biogenic silica record in the sediments of Little Round Lake, Ontario. Hydrobiologia 143:293–300

Officer CB, Ryther JH (1980) The possible importance of silicon in marine eutrophication. Mar Ecol Prog Ser 3:83–91

Rippey B (1983) A laboratory study of the silicon release process from a lake sediment (Lough Neagh, Northern Ireand). Arch Hydrobiology 96:417–433

Redfield AC, Ketchum BH, Richards FA (1963) The influence of organismson the composition of sea-water. In: Hill MN (eds) The sea. (Comparative and descriptive oceanography, vol 2) John Wiley & Sons, New York, pp 26–77

Reynolds CS (1973) The seasonal periodicity of planktonic diatoms in a shallow

eutrophic lake. Freshwater Biol 3:89–l10

Scavia D, Fahnenstiel GL (1987) Dynamics of Lake Michigan phytoplankton: mechanisms controlling epilmnetic communities. J Great Lakes Res 13(2):103–120

Schelske CL (1985) Biogeochemical silica mass balances in Lake Michigan. Biogeochemistry 1:197–218

Schelske CL (1999) Diatoms as mediators of biogeochemical silica depletion in the Laurentian Great Lakes. In: Stoermer EF, Smol JP (eds) The diatoms: Applications for the environmental and earth science. Cambridge University, Cambridge, pp 73–84

Schelske CL, Stoermer EF (1971) Eutrophication, silica depletion, and predicted changes in algal quality in Lake Michigan. Science 173:423–424

Schelske CL, Conley DJ, Stoermer EF, Newberry TL, Campbell CD (1986) Biogenic silica and phosphorus accumulation in sediments as indices of eutrophication in the Laurentian Great Lakes. Hydrobiologia 143:79–86

Schelske CL, Züllig H, Boucherle M (1987) Limnological investigation of biogenic silica sedimentation and silica biogeochemistry in Lake St. Moritz and Lake Zürich. Schweiz Z Hydrol 49:42–50

Schelske CL, Robbins JA, Gardner WS, Conley DJ, Bourbonnier RA (1988) Sediment record of biogeochemical responses to anthropogenic perturbations of nutrient cycles in Lake Ontario. Can J Fish Aquat Sci 45:1291–1303

Seki T, Fukushima T, Imai A, Matsushige K (2006) Turbidity increase and sediment resuspension in Lake Kasumigaura (in Japanese with English abstract). Doboku Gakkai Ronbunshuu G 62:122–134

Sicko-Goad L, Schelske CL, Stoermer EF (1984) Estimation of intracellular carbon and silica content of diatoms from natural assemblages using morphometric techniques. Limnol Oceanogr 29:1170–1178

Sommer U, Stabel HH (1983) Silicon consumption and population density changes of dominant planktonic diatoms in Lake Constance. J Ecol 71:119–130

Sommer M, Kaczorek D, Kuzyakov Y, Breuer J (2006) Silicon pools and fluxes in soils and landscapes—a review. J Plant Nutr Soil Sci 169:310–329

Szczepocka E, Szulc B (2006) Benthic diatoms in the central section of the Pilica River and Sulejow Reservoir. Oceanol Hydrobiol Stud 35:171–178

Takano K, Hino S (1994) What caused the summer replacement of dominant planktonic algae in Lake Barato? Jpn J Limnol 55:279–286

Takano K, Hino S (1996) The effect of silicon concentration on replacement of dominant diatom species in a silicon-rich Lake. Jpn J Limnol 57:153–162

Teodoru C, Dimopoulos A, Wehrli B (2006) Biogenic silica accumulation in the sediments of Iron Gate I Reservoir on the Danube River. Aquat Sci 68:469–481

Tilman D, Kilham P (1976) Sinking in freshwater phytoplankton: Some ecological implications of cell nutrient status and physical mixing processes. Limnol Oceanogr 21:409-417

Triplett LD, Engstrom DR, Conley DJ, Schellhaass SM (2008) Silica fluxes and trapping in two contrasting natural impoundments of the upper Mississippi River. Biogeochemistry 87:217–230

Tsunogai S (1979) Dissolved silica as a primary factor determining the composition of phytoplankton classes in the ocean (in Japanese with English abstract). Bull Faculty Fisheries Hokkaido Univ 30:314–322

Van Cappellen P, Dixit S, Van Beusekom J (2002) Biogenic silica dissolution in the oceans: Reconciling experimental and field-based dissolution rates. Glob Biogeochem Cycles 16:1075

Vesely J, Majer V, Kopacek J, Safanda J, Norton SA (2005) Increasing silicon concentrations in Bohemian Forest lakes. Hydrol Earth Syst Sci 9:699–706

Glossary

Symbols	Definition and dimension in SI units	Introduced in chapter
a	constant (K)	4
A	area of Lake Kasumigaura (1.715×10^8 m^2)	5
A'	watershed area (km^2)	6
A'_{total}	watershed area of Lake Kasumigaura (1426 km^2)	6
b	BSi content of freshwater diatom frustules (g cm^{-3})	6
BSi	BSi content in the sediment cores (g kg^{-1})	5
BSi_w	BSi concentration in water (g m^{-3})	5
c	diatom sinking rate (m day^{-1})	5, 6
C_{BSi}	BSi concentration (mg l^{-1} = g m^{-3})	4
$C_{diatoms}$	diatom abundance (cm^3 m^{-3})	6
C_{DSi}	DSi concentration (mg l^{-1} = g m^{-3})	4, 6
C_e	equilibrium concentration of DSi (mg l^{-1})	4
d_{WT}	constant (^oC)	6
DSi_{base}	DSi concentration of the base flows (g m^{-3})	5
DSi_{rain}	DSi concentration of rainwater (g m^{-3})	5
E	root mean squared error (DSi in g m^{-3}; diatoms in cm^3 m^{-3})	6
f_I	function representing the influence of irradiation	6

Symbols	Definition and dimension in SI units	Introduced in chapter
f_{I}'	vertically-averaged light influence function	6
f_{Si}	function representing the influence of DSi concentration	6
f_{T}	function representing the influence of temperature	6
h	depth of water from water surface to bottom surface (m)	4
I	(D + B) Si load from the inflows (g y^{-1})	5
$I_{diatoms}$	diatom load from the inflows (g day^{-1})	6
I_{DSi}	DSi load from the inflows (g day^{-1})	6
I_{max}	maximum DSi load from the inflows (g y^{-1})	5
I_{min}	minimum DSi load from the inflows (g y^{-1})	5
IRR	irradiation in water at a certain depth (MJ m^{-2} h^{-1})	6
IRR_0	solar irradiation at the water surface (MJ m^{-2} h^{-1})	6
k	dissolution rate constant (day^{-1})	4
k_f	dissolution rate constant of fresh diatom frustules (day^{-1})	4
k_o	dissolution rate constant of old diatom frustules (day^{-1})	4
K	release rate constant from bottom sediments (day^{-1})	4
K_d	light attenuation coefficient (m^{-1})	6
K_I	constant (MJ m^{-2} h^{-1})	6
K_{Si}	half-saturation constant of DSi concentration for diatoms (g m^{-3})	6
L_{exch}	load from the inflowing rivers (DSi in g s^{-1}; diatoms in cm^3 s^{-1})	6
L_{piston}	load from the inflowing rivers (DSi in g s^{-1}; diatoms in cm^3 s^{-1})	6
L_{river}	load from the inflowing rivers (DSi in g s^{-1}; diatoms in cm^3 s^{-1})	6
M	rate of change in the (D + B) Si amounts in water (g y^{-1})	5

Symbols	Definition and dimension in SI units	Introduced in chapter
N	area-averaged net sedimentation rate of BSi (g m^{-2} y^{-1})	5
O	(D + B) Si load from the outflow (g y^{-1})	5
O_{DSi}	DSi load from the outflow (g day^{-1})	6
$O_{diatoms}$	diatom load from the outflow (g day^{-1})	6
$OFUNC$	object function	6
q_{base}	daily discharge of the base flows (m^3 day^{-1})	5
q_{mean}	annual mean daily discharge of the inflows (m^3 day^{-1})	5
Q'_{total}	annual total discharge of the inflows (m^3 y^{-1})	5
Q	river discharge inflowing to each box (m^3 s^{-1})	6
Q_{total}	total river discharge inflowing to Lake Kasumigaura (m^3 s^{-1})	6
r	Mean ratio of river discharge inflowing to the each box to that inflowing to the entire lake	6
R	area-averaged DSi release rate (g m^{-2} y^{-1})	5
R_{bottom}	DSi release rate from bottom sediments (g m^{-2} day^{-1})	4
D	Si dissolution rate of SS (mg g^{-1} day^{-1})	4
R_{SS}	DSi release rate from SS (mg g^{-1} day^{-1})	6
S	area-averaged gross sedimentation rate of BSi (g m^{-2} y^{-1})	5
S_M	mass sedimentation rate (kg m^{-2} y^{-1})	5
SS	suspended solids concentration derived from sediments (g l^{-1})	4
SS_{sed}	suspended solids concentration derived from sediments (g m^{-3})	6
t	time (day)	4, 6
T	water temperature (K)	4

Symbols	Definition and dimension in SI units	Introduced in chapter
T_a	constant (298.15 K)	4
V_{total}	water volume of Lake Kasumiguara (6.6×10^8 m^3)	4
V	water volume (m^3)	6
WT	water temperature (^oC)	6
X	carrier content of SS ($mg\ g^{-1}$)	4
Y	annual amount of DSi released from SS ($g\ y^{-1}$)	4
z	water depth (m)	6
Z	apparent accumulation rate of BSi ($g\ m^{-2}\ y^{-1}$)	5
α	Si adsorbed on the surface of SS ($mg\ g^{-1}$)	4
α'	Si adsorbed on the carrier ($mg\ g^{-1}$)	4
β	BSi content of SS ($mg\ g^{-1}$)	4
β_f	fresh BSi content of SS ($mg\ g^{-1}$)	4
β_o	old BSi content of SS ($mg\ g^{-1}$)	4
γ	adsorption equilibrium constant	4
μ	growth rate of freshwater diatoms (day^{-1})	6
μ_{max}	maximum growth rate of freshwater diatoms (day^{-1})	6
τ	time (day)	4